Homoclinic Bifurcations in Reversible Systems

Dissertation

zur Erlangung des akademischen Grades

Dr. rer. nat.

vorgelegt von
Dipl.-Math. Thomas Wagenknecht

eingereicht bei der Fakultät für Mathematik und Naturwissenschaften
der Technischen Universität Ilmenau am 17. Juni 2003
öffentlich verteidigt am 12. Dezember 2003

Gutachter: Prof. Dr. A. R. Champneys (University of Bristol)
Prof. Dr. B. Fiedler (Freie Universität Berlin)
Prof. Dr. B. Marx (Technische Universität Ilmenau)

Zusammenfassung

Die vorliegende Arbeit untersucht Bifurkationen homokliner Lösungen in gewöhnlichen Differentialgleichungen. Homokline Lösungen sind in positiver und negativer Zeit asymptotisch zu einer Gleichgewichtslage, d.h. zu einer konstanten Lösung der Differentialgleichung. Die Arbeit betrachtet solche homokline Bifurkationen, die von einer Veränderung des Typs dieser assoziierten Gleichgewichtslage herrühren. Verschiedene Szenarien werden in der Klasse der reversiblen Differentialgleichungen analysiert.

Der Hauptteil der Arbeit beschäftigt sich mit Homoklinen an Gleichgewichtslagen, welche selbst in einer lokalen Bifurkation verzweigen. Dabei verändert sich der Typ der Gleichgewichtslage vom reellen Sattel (mit führenden reellen Eigenwerten) zum Sattel-Zentrum (mit einem Paar rein imaginärer Eigenwerte). Das Miteinander lokaler und globaler Bifurkationseffekte erfordert eine neuartige Behandlung: Durch eine Kombination analytischer und geometrischer Techniken wird eine Beschreibung verzweigender Homoklinen gewonnen. Dabei werden sowohl rein reversible Systeme als auch Systeme mit zusätzlicher Symmetrie und Hamilton-Struktur betrachtet.

Im zweiten Teil der Arbeit werden homokline Bifurkationsphänomene untersucht, die von einer Typveränderung der Gleichgewichtslage von rellem Sattel zu komplexem Sattel-Fokus (mit komplexen führenden Eigenwerten) herrühren. Dabei wird die Existenz von zwei Ausgangshomoklinen in sogenannter Blasebalg-Konfiguration *(homoclinic bellows configuration)* vorausgesetzt. Unter Verwendung einer auf Lin zurückgehenden analytischen Methode werden Bifurkationsresultate für verzweigende N-Homoklinen erzielt.

Die allgemeinen Bifurkationsresultate werden auf physikalische Probleme der nichtlinearen Optik und Wasserwellentheorie, sowie auf zwei mathematischen Modellgleichungen angewendet und in numerischen Untersuchungen bestätigt.

Abstract

The thesis investigates bifurcations from homoclinic solutions of ordinary differential equations. Homoclinic solutions are characterised by approaching an equilibrium, i.e. a constant solution of a differential equation, in both positive and negative time. The thesis is devoted to the analysis of homoclinic bifurcations that originate from a change in the type of the associated equilibrium. Several scenarios are considered in the class of reversible ordinary differential equations.

The main part of the thesis deals with solutions homoclinic to equilibria that themselves undergo a local bifurcation. In this process the type of the equilibrium changes from a real saddle (with real leading eigenvalues) to a saddle-centre (with a pair of imaginary eigenvalues). The interplay of local and global bifurcation effects requires a new analytical approach. By a combination of analytical and geometric techniques a description of bifurcating homoclinic solutions is derived. Thereby both purely reversible systems and systems with additional symmetry or Hamiltonian structure are considered.

The second part of the thesis discusses a homoclinic bifurcation in which the associated equilibrium undergoes a transition from real saddle to complex saddle-focus (with complex leading eigenvalues). The existence of two primary homoclinic solutions forming a so-called bellows structure is assumed. Using an analytical technique known as Lin's method results about the bifurcation of N-homoclinic orbits are derived.

The theory is applied to physical problems from nonlinear optics and water wave theory as well as to two mathematical model systems. Numerical investigations confirm the general bifurcation results.

Contents

CHAPTER 1

Introduction

1.1. Prologue

There has been a long fascination with homoclinic and heteroclinic phenomena in ordinary differential equations (ODEs) and discrete dynamical systems, motivated by both mathematical and applied questions. From a mathematical point of view homoclinic phenomena are of interest because they represent a possible source for complex dynamics. From Poincare's studies on celestial mechanics [72], over Birkhoff's and Smale's work on discrete systems [5, 80], or Shilnikov's analysis of saddle focus homoclinic orbits [78], researchers have always searched for a suitable description and understanding of the complicated behaviour caused by the seemingly simple primary configuration. It has been recognized that connecting orbits and their bifurcations play an important role in the qualitative theory of dynamical systems since they can be thought of as organizing centres for the dynamics of a system in their neighbourhood. Strong effort has gone into describing the different bifurcations that can occur in terms of genericity and into determining the different types of behaviour in systems undergoing homoclinic and heteroclinic bifurcations.

In applications the role of certain travelling (or standing) waves played by homoclinic and heteroclinic orbits is of immediate interest. Travelling wave solutions form a particular important set of solutions or patterns of partial differential equation (PDE) models. In mathematical biology they can describe impulse propagation in nerve fibres [69]. In water-wave theory they arise as solitary waves of elevation or depression [26, 15]. In nonlinear optics they are of interest for the transition of beams and pulses through optical fibres [1, 73]. Standing waves can model localized structures in solid mechanics [76].

By an appropriate travelling wave ansatz the PDE system can be reduced to a system of ODEs, and hence dynamical systems theory for ODEs can be employed in the study

of PDEs. Homoclinic orbits in the travelling wave system describe pulses in the PDE model. Often such waves are also referred to as *solitary waves* or *solitons* (although no integrability is assumed here). Heteroclinic orbits in the travelling wave system correspond to fronts or kinks in the PDE model. In many situations it is of interest whether given pulses or kinks are accompanied by N-pulses, i.e. by waves that consist of N well-separated copies of the primary waves. This amounts to the study of the existence of N-homoclinic orbits in the travelling wave system.

Often this system has the structure of being reversible, because of spatial symmetries in the underlying PDE model. A number of examples is given in [22] or Section 3.6 below. Consequently, substantial progress in the understanding of the associated phenomena has been made. A comprehensive overview is given in [22, 23].

Most of the bifurcation results in the literature, however, concern a *single* homoclinic orbit (or heteroclinic cycle) to a *hyperbolic* equilibrium [22]. Other scenarios, such as homoclinic orbits to equilibria of saddle centre type, have attracted attention only recently [23]. The purpose of this thesis is to take a further step and to analyse two new types of bifurcations from homoclinic orbits in reversible systems, using a mixture of geometric, topological and functional-analytical techniques. Both types of bifurcations can be characterized by a change in the type of the associated equilibrium.

In the main part we consider a family of reversible systems that possesses a symmetric homoclinic orbit to an equilibrium of real saddle type, i.e. to an equilibrium whose leading eigenvalues are real. Such homoclinic orbits are of codimension-zero in the class of reversible systems and can therefore be continued in the considered family. We are interested in the bifurcation that occurs when the leading eigenvalues merge at 0 and become imaginary. In this process the equilibrium changes its type to a saddle centre, and the investigation of this process amounts to discuss bifurcations from homoclinic orbits to degenerate equilibria, that is, to equilibria which possess a singular linearization. Because of this singularity the global behaviour near the homoclinic solution is strongly affected by a local bifurcation of the equilibrium. We discuss this influence for several classes of reversible system. A complete description of bifurcating one-homoclinic orbits is derived.

In the second part we study what happens when the equilibrium, associated to a homoclinic orbit, undergoes a transition from a real saddle to a complex saddle focus. In the usual way, we refer to equilibria as saddle foci, if their leading eigenvalues are complex. This time we do not consider the case of a single homoclinic orbit, which has been discussed in the literature before, see for instance [21]. Instead we are interested in bifurcations from two homoclinic orbits that form a so-called *bellows configuration*. This means that both orbits approach the equilibrium in the same direction for positive and negative time, respectively. Our studies focus on bifurcating N-homoclinic orbits.

The rest of this introductory section is devoted to a comprehensive description of the bifurcation phenomena that we deal with in this thesis. We do not intend to give a summary of the thesis; in particular, we discuss the general bifurcation problems and

the techniques for their analysis only in brief. We rather want to arouse the reader's interest by presenting numerical results that have been derived for two systems of second order ODEs. These *umbilic systems* are unfoldings of a degenerate equilibrium with fourfold eigenvalue zero in a class of reversible Hamiltonian systems. Our analysis of the umbilic systems is mainly concerned with the existence and bifurcations of homoclinic and heteroclinic orbits. Starting from rigorous existence results for such orbits, obtained in [88, 91], we have numerically studied bifurcations of connecting orbits in the system, see for instance [58]. These studies have been the main motivation for the investigations in this thesis.

In the following we use the numerical results to illustrate some of the problems we will deal with, and to give the reader an idea of what we are interested in. But it is important to note that the umbilic systems are not only suitable examples for numerical computations. On the contrary, being unfoldings of a highly degenerate equilibrium they are of interest in their own right. We will therefore repeatedly return to the systems throughout the thesis and explain how general bifurcation results apply to these specific systems. Furthermore, we have compiled some material in Appendix A, where we give information about the origin of the umbilic systems and list analytical results that lay the foundations for the numerical analysis.

1.2. Two model systems

Our studies revolve around bifurcations of connecting orbits that have been observed numerically in two systems of second order ODEs, called the umbilic systems. These systems have been obtained as unfoldings of a degenerate equilibrium with fourfold eigenvalue zero in a class of reversible Hamiltonian systems in the author's Diploma thesis [88], see also [91]. They read

$$\dot{x} = f^{\pm}(x, \alpha, \beta) = \begin{pmatrix} x_2 \\ 2x_1x_3 + 2\alpha x_1 \\ x_4 \\ -x_1^2 \pm x_3^2 \mp 2\alpha x_3 - \beta \end{pmatrix} \tag{1.1}$$

with $x = (x_1, x_2, x_3, x_4) \in \mathbb{R}^4$, and with real parameters α, β. Our analysis of the umbilic systems is mainly concerned with the existence and bifurcation of orbits connecting equilibria. Corresponding results have been obtained in [88, 91] and are reviewed in Section A.2. In the present introductory part we discuss some fundamental properties.

It is important to note that the umbilic systems belong to the class of reversible Hamiltonian systems. To fix thoughts let us first introduce what we will understand by reversibility throughout this thesis. Consider an ODE

$$\dot{u} = f(u), \ u \in \mathbb{R}^{2n}. \tag{1.2}$$

We call the equation (or equivalently the corresponding vector field f) *R-reversible* if there exists a linear involution R, i.e. a linear map on $\mathbb{R}^{2n}$ satisfying $R^2 = id$, with a fixed space $\mathrm{Fix}\,(R) := \{u : Ru = u\}$ of dimension n such that

$$f(Ru) + Rf(u) = 0.$$

We remark that there exist more general definitions of reversibility. Some authors, for instance, allow both the phase space of the system and the fixed space $\mathrm{Fix}\,(R)$ to have arbitrary dimension [63, 67]. But the scenarios that we are interested in will lead to situations in which a hyperbolic equilibrium point is contained in the space $\mathrm{Fix}\,(R)$. In this case the dimension of $\mathrm{Fix}\,(R)$ is necessarily half the dimension of the phase space as demanded above, see [81]. Consequently, we have chosen the restrictive definition of reversibility to avoid constant technical considerations.

It is easy to verify that the umbilic systems are reversible with respect to the involutions

$$R_1 : (x_1, x_2, x_3, x_4) \mapsto (x_1, -x_2, x_3, -x_4),$$

and

$$R_2 : (x_1, x_2, x_3, x_4) \mapsto (-x_1, x_2, x_3, -x_4).$$

Moreover, for the map $S := R_1 \circ R_2$ we find that $f^{\pm}(Sx, \alpha, \beta) = Sf^{\pm}(x, \alpha, \beta)$, i.e. this map describes a $\mathbb{Z}_2$-symmetry for (1.1).

In addition to being reversible and $\mathbb{Z}_2$-symmetric the umbilic systems are also *Hamiltonian* with Hamilton functions $H^{\pm}$ given by

$$H^{\pm}(x, \alpha, \beta) = -\frac{1}{2}x_2^2 + \frac{1}{2}x_4^2 + x_1^2 x_3 \mp \frac{1}{3}x_3^3 + \alpha(x_1^2 \pm x_3^2) + \beta x_3.$$

Because of the indefinite quadratic form in $H^{\pm}$ the systems belong to the class of *indefinite Hamiltonian systems*, as introduced in [44]. Setting $q = (x_1, x_3)$ they can be written as

$$S\ddot{q} + \nabla V(q, \alpha, \beta) = 0,$$

with an indefinite matrix

$$S = \begin{pmatrix} -1 & 0 \\ 0 & 1 \end{pmatrix}$$

and potential V. The Hamiltonian is then given by $\widetilde{H}^{\pm}(q, \dot{q}, \alpha, \beta) = \frac{1}{2}\langle S\dot{q}, \dot{q}\rangle + V(q, \alpha, \beta)$. This property is of importance in Sections A.2 and A.3, where we investigate the existence of heteroclinic cycles for (1.1).

We have mentioned before that the umbilic systems are unfoldings of a highly degenerate equilibrium point. Indeed, setting $\alpha = \beta = 0$ we find that $x = 0$ is an equilibrium which possesses a fourfold eigenvalue zero. Our interest in equilibria of this type stems from a problem in nonlinear optics which is described in Appendix A. In that Appendix we also explain the origin of the systems and their mathematical relevance.

For the time being, however, we can consider the umbilic systems as model systems for the homoclinic bifurcations that will be studied in this thesis. The corresponding numerical analysis is based on rigorous existence results for homoclinic and heteroclinic orbits. We have put together these results in Appendix A and the interested reader is referred to this part for detailed information.

In the first Section A.2 we review results about the bifurcation of equilibria and the existence of connecting orbits, mainly obtained in [88, 91]. The results about bifurcations of equilibria are compiled in bifurcation diagrams in Figures A.1 and A.3, respectively.

The results about the existence of connecting orbits are completely analogous for both systems. In most cases, we therefore only consider the reversible hyperbolic umbilic f^- in detail. For this system two results are of particular importance in the following:

- The existence of a homoclinic orbit γ_{hom} to an equilibrium ξ_2 for all parameter values where ξ_2 exists, that is for $\beta < \alpha^2$ (see Figure A.1 and Theorem A.1).
- The existence of a symmetric heteroclinic cycle $\{\gamma_{het}, R_1\gamma_{het}\}$ between equilibria ξ_3 and $\xi_4 = R_2\xi_3$ for all parameter values where these equilibria are real saddles, i.e. for $-4\alpha^2 \leq \beta < -3\alpha^2$, $\alpha > 0$ (see Figure A.1 and Theorem A.2).

Both the homoclinic orbit and the heteroclinic cycle are subject to numerical studies.

We also discuss two techniques that are of advantage for the (numerical) analysis of the systems. We first show that in most cases one of the two parameters α, β can be eliminated by a suitable scaling. In particular, we will see that bifurcation results are independent of the size of α and β. This simplifies the numerical analysis since we are not chained to a local regime. Moreover, we demonstrate how to factor out the $\mathbb{Z}_2$-symmetry of the systems. This allows us to unify the treatment of homoclinic and heteroclinic orbits to the equilibria ξ_3 and ξ_4. The latter point is again used in Chapter 4.

Section A.3 of the appendix is devoted to a detailed treatment of the heteroclinic cycle $\{\gamma_{het}, R_1\gamma_{het}\}$. One of the open questions in [88] has been whether this cycle persists the transition of the equilibria $\xi_{3,4}$ from real saddles to complex saddle foci. This transition occurs for parameter values $\beta = -4\alpha^2$, $\alpha > 0$. In Section A.3 we show that the cycle exists because of a *topologically transverse intersection* of corresponding stable and unstable manifolds and therefore survives the associated equilibria's change in type.

1.3. Homoclinic orbits to degenerate equilibria

The main part of this thesis is devoted to the study bifurcations from homoclinic orbits to degenerate equilibria in reversible systems. In Chapter 2 we deal with such a bifurcation in a class of reversible and $\mathbb{Z}_2$-symmetric systems, motivated by numerical investigations on the umbilic systems. In Chapter 3 we extend these studies to the class of purely reversible systems.

We have introduced the concept of reversibility above. A characteristic property of reversible systems is that if $u(\cdot)$ is a solution of (1.2), then so is $\tilde{u}(t) = Ru(-t)$. If we have $u(0) \in \mathrm{Fix}\,(R)$ then $u(t) = Ru(-t)$, and for the corresponding orbit $U := \{u(t) : t \in \mathbb{R}\}$ we find that $RU = U$. We call such orbits and the corresponding solutions *R-symmetric* or *symmetric*, in short. They are of particular concern in the theory of reversible systems since they enjoy special properties. For an overview we refer to [63, 81].

Consequently, we are interested in symmetric homoclinic orbits. We assume such an orbit to be contained in the intersection of the stable and unstable manifold of a degenerate equilibrium. Here, degenerate means an equilibrium with singular linearization. More precisely, we assume the spectrum of this linearization to consist of a double, non-semisimple eigenvalue zero and hyperbolic eigenvalues, that is, eigenvalues with non-zero real part. (From now on we follow the usual convention and speak of the eigenvalues of the equilibrium.) Hence, the scenario requires a phase-space that is a least four-dimensional. In the four-dimensional case the equilibrium is assumed to have a double zero and a pair of real eigenvalues. Note that the equilibrium's eigenvalues necessarily come in pairs because of the reversibility.

It is not hard to see, that this scenario is non-generic. Already the existence of an equilibrium of the above type is a codimension-one phenomenon in the class of reversible systems. The additional assumption concerning the existence of a homoclinic orbit typically increases the codimension of the problem further. We therefore consider an unfolding of the degenerate situation. We are interested in how homoclinic orbits bifurcate from the primary one.

We first encountered a problem of this type in numerical studies on the umbilic systems, undertaken in [58]. Let us briefly describe these studies since they give an idea of what we are interested in. We concentrate on the case of the hyperbolic umbilic f^-.

A new type of homoclinic bifurcation - numerical results

We are concerned with the homoclinic orbit γ_{hom} of f^-, asymptotic to the equilibrium ξ_2, whose existence is asserted in Theorem A.1 in Section A.2. This orbit is symmetric with respect to both involutions R_1 and R_2. Consequently it is contained in the invariant space $\mathrm{Fix}\,(S)$. An analytical expression for the corresponding homoclinic solution is given in Theorem A.1.

We are interested in a bifurcation from γ_{hom} that occurs at parameter values $\beta = -3\alpha^2$, $\alpha > 0$. (In the bifurcation diagram in Figure A.1 this corresponds to the curve $\mathcal{B}_4$.) For simplicity we make use of a scaling property of f^-, established in Lemma A.5. Roughly speaking Lemma A.5 states that systems (1.1) to different parameter values are equivalent if these parameter values lie on the same arc of a parabola $\beta = c\alpha^2$ with $c \in \mathbb{R}$. In studying a bifurcation it is therefore important to vary the parameters such that these curves are crossed. In the following we keep $\alpha = 1$ fixed and consider f^- under variation of β only.

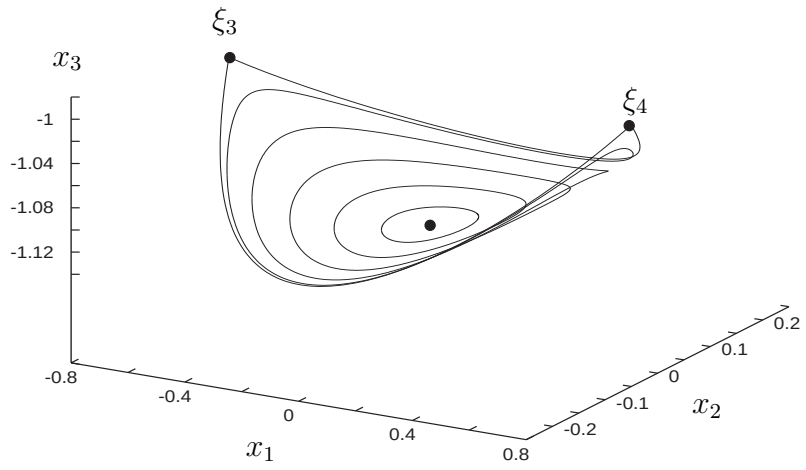

Figure 1.1.: Phase portrait after the reversible pitchfork bifurcation of ξ_2. This figure shows plots of periodic orbits and of the heteroclinic cycle $\{\gamma_{het}, R_1\gamma_{het}\}$ for $\alpha = 1$, $\beta = -3.2$, projected in (x_1, x_2, x_3)-space.

Let us first consider the associated equilibrium ξ_2. As the bifurcation diagram in Figure A.1 shows the equilibrium has a double zero and a pair of real eigenvalues for $\alpha = 1$, $\beta = -3$. Moreover, if the critical value, $\beta = -3$, is crossed with decreasing β, the equilibrium undergoes a reversible pitchfork bifurcation, giving rise to two saddles ξ_3 and $\xi_4 = R_2\xi_3$ and turning from a real saddle into a saddle centre itself.

A numerical analysis of the local bifurcation of ξ_2 yields the 'phase portrait' in Figure 1.1. This figure shows plots of projections of periodic orbits in (x_1, x_2, x_3)-space for $\alpha = 1$, $\beta = -3.2$, i.e. 'after the bifurcation'. In addition it shows a heteroclinic cycle between ξ_3 and ξ_4. Because of its characteristic shape we refer to this local scenario as the *eye case* of a reversible pitchfork bifurcation.

Now let us return to the homoclinic orbit γ_{hom}. According to Theorem A.1 this orbit exists for all $\beta < \alpha^2$. In particular, the existence of γ_{hom} is unaffected by the local bifurcation above. At a first glance this is a rather remarkable result. It is well known that symmetric homoclinic orbits to hyperbolic equilibria are of codimension-zero in R-reversible systems [29]. The reason for this lies in the possibility for a transverse intersection of the stable manifold of the equilibrium and the space $\mathrm{Fix}\,(R)$. Since the stable and unstable manifold of a symmetric equilibrium are R-images of each other, the orbit through such an intersection point is homoclinic to the equilibrium and thus exists robustly. Hence, this can explain the stable existence of γ_{hom} for parameter values where ξ_2 is a real saddle. (For the particular case of γ_{hom} it is indeed possible to prove

that the stable manifold of ξ_2 intersects the fixed space of the involution transversally, see Lemma 2 in [91].)

For $\beta \leq -3\alpha^2$, however, ξ_2 is nonhyperbolic and the above transversality arguments do not apply in the full four-dimensional phase space. But we can now use the fact that $\gamma_{hom} \subset \mathrm{Fix}\,(S)$. Reduced to this space f^- is still reversible and therefore we can repeat the above arguing within $\mathrm{Fix}\,(S)$. Hence, the symmetries of f^- imply the robust existence of γ_{hom}. Nevertheless, the loss of hyperbolicity of ξ_2 (in the full system) should have consequences for the dynamics in a neighbourhood of the orbit. Hence, it is interesting to investigate bifurcations from γ_{hom}.

We have studied the situation numerically, using the software package AUTO/HomCont [32] and have searched for homoclinic orbits to the equilibria ξ_3 and ξ_4. (Note that no other homoclinic orbits to ξ_2 can exist since its stable and unstable manifold agree along γ_{hom} if $\beta < -3\alpha^2$.) Because of the reversing symmetry of f^- it suffices to compute homoclinic orbits to ξ_3. The numerical techniques for this are based on the continuation methods for symmetric homoclinic orbits that are implemented in AUTO/HomCont.

Our idea for the computation of homoclinic orbits to ξ_3 is as follows: We start a continuation of γ_{hom} with parameter values $\alpha = 1$, $\beta > -3$. (Here we use the known analytical expression of γ_{hom}.) The continuation is performed with decreasing β such that the critical value $\beta = -3$ is crossed. Upon crossing we do not compute homoclinic orbits to ξ_2 but switch to the equilibrium ξ_3. In this way homoclinic orbits to ξ_3 can be found which look like 'copies' of γ_{hom}.

In a first run γ_{hom} has been continued as an R_1-symmetric homoclinic solution. As a result, only R_1-symmetric homoclinic orbits could be detected by the above procedure. It turns out that when we move the parameter β through $\beta = -3$ then not only the equilibrium ξ_2 undergoes a pitchfork bifurcation but also the orbit γ_{hom} follows a similar scenario. Indeed, for $\beta < -3$ we find a new homoclinic orbit to the equilibrium ξ_3, and - by reversibility - another one to ξ_4, both bifurcating from the primary orbit γ_{hom}. We term this scenario a *reversible homoclinic pitchfork bifurcation*.

In Figure 1.2 we present plots of solutions that have been produced by the above procedure. Panel (a) shows the primary solution γ_{hom} for parameter values $\alpha = 1$, $\beta = -2.8$. The right part of the panel contains plots of the x_1-component and x_3-component of the homoclinic solution x_{hom}. In the left part we give an impression of the situation in phase space and show a projection of the corresponding orbit in (x_1, x_2, x_3)-space. Because of the chosen projection γ_{hom} is completely contained in the x_3-axis. In the lower panel of Figure 1.2 the situation for $\alpha = 1$, $\beta = -3.5$ is illustrated. For an impression of the proportions we have also incorporated the heteroclinic cycle $\{\gamma_{het}, R_1\gamma_{het}\}$ into the 3D-picture. Note the different scales of the x_1- and x_2-axis, and of the x_3-axis.

Since γ_{hom} is symmetric with respect to both involutions R_i, $i = 1, 2$, we can repeat the above computations and continue γ_{hom} as an R_2-symmetric solution. In this way R_2-symmetric solutions between ξ_3 and ξ_4, i.e. heteroclinic cycles, have been computed.

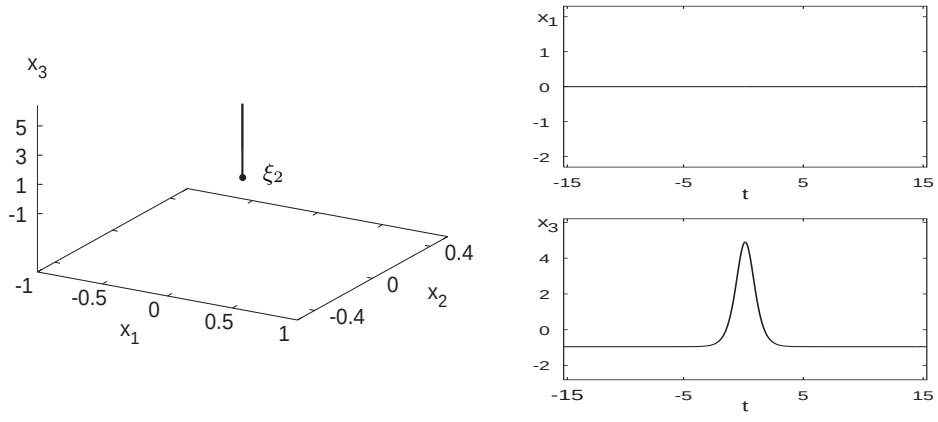

(a) $\alpha = 1,\ \beta = -2.8$

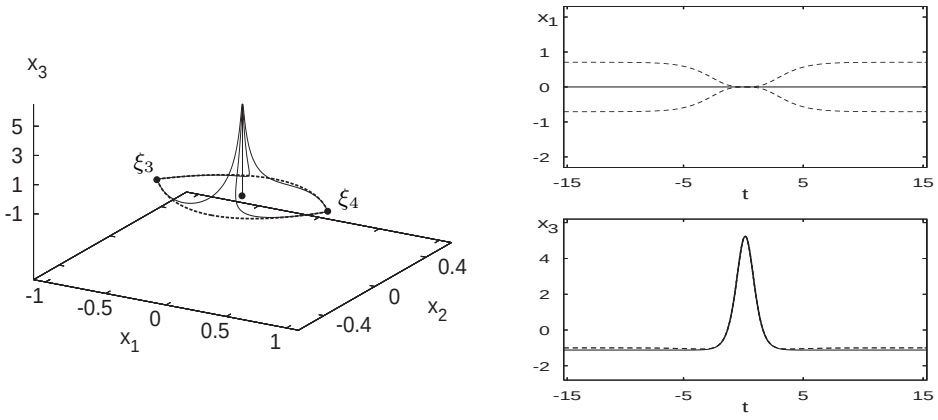

(b) $\alpha = 1,\ \beta = -3.5$

Figure 1.2.: Reversible homoclinic pitchfork bifurcation for $f^-(x, \alpha, \beta)$. The shown homoclinic solutions have been computed by the continuation method described in the text. A plot of the (small) heteroclinic cycle between ξ_3 and ξ_4 is added in the lower panel.

The results are completely analogous to the homoclinic scenario. The local bifurcation is followed by the global bifurcation, in which heteroclinic orbits between ξ_3 and ξ_4 emerge for $\beta < -3$. These orbits are 'copies' of the primary homoclinic solution and form a cycle. In Figure 1.3 we show a plot of the cycle at $\beta = -3.5$ in (x_1, x_2, x_3)-space. Note the similarity to the homoclinic structure in the lower panel of Figure 1.2.

Let us summarize these results. The computations suggest that the local bifurcation of

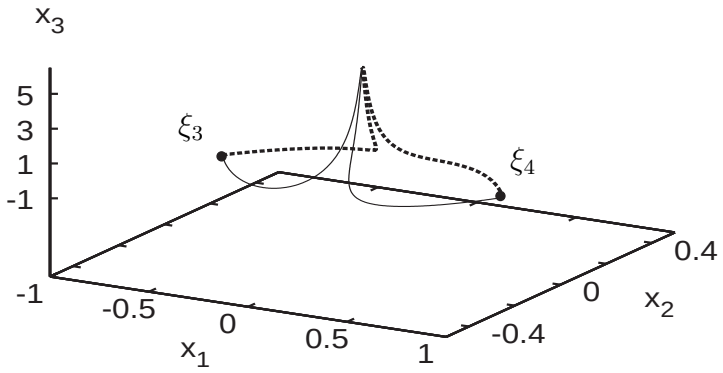

Figure 1.3.: Plot of the heteroclinic cycle that emerges in the bifurcation of γ_{hom}. The shown solutions have been computed for $\alpha = 1$, $\beta = -3.5$. Different orbits have been plotted differently.

ξ_2 is accompanied by a similar global bifurcation of the homoclinic orbit γ_{hom}. While the local reversible pitchfork bifurcation leads to the emergence of two additional R_1-symmetric equilibria $\xi_{3,4}$, we find a global *reversible homoclinic pitchfork bifurcation* in which two R_1-symmetric homoclinic orbits bifurcate from γ_{hom}. These orbits are bi-asymptotic to ξ_3 and ξ_4, respectively. Moreover, both the local and the global bifurcation leads to the emergence of a symmetric heteroclinic cycle between ξ_3 and ξ_4.

Our aim in Chapter 2 is to understand the homoclinic bifurcation of γ_{hom} analytically. Instead of restricting to the specific systems (1.1) we study the bifurcation in a general class of reversible and $\mathbb{Z}_2$-symmetric ODEs. The results in this chapter are based on the article [90].

Remark 1.1. We have seen that the umbilic systems have the additional property of being Hamiltonian. This has been used extensively to prove the existence of γ_{hom} and of the heteroclinic cycle $\{\gamma_{het}, R_1\gamma_{het}\}$ in [88, 91], see also Section A.2. Nevertheless, we neglect this Hamiltonian property in the general bifurcation analysis. The reason for this is simple. The reversing symmetries govern the behaviour of the system to such an extent that we can analyse the bifurcation scenario without relying on a possible Hamiltonian structure.

The general problem

As announced above we will not consider the umbilic systems alone, but we will turn to a general class of reversible and $\mathbb{Z}_2$-symmetric ODEs that possess an equilibrium which undergoes a reversible pitchfork bifurcation and which is connected to itself by a symmetric homoclinic orbit. We are interested in bifurcations from this homoclinic orbit, in particular, in the bifurcation of homoclinic and heteroclinic orbits to equilibria.

Hopefully the numerical example above has already convinced the reader that it is worth investigating this bifurcation. But there are further reasons why this is an interesting problem.

The analytical challenge for the analysis lies in the interplay of local and global effects. Indeed, we are interested in the *global* bifurcation of a homoclinic orbit which is strongly influenced by the *local* bifurcation of an equilibrium. This requires us to take a further step in the analysis of homoclinic bifurcations in reversible systems. Let us, for simplicity, explore this point in the case of four-dimensional systems.

Symmetric homoclinic orbits to hyperbolic equilibria are a classic issue of the theory of reversible systems, with studies dating back to Devaney [29, 30]. We have already observed that such orbits are of codimension-zero, i.e that they generically exist robustly in reversible systems. A sufficient condition for the robustness is the *non-degeneracy* of the orbit, which means that the intersection of the corresponding stable and unstable manifold along the orbit only contains the vector field direction [81]. Devaney has proved that in this case the homoclinic orbit is accompanied by a family of periodic orbits. These orbits accumulate on the homoclinic orbit with a period tending to infinity, see also [81].

It is well-known that the complexity of the dynamics near the homoclinic orbit is essentially determined by the type of the associated equilibrium. In a generic situation, the behaviour near homoclinic orbits to real saddles (with four real eigenvalues) is rather simple, whereas homoclinic orbits to complex saddle foci (with four complex eigenvalues) are accompanied by a very complex dynamics, see for instance [22, 41]. In particular, one can often prove uniqueness results for homoclinic orbits to real saddles, whereas in a neighbourhood of homoclinic orbits to complex saddle foci infinitely many N-homoclinic orbits exist [41]. These are homoclinic orbits which make N windings in a neighbourhood of the primary orbit. We return to these differences in detail in the next section.

More recently, also the case of homoclinic orbits to saddle centre equilibria has attracted substantial attention. In the case of four-dimensional systems a saddle centre possesses one pair of imaginary eigenvalues and one pair of real eigenvalues. Note that such equilibria are of codimension-zero in the class of reversible systems. By the Lyapunov Centre Theorem [29] the two-dimensional centre manifold of the equilibrium is filled with periodic orbits and, in particular, no local bifurcation occurs.

A symmetric homoclinic orbit to a saddle centre exists if the one dimensional stable and unstable manifolds intersect the two-dimensional fixed space of the involution. By

a simple count of dimensions we conclude that symmetric homoclinic orbits to saddle centres are of codimension one and therefore generically exist at isolated parameter values in one-parameter families of reversible ODEs. General studies in [68, 62] for reversible Hamiltonian systems and [16] for purely reversible systems deal with the question of how N-homoclinic orbits accumulate on parameter values for which a primary homoclinic orbit exists.

Our studies in Chapter 2 (and Chapter 3) take the natural next step and deal with homoclinic orbits to equilibria which themselves undergo a local bifurcation. We note that we do not aim to give complete description of the bifurcation scenario. Our main interest lies in the bifurcation of one-homoclinic orbits to equilibria. We will derive a complete description of the bifurcations of one-homoclinic orbits. The case of bifurcating N-homoclinic orbits is analytically more involved and is briefly discussed.

The general approach

We now outline how we will treat the homoclinic bifurcation in Chapter 2. We note that although our primary interest lies in four-dimensional systems, the analysis in that chapter mainly concerns systems of arbitrary (even) dimension. This is done merely to show that the results are not restricted to four dimensions, but can easily be extended under appropriate transversality conditions. Nevertheless, in the short description below we will only consider four-dimensional systems since the higher-dimensional case requires additional technical considerations.

Our bifurcation analysis uses two supplementary concepts. On the one hand we present an analytical technique for the detection of one-homoclinic orbits, namely a generalization of Lin's method [66, 75, 81]. On the other hand, the analysis is inspired by a geometric approach for the study of singularly perturbed systems of ODEs, known as *geometric singular perturbation theory* [54, 55]. Of particular concern to us here are studies about homoclinic orbits to *slow manifolds*, presented in [45, 42] and references therein.

Let us give explanations and consider a system $\dot{x} = f(x, \lambda)$ with $x \in \mathbb{R}^4$, $n \geq 1$, and $\lambda \in \mathbb{R}$, which is reversible with respect to two involutions R_1 and R_2 and possesses an R_i-symmetric ($i = 1, 2$) homoclinic orbit Γ to the equilibrium 0. The 0-equilibrium is assumed to bifurcate in a reversible homoclinic pitchfork bifurcation and we want to analyse bifurcations of homoclinic orbits from Γ. (The precise setting for the problem is described in Section 2.2.)

We first determine suitable manifolds that contain the desired bifurcating orbits. For that we turn to the local bifurcation of 0 and apply centre manifold theory. We find that the local bifurcation can be described in a family of planar reversible and $\mathbb{Z}_2$-symmetric vector fields. Indeed, a straightforward application of the Centre Manifold Theorem [37] yields two-dimensional, locally invariant 'centre manifolds' $W^c_{loc,\lambda}$, that contain all small bifurcating solutions. We will see in Section 2.2.1 that we have to distinguish two generic

cases for the local bifurcation: the *eye case*, which appeared in the numerical example, and the *figure-eight case*.

Furthermore, centre manifold theory associates local stable and unstable manifolds $W_\lambda^{cs(cu)}$ to the centre manifolds. These manifolds can be extended to global manifolds along the primary homoclinic orbit Γ. Our main idea for the analysis is to determine the intersection $W_\lambda^{cs} \cap W_\lambda^{cu}$. In this way we compute homoclinic solutions to $W_{loc,\lambda}^c$, i.e. solutions that are asymptotic to $W_{loc,\lambda}^c$ as $t \to \pm\infty$. Afterwards we analyse the asymptotic behaviour of these solutions in detail.

The first step is accomplished by introducing a cross section Σ to Γ and by studying the traces of $W_\lambda^{cs(cu)}$ in Σ. For this purpose the symmetries of the system and of Γ are essential. It is possible to show that both manifolds have a common tangent space in Σ (Lemma 2.2), and that both manifolds intersect the fixed spaces $\mathrm{Fix}\,(R_1)$ and $\mathrm{Fix}\,(R_2)$ transversally (Lemma 2.9) in Σ. Consequently, we obtain one-parameter families of R_1-symmetric homoclinic orbits and R_2-symmetric homoclinic orbits to $W_{loc,\lambda}^c$, respectively, see Theorem 2.10.

The geometric considerations are backed up by a generalized version of Lin's method. Lin's method has proved to be a powerful tool in the bifurcation analysis of homoclinic orbits to hyperbolic equilibria [66, 75]. We use an adapted version from [57] to deal with the case of homoclinic orbits to nonhyperbolic equilibria. The main technical difference to the analysis for homoclinic orbits to hyperbolic equilibria lies in the circumstance that in the nonhyperbolic situation the variational equation along the homoclinic orbit possesses an exponential trichotomy, instead of an exponential dichotomy. This requires a modified approach.

It turns out that homoclinic orbits which approach 0 at some pre-described exponential rate play a distinguished role in the analysis. We call such orbits *fast decaying*. In Section 2.3.1 it is shown that for each λ there exists a unique fast decaying homoclinic orbit to 0. This perfectly agrees with the robust existence of γ_{hom} in the numerical example f^-. Afterwards we study the existence of homoclinic orbits to W_λ^c in Section 2.3.2. Using the presentation of $W_\lambda^{cs(cu)}$ as graphs over their common tangent space in Σ we derive bifurcation equations of Melnikov-type for the splitting of these manifolds. We remark that the results for homoclinic orbits to $W_{loc,\lambda}^c$ are independent of the type of reversible pitchfork bifurcation of 0.

Having described homoclinic orbits to $W_{loc,\lambda}^c$ we then go on to analyse their asymptotic behaviour in detail. For this we use the invariant foliation of W_λ^{cs} and perform a *projection along stable fibres*, see Section 2.4. This technique allows us to determine which orbits in $W_{loc,\lambda}^c$ are connected by homoclinic or heteroclinic orbits, simply by discussing the bifurcation diagrams in Figure 2.5 for the eye case and Figure 2.6 for the figure-eight case. We derive existence results for homoclinic and heteroclinic orbits to equilibria and periodic orbits. In particular, we prove that in the eye case a reversible homoclinic pitchfork bifurcation occurs, while in the figure-eight case no additional homoclinic orbits to equilibria exist. The results are summarized in the Theorems 2.11 and 2.12.

In principle, the outlined method can also be used to detect N-homoclinic orbits that bifurcate from the primary orbit Γ. This, however, requires to track the manifolds $W_\lambda^{cs(cu)}$ when they pass by the centre manifold $W_{loc,\lambda}^c$.

In Section 2.5 we discuss the bifurcation of two-homoclinic orbits to the centre manifolds $W_{loc,\lambda}^c$. This is accomplished by introducing a second cross section Σ_0 near the equilibrium and investigating intersections of $W_\lambda^{cs(cu)}$ with the fixed spaces $\mathrm{Fix}\,(R_i)$ in Σ_0. We set up a Poincare map which is studied geometrically for the eye case of the local bifurcation. Here two scenarios, which differ in the geometry of $W_\lambda^{cs(cu)}$ in Σ, are possible. For one of the two cases we prove the existence of a family of symmetric two-homoclinic orbits to $W_{loc,\lambda}^c$ 'after' the pitchfork bifurcation in Theorem 2.19. We show in particular that two-heteroclinic orbits between the additional equilibria exist. The difficulties caused by the non-trivial dynamics within $W_{loc,\lambda}^c$ already become apparent in this section.

Other scenarios

In Chapter 3 we continue the study of homoclinic orbits to degenerate equilibria. The investigations in Chapter 2 have concerned the corresponding bifurcation in the class of reversible $\mathbb{Z}_2$-symmetric systems. We now analyse what happens if we consider the homoclinic bifurcation in a purely reversible system.

At first glance answering this seems difficult. We have described above that the symmetries of the system (and the homoclinic orbit) are essential for the analysis in Chapter 2: The fact that W_λ^{cs} is the image of W_λ^{cu} under both involutions R_i is used to prove that W_λ^{cs} (and hence W_λ^{cu}) necessarily intersects both fixed spaces of the involutions transversally, thus giving rise to two one-parameter families of symmetric homoclinic orbits to W_λ^c.

It is clear that there is more freedom for the position of $W_\lambda^{cs(cu)}$ if only one reversing symmetry is present. In particular, we will see that a transverse intersection of these manifolds is no longer forbidden. But in this case the transverse intersection is *generic*. The corresponding non-degeneracy assumption (Hypothesis 3.5) will be the substitute for the additional symmetry in the last section.

It is straightforward to derive bifurcation diagrams for one-homoclinic orbits under this assumption, using the method developed in Chapter 2. Note that in purely reversible systems the local bifurcation of 0 is generically a reversible saddle-centre bifurcation or transcritical bifurcation. We concentrate on the latter case. This is consistent with our interest in the homoclinic bifurcation, in which the associated equilibrium changes its type from real saddle to saddle centre - such a transition cannot occur with a local saddle-centre bifurcation. Furthermore, note that the existence of fast decaying homoclinic orbits in purely reversible systems has to be controlled by a second parameter, such that the bifurcation is of codimension-two.

The details of the analysis are presented in Section 3.3.2. To shorten the presentation we will not employ the analytical machinery of Lin's method as before, but rely on a geometric argumentation. Consequently, we will exclusively consider four-dimensional systems in this part.

The investigations in that chapter are based on a joint paper with Alan Champneys [87]. In Section 3.3 we first discuss bifurcations of homoclinic orbits to degenerate equilibria in purely reversible systems. This part also contains the outline of the geometric approach. The bifurcation scenario is presented in a bifurcation diagram in Figure 3.3 and Theorem 3.3.

Afterwards we return to reversible systems that are additionally $\mathbb{Z}_2$-symmetric, but we assume a different action of the symmetries, compared to Chapter 2. Finally, in Section 3.5, we consider the important class of reversible Hamiltonian systems. It is interesting to note that reversible Hamiltonian systems are not generic in the sense of Chapter 3, since they cannot fulfill the non-degeneracy Hypothesis 3.5. Still, we prove that the bifurcation results for symmetric orbits, obtained before, are necessarily valid in Hamiltonian systems (Theorem 3.7). Nevertheless, additional non-symmetric orbits may bifurcate.

Our studies in Chapter 3 are motivated by a problem for solitary wave solutions of PDE models. In a number of examples a novel kind of solitary waves has been observed recently - so-called *embedded solitons*, see [18] and references therein. In the associated travelling wave system such waves are described by homoclinic orbits to saddle centres. On the other hand, *gap solitons* correspond to homoclinic orbits to real saddles. In this context our studies deal with the question of what happens, if a gap soliton is traced along a family of systems up to some parameter value where it passes over into being an embedded soliton. (Note that both types of homoclinic orbits arise in the bifurcation scenarios we study.) More details about this application are provided in Section 3.6, where the theory is shown to match numerical computations on examples from water-wave theory and nonlinear optics.

1.4. A broom bifurcation of homoclinic bellows

The investigations in Chapter 4 of this thesis concern bifurcations from symmetric homoclinic orbits, in which the associated equilibrium undergoes a transition from a real saddle to a complex saddle focus. Such a transition occurs if the leading real eigenvalues of the equilibrium merge with a second pair of eigenvalues on the real axis and split off into the complex plane. Note that complex eigenvalues of symmetric equilibria in reversible systems necessarily arise in quadruple $\{\mu, -\mu, \bar{\mu}, -\bar{\mu}\}$. Therefore, also this bifurcation can only occur in at least four-dimensional systems. Moreover, the bifurcation is of codimension one, with one parameter needed to control the spectrum of the equilibrium.

We have described before that homoclinic orbits to real saddles are usually accompanied

by simple dynamics. Observe that homoclinic orbits to real saddles can exist in planar reversible systems, where the trivial behaviour near the orbit is obvious. In higher dimensions there exist codimension-one mechanisms, such as the orbit flip [74] or non-elementary homoclinic orbits [34, 59] which can lead to a non-trivial behaviour near the orbit. In the generic situation, however, the planar picture can be recovered with a family of periodic orbits accumulating on the homoclinic orbit [29, 30, 81]. In fact, for a class of reversible and Hamiltonian systems it can be proved that except for this family no bounded solutions exist near the homoclinic orbit [2, 84]. In particular, no N-homoclinic or N-periodic orbits can exist.

The situation is completely different if the homoclinic orbit is asymptotic to a complex saddle focus. In reversible Hamiltonian systems a famous theorem by Devaney [28] implies the existence of shift dynamics near non-degenerate homoclinic orbits to saddle foci, see also [92]. His results imply in particular that such orbits are accompanied by infinitely many N-homoclinic orbits for each $N > 1$ [9]. More recently, Härterich has derived a similar result without relying on an extra Hamiltonian structure in [41]. (Note, however, that for reversible systems - in contrast to the Hamiltonian case - it has not been proved yet that shift-dynamics necessarily occurs near the primary orbit.)

The change in type of the equilibrium hence leads to a dramatic change in the dynamics near the homoclinic orbit and therefore makes it interesting to investigate the corresponding homoclinic bifurcation. We refer to this global bifurcation as *broom bifurcation*, following the notion in [4] where the equivalent bifurcation has been studied in the non-reversible context. For reversible indefinite Hamiltonian systems studies of this bifurcation have been undertaken in [21].

We do not consider the broom bifurcation of a single homoclinic orbit here. Instead we assume that two orbits approach an equilibrium from the same directions as $t \to \infty$ and $t \to -\infty$, respectively. Such a configuration has become known as *homoclinic bellows*, see [3, 47, 46]. In our analysis of the broom bifurcation with a bellows configuration we are again primarily interested in the bifurcation of homoclinic orbits. And again, this interest stems from numerical investigations on the umbilic systems (1.1). Let us conclude this introductory section with a presentation of the corresponding results and with a description of the analysis afterwards.

A bellows configuration in the umbilic systems

A bellows configuration in the umbilic systems can be numerically detected via computations for the heteroclinic cycle $\{\gamma_{het}, R_1\gamma_{het}\}$, connecting the equilibria $\xi_{3,4}$. Theorems A.2 and A.4 show the existence of this cycle for all parameter values where the equilibria are real saddles. It has been an open problem in [88] to describe the maximal range of parameter values for which a cycle exists. Note that the proof of Theorems A.2 and A.4 uses a shooting method developed by Hofer and Toland [44], which implies a certain monotonicity of the detected orbits. Therefore the shooting cannot yield orbits

that are asymptotic to complex saddle foci.

In Section A.3 we demonstrate in a first step that the cycle persists the transition of $\xi_{3,4}$ from real saddles to saddle foci. This is accomplished by showing the cycle to exist because of a *topologically transverse intersection* of the stable and unstable manifolds of $\xi_{3,4}$. Note that topological transversality is weaker than the usual notion of transversality. (A precise definition is included in Section A.3.) Yet, this property allows us to continue the heteroclinic cycle to some region in parameter space where the equilibria $\xi_{3,4}$ are complex saddle foci.

The whole range of parameter values for which the cycle exists has been detected numerically in [58], using standard continuation methods from AUTO/HomCont. Let us describe the procedure for the hyperbolic umbilic f^-. Similar to the numerical analysis in Section 1.3 we can analyse the problem by keeping one of the two parameters constant. This time we set $\beta = -3.5$ and consider f^- under variation of α only.

The continuation has been started at $\alpha = 1$ where $\xi_{3,4}$ are real saddles, as it can be seen in the bifurcation diagram in Figure A.1. The starting solution has been obtained by a period blow-up of a periodic orbit as in Figure 1.1. This solution has been continued with decreasing α, such that the region in parameter space where $\xi_{3,4}$ are complex saddle foci has been reached. It has been found that there exists a bifurcation curve in the saddle foci region, on which the cycle coalesces with another cycle $\{\tilde{\gamma}_{het}, R_1\tilde{\gamma}_{het}\}$ between $\xi_{3,4}$ in a heteroclinic saddle node bifurcation. This occurs for parameter values $\alpha < 0$, $\beta \approx -5.5\alpha^2$.

The heteroclinic bifurcation is not of concern to us here. Instead we focus on the second cycle. It is possible to continue $\{\tilde{\gamma}_{het}, R_1\tilde{\gamma}_{het}\}$ with increasing α until we reach parameter values where $\xi_{3,4}$ become real saddles again, i.e. close to $\alpha = 0.92$. A plot of the orbit $\tilde{\gamma}_{het}$ for this parameter value is shown in Figure 1.4.

The orbit $\tilde{\gamma}_{het}$ in Figure 1.4 is composed of 'homoclinic loops' near the equilibria and of a 'heteroclinic part' in the middle. These parts have already appeared separately in this thesis. To see this consider Figure 1.5, where different orbits that have been computed for $\alpha = 0.92$, $\beta = -3.5$ are shown. The diagram shows a plot of the heteroclinic orbit γ_{het} and, in addition, plots of the homoclinic orbits that emerge in the reversible homoclinic pitchfork bifurcation of γ_{hom}. (Note that this bifurcation occurs for $\alpha = 1.08$, $\beta = -3.5$.) The similarity to Figure 1.4 is obvious. In fact, it is possible to continue the separate parts of $\tilde{\gamma}_{het}$ as orbits themselves, and these orbits show the same behaviour as γ_{het} and the respective homoclinic orbits.

We can summarize the results as follows. For parameter values $\beta = -4\alpha^2$, $\alpha > 0$ the equilibria $\xi_{3,4}$ are connected by a heteroclinic cycle. Furthermore, there exists a homoclinic orbit to each of the equilibria and all orbits approach the equilibria in the weak stable direction. We also refer to this formation as a bellows configuration, although both homoclinic and heteroclinic orbits belong to it. (We discuss below that heteroclinic cycles between $\xi_{3,4}$ can be viewed as homoclinic orbits if one chooses an appropriate phase

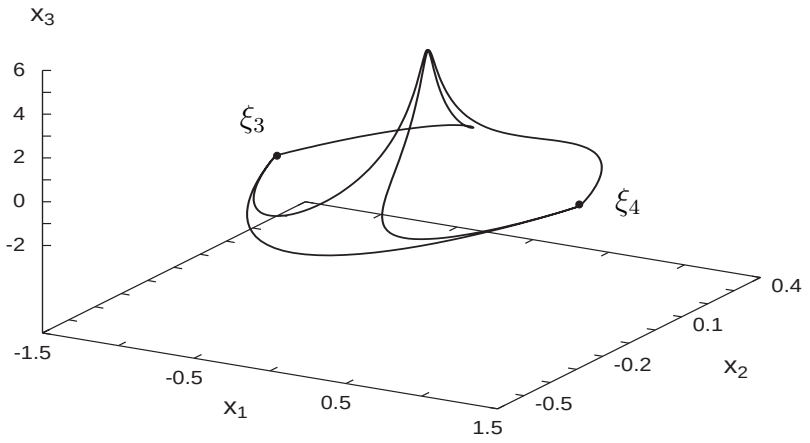

Figure 1.4.: Plot of the orbit $\tilde{\gamma}_{het}$ of f^- for $\alpha = 0.92$, $\beta = -3.5$ in (x_1, x_2, x_3)-space.

space.) Finally, if the parameters are varied such that $\xi_{3,4}$ become complex saddle foci, there emerges a second heteroclinic cycle $\{\tilde{\gamma}_{het}, R_1\tilde{\gamma}_{het}\}$ which is composed of parts of both primary orbits.

Let us discuss this further. We have described before that homoclinic orbits to complex saddle foci are generically accompanied by a plethora of N-homoclinic orbits. Therefore one would expect that such a plethora exists near the homoclinic orbits to $\xi_{3,4}$, if $\xi_{3,4}$ are complex saddle foci. Similarly, there should exist N-homoclinic and N-heteroclinic orbits near the heteroclinic cycle. The numerical results now suggest that in addition there exist orbits that follow the homoclinic and heteroclinic orbits in the bellows configuration alternately. And even more so, these orbits emerge in the broom bifurcation for parameter values $\beta = -4\alpha^2$, $\alpha > 0$.

Similar to the last section we aim at an analytical understanding of this observation. Nevertheless, there is a difference. Our results in Chapter 2 imply that the reversible homoclinic pitchfork bifurcation necessarily occurs in (1.1), i.e. we can *prove* the numerical results. This time the analysis will rely on genericity assumptions that have not been verified for the umbilic systems. In particular, we assume all connecting orbits to be non-degenerate. Therefore the analysis will support the numerics, but does not yield rigorous results. We return to this point in Section 4.4.

Before starting the analysis it is convenient to use a little trick which allows us to unify the treatment of heteroclinic and homoclinic orbits in the present case. This can be achieved by factoring out the $\mathbb{Z}_2$-symmetry of the system and working in *orbit space*, i.e.

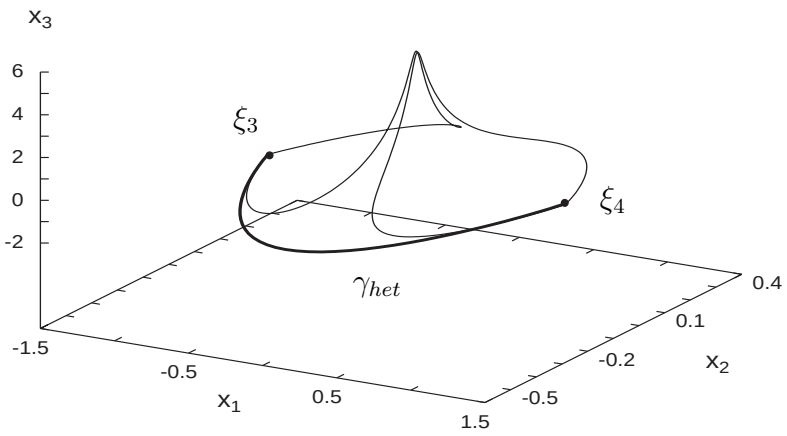

Figure 1.5.: Plots of the orbit γ_{het} (thick) and the one-homoclinic orbits (regular) that emerge in the reversible homoclinic pitchfork bifurcation. The orbits have been computed at the same parameter values as in Figure 1.4.

in the space of orbits of the system's symmetry group $\{id, S\}$. This symmetry reduction is performed explicitly for (1.1) in Section A.2.3 in the appendix. The reduced vector field in orbit space is still reversible. The equilibria ξ_3 and $\xi_4 = S\xi_3$ correspond to the same equilibrium $\hat{\xi}$. Hence, both homoclinic and heteroclinic orbits of the original system are described by homoclinic orbits of the reduced systems. In particular, the bellows structure of the heteroclinic cycle and homoclinic orbits now becomes a bellows of two symmetric homoclinic orbits. Our general analysis will therefore concern reversible systems possessing a homoclinic bellows.

Remark 1.2. Note that the reduction in general leads to a loss of smoothness. In fact, the reduced vector field in orbit space is smooth except for points in $\mathrm{Fix}\,(S)$. But these points are not of interest for us, since $\mathrm{Fix}\,(S)$ is an invariant subspace of the original system. Thus, orbits which are asymptotic to $\xi_{3,4} \notin \mathrm{Fix}\,(S)$ cannot visit this space.

The analysis

We describe the setting for the general analysis in Section 4.2. As explained before we are concerned with homoclinic bellows in reversible systems, and we assume that the associated equilibrium undergoes a transition from real saddle to complex saddle focus. This transition can be achieved by considering one-parameter families of reversible ODEs. The corresponding parameter will be introduced by deriving a suitable linear

normal form for the equilibrium.

The analysis of the global bifurcation relies on Lin's method. In the present case we are concerned with homoclinic orbits to a hyperbolic equilibrium and it is therefore straightforward to derive bifurcation equations for homoclinic orbits near the primary ones, using general results from [75]. General technical considerations are quoted briefly.

In Section 4.4 we solve the bifurcation equations and discuss the bifurcation scenario for N-homoclinic orbits. We prove that beside the homoclinic bellows no homoclinic orbits exist if the equilibrium is a real saddle. This confirms results in [34, 46].

If the equilibrium is a complex saddle focus, then there exist infinitely many homoclinic orbits near the bellows configuration. More precisely, let Γ_1 ,Γ_2 denote the homoclinic orbits in bellows configuration. To an N-homoclinic orbit we can associate a sequence of N-numbers $\kappa = (\kappa_j) \in \{1, 2\}^N$, that denote the order in which the orbit follows Γ_1, Γ_2. The sequence κ is called *symmetric*, if $\kappa_{N+1-j} = \kappa_j$ for all $j = 1, \ldots, N$. We prove that for each N and for any symmetric sequence κ of length N, there exist infinitely many N-homoclinic orbits which follow the bellows structure according to κ (Theorem 4.6).

CHAPTER 2

The reversible homoclinic pitchfork bifurcation

2.1. Introduction

The main part of the thesis is dedicated to the study of homoclinic orbits to degenerate equilibria. In this chapter we consider reversible and $\mathbb{Z}_2$-symmetric ODEs that possess a homoclinic orbit Γ to an equilibrium which itself undergoes a homoclinic pitchfork bifurcation. We are interested in bifurcations from the primary homoclinic orbit.

In the next section we introduce the general setting for the problem in detail. The local bifurcation of the equilibrium is described via centre manifold reduction. We have to distinguish two cases for the local bifurcation that differ in the sign of a third order term in the equilibrium's normal form. We also introduce suitable 'centre manifolds' $W^c_{loc,\lambda}$ and 'centre (un)stable' manifolds $W^{cs(cu)}_\lambda$.

In Section 2.3 we study the intersection $W^{cs}_\lambda \cap W^{cu}_\lambda$ in some suitable cross section to describe homoclinic orbits to $W^c_{loc,\lambda}$ (Theorem 2.10). This is accomplished by a generalized version of Lin's method. Afterwards we use the invariant foliation of W^{cs}_λ to study the asymptotic behaviour of the detected homoclinic orbits in Section 2.4. We obtain a complete description of bifurcating one-homoclinic orbits to $W^c_{loc,\lambda}$ in Theorems 2.11 and 2.12. In particular, we find excellent agreement of the general analysis with the numerical studies in Section 1.3.

These parts of the chapter are based on the article [90].

In the final Section 2.5 we investigate bifurcating two-homoclinic solutions. We locate R_2-symmetric two-homoclinic solutions by studying intersections of W^{cs}_λ with $\mathrm{Fix}\,(R_2)$ near 0. This requires a detailed analysis of the behaviour near $W^c_{loc,\lambda}$. In one possible scenario for the reversible homoclinic pitchfork bifurcation Theorem 2.19 shows the existence of a one-parameter family of two-homoclinic orbits to $W^c_{loc,\lambda}$ for parameter

values where three equilibria exist. This family contains in particular two-heteroclinic orbits to the additional equilibria.

2.2. Basic assumptions and conclusions

Throughout this part we consider a family of ODEs

$$\dot{x} = f(x, \lambda), \quad (x, \lambda) \in \mathbb{R}^{2n+2} \times \mathbb{R} \tag{2.1}$$

with a smooth vector field f and λ as a real parameter. The attribute smooth here means C^∞ or C^k with k sufficiently large. We assume the system to be *reversible* and $\mathbb{Z}_2$-*symmetric*, more precisely we assume

Hypothesis 2.1. There exist linear involutions $R_i : \mathbb{R}^{2n+2} \to \mathbb{R}^{2n+2}$, $i = 1, 2$ with $\dim(\mathrm{Fix}\,(R_i)) = n + 1$ and with $R_1 R_2 = R_2 R_1$, such that

$$R_i f(x, \lambda) + f(R_i x, \lambda) = 0 \quad \forall (x, \lambda), \quad i = 1, 2.$$

Of course, we assume R_1, R_2 to be distinct (see Hypothesis 2.2 below for a detailed statement). In the same way as for the umbilic systems (1.1), Hypothesis 2.1 implies a $\mathbb{Z}_2$-symmetry for (2.1), namely with $S := R_1 R_2$ we have

$$S f(x, \lambda) - f(Sx, \lambda) = 0 \quad \forall (x, \lambda). \tag{2.2}$$

In particular this equality shows that the space $\mathrm{Fix}\,(S) := \{x : Sx = x\}$ is an invariant subspace for (2.1). It is an immediate consequence from Hypothesis 2.1 that within this space the involutions R_i agree, i.e.

$$R_1 \big|_{\mathrm{Fix}(S)} = R_2 \big|_{\mathrm{Fix}(S)} =: R_S.$$

Furthermore, when equation (2.1) is reduced to $\mathrm{Fix}\,(S)$, the system is reversible with respect to R_S.

Remark 2.1. In [65] Lamb has introduced the concept of *reversing symmetry groups*. Using this formal notion we can reformulate Hypothesis 2.1 by saying that equation (2.1) possesses the *reversing symmetry group* $G := \{I, R_1, R_2, S\}$. It is important to note that G is finite and therefore we can introduce an inner product in $\mathbb{R}^{2n+2}$ such that each element of G is self-adjoint.

Let us discuss a further property associated to the reversing symmetry group of (2.1). In the following we will often use the fact that

$$R_i(\mathrm{Fix}\,(\pm R_j)) \subset \mathrm{Fix}\,(\pm R_j), \quad i, j \in \{1, 2\}. \tag{2.3}$$

This is obvious for $i = j$. For $i \neq j$ let us choose $x \in \mathrm{Fix}\,(R_1)$. (The arguments for the other cases are the same.) Then

$$R_1(R_2x) = R_2R_1x = R_2x,$$

and therefore $R_2x \in \mathrm{Fix}\,(R_1)$, also. (Note that in (2.3) we even have equality since the R_i are bijective maps.)

2.2.1. Assumptions about the equilibrium

Our main interest lies in bifurcations of a global object, namely a homoclinic orbit. But first we deal with the associated equilibrium and describe its local bifurcation. We assume the following.

Hypothesis 2.2. Let $f(0,0) = 0$ and assume that

$$\sigma(D_1f(0,0)) = \{0\} \cup \{\pm\mu\} \cup \sigma^{ss} \cup \sigma^{uu},$$

with 0 being a double, non-semisimple eigenvalue. Furthermore let $\mu \in \mathbb{R}^+$, and let $|\Re(\tilde{\mu})| > \mu \ \forall \tilde{\mu} \in \sigma^{ss} \cup \sigma^{uu}$. Here $\sigma^{ss(uu)}$ denotes the strong stable (strong unstable) spectrum of $D_1f(0,0)$.

Thus, 0 is an R_i-symmetric equilibrium (i=1,2) which, in particular, implies

$$R_iD_1f(0,0) + D_1f(0,0)R_i = 0.$$

Therefore, $D_1f(0,\lambda)$ is an R_i-reversible linear operator, and so its spectrum is symmetric with respect to zero (in the complex plane). We conclude, that Hypothesis 2.2 describes equilibria which generically occur in one-parameter families of reversible vector fields, see also [64].
In order to study the local bifurcation of 0 we first distinguish the involutions R_i. For this let $X^c_{\lambda=0}$ denote the centre subspace of $D_1f(0,0)$. Observe that $X^c_{\lambda=0}$ is invariant under the action of the involutions R_i, $i = 1, 2$. We want to study the situation when the involutions act differently (and non-trivially) on $X^c_{\lambda=0}$ and demand

Hypothesis 2.3. $X^c_{\lambda=0} \not\subset \mathrm{Fix}\,(\pm R_i)$ for $i = 1, 2$, and $X^c_{\lambda=0} \cap \mathrm{Fix}\,(S) = \{0\}$.

For the description of the local bifurcation of 0 we apply centre manifold theory and perform a reduction of the local problem to a family of two-dimensional reversible vector fields. For this purpose, let us consider the extended system

$$\begin{aligned} \dot{x} &= f(x,\lambda) \\ \dot{\lambda} &= 0. \end{aligned} \tag{2.4}$$

Owing to Hypothesis 2.2 this system possesses the equilibrium $(0,0)$ with a 3-dimensional local centre manifold $\mathfrak{W}^c_{loc}$ at $(0,0)$. This manifold is foliated into two-dimensional invariant slices $\{\lambda = const.\}$ which we denote by $W^c_{loc,\lambda}$. Now, the Centre Manifold Theorem [82, 37] shows that all small bounded solutions of (2.4) are contained in $\mathfrak{W}^c_{loc}$ which means that for (2.1) we can follow the evolution of small bifurcating solutions within the two-dimensional slices $W^c_{loc,\lambda}$. Similarly, the manifolds $W^{cs(cu)}_{loc,\lambda}$, $W^{s(u)}_{loc,\lambda}$ are defined as slices of the local centre (un)stable $\mathfrak{W}^{cs(cu)}_{loc}$ and (un)stable manifold $\mathfrak{W}^{s(u)}_{loc}$ of $(0,0)$ in (2.4).

Remark 2.2. Later we will deal with the globalized versions of the local manifolds $W^{cs(cu)}_{loc,\lambda}$, $W^{s(u)}_{loc,\lambda}$ and we will denote them by dropping the *loc*-index. Note that the manifolds $W^{cs(cu)}_{\lambda}$ are stable and unstable manifolds for $W^c_{loc,\lambda}$, respectively. By a slight abuse of language we will, for instance, also refer to the slices W^{cs}_{λ} as centre stable manifolds.

The centre stable, centre unstable and centre manifolds are not unique, in general. The next lemma shows that they can be chosen, such that the symmetries of (2.1) are preserved.

Lemma 2.1. *The manifolds $W^{cs}_{loc,\lambda}$, $W^{cu}_{loc,\lambda}$ can be chosen such that $W^{cs}_{loc,\lambda} = R_i W^{cu}_{loc,\lambda}$, $i = 1, 2$.*

Proof. We consider (2.4), which is easily seen to possess the reversing symmetry group $\mathfrak{G} := \{\mathfrak{I}, \mathfrak{R}_1, \mathfrak{R}_2, \mathfrak{S}\}$, where

$$\mathfrak{R}_i := \begin{pmatrix} R_i & 0 \\ 0 & 1 \end{pmatrix}$$

and $\mathfrak{S} = \mathfrak{R}_1\mathfrak{R}_2$. The key argument of the proof is that we can choose $\mathfrak{W}^{cs(cu)}_{loc}$ such that $\mathfrak{R}_i\mathfrak{W}^{cs}_{loc} = \mathfrak{W}^{cu}_{loc}$. In fact, this is a standard result for systems that are reversible with respect to *one* involution, [49] or for systems symmetric with respect to a compact symmetry group, [25]. The corresponding proofs can easily be generalized to the case of a compact reversing symmetry group. The symmetry properties of the corresponding slices $W^{cs(cu)}_{loc,\lambda}$ are then apparent. □

For later considerations it is useful to further simplify equation (2.1) around 0. Let $\mathfrak{X}^{cs(cu)}$ denote the centre stable (centre unstable) subspace of the linearization at (0,0) in (2.4). We can then assume that

$$\mathfrak{W}^{cs(cu)}_{loc} \subset \mathfrak{X}^{cs(cu)}.$$

In fact, there exists a transformation $\mathfrak{T}$ which pushes the manifolds into their respective subspaces, and moreover $\mathfrak{T}$ can be chosen such that the symmetries of (2.4) are preserved, since $\mathfrak{G}$ is a compact reversing symmetry group. See for instance [57] for a computation of $\mathfrak{T}$. Now setting $\mathfrak{W}^c_{loc} := \mathfrak{W}^{cs}_{loc} \cap \mathfrak{W}^{cu}_{loc}$ we obtain a 'flat' centre manifold for (2.4) and

by Lemma 2.1 we have $\mathfrak{R}_i\mathfrak{W}^c_{loc} = \mathfrak{W}^c_{loc}$ for $i = 1, 2$. Finally, for the invariant slices we conclude that

$$W^{cs(cu)}_{loc,\lambda} \subset X^{cs(cu)}_{\lambda}, \tag{2.5}$$

where $X^{cs(cu)}_{\lambda}$ denote the corresponding slices of the linear spaces $\mathfrak{X}^{cs(cu)}$, and moreover that $R_i W^c_{loc,\lambda} = W^c_{loc,\lambda}$ for $i = 1, 2$.
An immediate consequence of Lemma 2.1 and the considerations below is that the vector field in $W^c_{loc,\lambda}$ is also reversible with respect to two distinct involutions. Let us denote the corresponding system by

$$\dot{y} = g(y, \lambda). \tag{2.6}$$

Hypothesis 2.2 yields

$$g(0,0) = 0, \quad D_1 g(0,0) = \begin{pmatrix} 0 & 1 \\ 0 & 0 \end{pmatrix},$$

and in suitably chosen coordinates we find the following normal form for the corresponding involutions R_i

$$R_1 : y := (y_1, y_2) \mapsto (y_1, -y_2), \quad R_2 : (y_1, y_2) \mapsto (-y_1, y_2).$$

The bifurcation of the equilibrium 0 of (2.6) can be studied in a planar normal form of the vector field. More precisely, results by Dumortier [33] demonstrate that equilibria of finite codimension are *finitely determined* in planar systems. This means that for the study of local bifurcations one might always restrict to consider only polynomial systems. Hence, it suffices to deal with normal forms which can in addition be chosen such that the symmetries of the original system are preserved. In the present case this normal form is given in [65, 64] and reads

$$\begin{aligned} \dot{y}_1 &= y_2 \\ \dot{y}_2 &= \sum_{k \ odd} a_k(\lambda) y_1^k. \end{aligned} \tag{2.7}$$

By Hypothesis 2.2 we have $a_1(0) = 0$ in (2.7) and we consider a generic bifurcation by demanding

Hypothesis 2.4. $a_3(0) \neq 0$.

Depending on the sign of $a_3(0)$ we are led to two unfoldings of the corresponding singular systems. If $a_3(0) > 0$ we obtain

$$\begin{aligned} \dot{y}_1 &= y_2 \\ \dot{y}_2 &= \lambda y_1 + y_1^3. \end{aligned} \tag{2.8}$$

Note that we have neglected terms of order larger than three in (2.8). These terms do not influence the qualitative local behaviour of the systems since (2.8) describes a universal

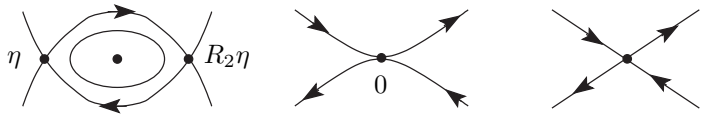

Figure 2.1.: Phase portraits in for the reversible pitchfork bifurcation I: The eye case with normal form (2.8).

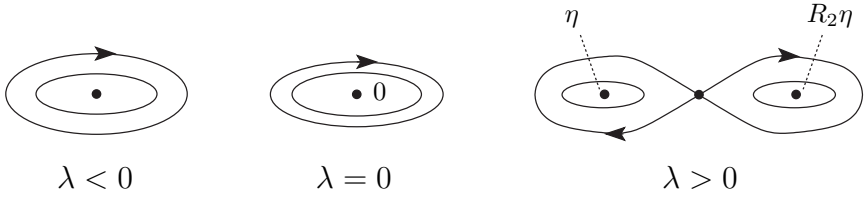

Figure 2.2.: Phase portraits for the reversible pitchfork bifurcation II: The figure-eight case with normal form (2.9).

unfolding of the singularity, see again [64]. We remark that the normal form for the reversible problem (2.6) possesses the additional property of being Hamiltonian.

System (2.8) is easily analysed and it is straightforward to derive the corresponding phase portraits in Figure 2.1. Here we find the situation that was encountered for the illustrating example in Section 1.3. For $\lambda < 0$ there exist two additional equilibria $\eta = (-\sqrt{-\lambda}, 0)$, $R_2\eta = (\sqrt{-\lambda}, 0)$ which are saddles while 0 has turned from a real saddle (for $\lambda > 0$) into a centre. Moreover, we find a (small) symmetric heteroclinic cycle between $\eta, R_2\eta$. As before we refer to this bifurcation scenario as the *eye case*.

If $a_3(0) < 0$ a universal unfolding is given by

$$\begin{aligned} \dot{y}_1 &= y_2 \\ \dot{y}_2 &= \lambda y_1 - y_1^3. \end{aligned} \tag{2.9}$$

The phase portraits can be found in Figure 2.2. For $\lambda > 0$ the additional equilibria $\eta = (-\sqrt{\lambda}, 0)$, $R_2\eta = (\sqrt{\lambda}, 0)$ are centres in this case and the equilibrium at 0 has become a saddle which is connected to itself by two homoclinic orbits. Therefore we name this scenario the *figure-eight case*.

Remark 2.3. The local bifurcation of 0 leads to the existence of a symmetric hyperbolic equilibrium, and therefore the dimension of $\mathrm{Fix}\,(R_i)$ is necessarily half the dimension of phase space [81]. This explains our general definition of reversibility in the first chapter, see also Hypothesis 2.1. Moreover, the same argument shows that the space $\mathrm{Fix}\,(S)$ must be even-dimensional.

The parameter λ was chosen to control the local bifurcation of the equilibrium 0. Since, however, we are interested in the bifurcation of a homoclinic orbit one would expect at a first sight that this requires additional parameters. But in the next section we will assume sufficient transversality conditions for the homoclinic orbit which ensure the problem to be of codimension one.

2.2.2. Assumptions about the homoclinic orbit

Let us now describe the homoclinic orbit which will be of concern in the following.

Hypothesis 2.5. For $\lambda = 0$ equation (2.1) possesses a solution $\gamma(\cdot)$ homoclinic to 0, that is,

$$\lim_{t\to\pm\infty} \gamma(t) = 0.$$

The corresponding orbit $\Gamma := \{\gamma(t) : t \in \mathbb{R}\}$ is symmetric with respect to both R_1 and R_2.

The R_1-symmetry of Γ implies that the orbit intersects the fixed space $\mathrm{Fix}\,(R_1)$ in some point, say $\gamma(0)$. Moreover, by Lemma 3 in [81] this point is unique. Since $R_2\gamma(0) \in \mathrm{Fix}\,(R_1)$ by (2.3) we thus obtain $\gamma(0) \in \mathrm{Fix}\,(R_2)$, as well. This implies $\gamma(0) \in \mathrm{Fix}\,(S)$ and the invariance of $\mathrm{Fix}\,(S)$ shows

$$\Gamma \subset \mathrm{Fix}\,(S).$$

This trivially shows $\mathrm{Fix}\,(S) \neq \{0\}$ and thus $\dim(\mathrm{Fix}\,(S)) \geq 2$.
From Hypothesis 2.2 we can immediately conclude that the orbit Γ is a global object which lies in the intersection of $W^s_{\lambda=0}$ and $W^u_{\lambda=0}$.

Remark 2.4. The considerations show in particular that Γ does not approach the origin at the lowest possible speed. Generically, such a situation results in a reversible orbit flip bifurcation, see [74]. Here, however, this behaviour is forced by the symmetries of Γ and the forthcoming analysis proves that no orbit flip bifurcation occurs.

Let us impose a transversality condition upon the homoclinic orbit Γ. In order to consider a generic situation we assume that at $\lambda = 0$ the stable manifold of 0 intersects the centre unstable manifold as cleanly as possible. More precisely, for $\lambda = 0$ we denote the tangent space of the (un)stable manifold of 0 at the point $\gamma(0)$ by $T_{\gamma(0)}W^{s(u)}_{\lambda=0}$ and demand

Hypothesis 2.6. We have

$$\dim(T_{\gamma(0)}W^s_{\lambda=0} \cap T_{\gamma(0)}W^{cu}_{\lambda=0}) = 1.$$

We note that this assumption is automatically fulfilled in $\mathbb{R}^4$, since in this case the stable manifold of the equilibrium 0 is one-dimensional.

Hypothesis 2.6 has important consequences for the dynamics near Γ. Let us first consider the situation within the invariant subspace $\mathrm{Fix}\,(S)$. Here the equilibrium 0 is hyperbolic and moreover, the trace of the centre unstable manifold $W^{cu}_{\lambda=0}$ is the unstable manifold W^u_S of this equilibrium. This immediately follows from $\mathrm{Fix}\,(S) \cap W^c_{loc,\lambda} = \{0\}$, because of Hypothesis 2.4. Thus, under Hypothesis 2.6 the intersection of W^u_S and W^s_S along Γ only contains the vector field direction, i.e. the orbit is *non-degenerate* within $\mathrm{Fix}\,(S)$. As a consequence, we find that the intersection of W^u_S and $\mathrm{Fix}\,(R_S)$ is transverse, see Lemma 4 in [81]. (Recall that R_S is the restriction of the R_i to $\mathrm{Fix}\,(S)$.) This point will be of importance in the proof of Lemma 2.2 below.

In the next section we determine one-homoclinic orbits to $W^c_{loc,\lambda}$ by investigating the intersection of W^{cs}_λ and W^{cu}_λ. Related studies in [57] reveal that the results crucially depend on the relative position of the tangent spaces of the centre (un)stable manifold and the fixed spaces of the involutions. Due to the symmetries of our problem we can determine this position (see Lemmas 2.2 and 2.9 below). As a first result in this context we obtain

Lemma 2.2. *Under the assumptions above the intersection of $W^{cs}_{\lambda=0}$ and $W^{cu}_{\lambda=0}$ along Γ is non-transverse with*

$$\dim\left(T_{\gamma(0)}W^{cs}_{\lambda=0} \cap T_{\gamma(0)}W^{cu}_{\lambda=0}\right) = 3.$$

Proof. First observe that it suffices to prove the non-transversality of the intersection of the manifolds. The second assertion can then be obtained by a simple count of dimensions and consideration of Hypothesis 2.6.

Seeking a contradiction, let us assume that the intersection of $W^{cs(cu)}_{\lambda=0}$ is transverse and let us introduce a space Y^c by setting

$$\mathrm{span}\{f(\gamma(0),0)\} \oplus Y^c := T_{\gamma(0)}W^{cs}_{\lambda=0} \cap T_{\gamma(0)}W^{cu}_{\lambda=0}.$$

(Here, all appearing decompositions are assumed to be orthogonal with respect to the R_i-invariant inner product.) Since $\dim W^{cs(cu)}_{\lambda=0} = n+2$ we have $\dim Y^c = 1$. Another count of dimensions reveals

$$\dim\left(T_{\gamma(0)}W^{cs}_{\lambda=0} \cap \mathrm{Fix}\,(R_i)\right) = 1,$$

for $i = 1, 2$. By reversibility components of $T_{\gamma(0)}W^{cs}_\lambda$ that are contained in $\mathrm{Fix}\,(R_i)$ also belong to $T_{\gamma(0)}W^{cu}_\lambda$, and therefore $Y^c \subset \mathrm{Fix}\,(R_1) \cap \mathrm{Fix}\,(R_2)$, i.e. we have $Y^c \subset \mathrm{Fix}\,(S)$. We will show that this is impossible because of Hypothesis 2.6. For this introduce a space $\widetilde{Y}^{cs}$ by letting

$$T_{\gamma(0)}W^{cs}_{\lambda=0} = \mathrm{span}\{f(\gamma(0),0)\} \oplus Y^c \oplus \widetilde{Y}^{cs}.$$

An important observation is that

$$R_1\widetilde{Y}^{cs} = R_2\widetilde{Y}^{cs}. \tag{2.10}$$

In fact, since the spaces $T_{\gamma(0)}W^{cs}_{\lambda=0}$ and $\operatorname{span}\{f(\gamma(0),0)\}\oplus Y^c$ are invariant under S this also applies to $\widetilde{Y}^{cs}$, i.e. we have $S\widetilde{Y}^{cs} = \widetilde{Y}^{cs}$. In particular, $R_1R_2\widetilde{Y}^{cs} = R_1R_1\widetilde{Y}^{cs}$, and this yields (2.10). So we can similarly decompose

$$T_{\gamma(0)}W^{cu}_{\lambda=0} = \operatorname{span}\{f(\gamma(0),0)\}\oplus Y^c\oplus\widetilde{Y}^{cu},$$

with $\widetilde{Y}^{cu} := R_i\widetilde{Y}^{cs}$.
We can represent the manifolds $W^{cs(cu)}_{\lambda=0}$ near $\gamma(0)$ as graphs of functions

$$h^{cs(cu)} : \operatorname{span}\{f(\gamma(0),0)\}\oplus Y^c\oplus\widetilde{Y}^{cs(cu)} \to \widetilde{Y}^{cu(cs)},$$

with $Dh^{cs(cu)}(0) = 0$. Choosing $(y_c, h^{cu}(y_c)) \in W^{cu}$ with $y_c \in Y^c \subset \operatorname{Fix}(S)$ we have

$$R_1(y_c, h^{cu}(y_c)) \in W^{cs}, \quad R_2(y_c, h^{cu}(y_c)) \in W^{cs}$$

and thus $R_1h^{cu}(y_c) = R_2h^{cu}(y_c)$, wherefore $(y_c, h^{cu}(y_c)) \in \operatorname{Fix}(S)$.
Thus, we can again consider the reduced system within $\operatorname{Fix}(S)$. We recall that this system is R_S-reversible, and as above we denote the unstable manifold of the (hyperbolic) equilibrium 0 by W^u_S. Then $W^u_S = W^{cu}_{\lambda=0}\cap\operatorname{Fix}(S)$, and a consequence of our considerations is that W^u_S intersects $\operatorname{Fix}(R_S)$ non-transversally. Indeed, letting $\dim\operatorname{Fix}(S) = 2k$ (recall that because of reversibility $\operatorname{Fix}(S)$ is even-dimensional) we have

$$\dim T_{\gamma(0)}W^u_S = \dim\operatorname{Fix}R_S = k,$$

and since $y_c \in \operatorname{Fix}(R_1)\cap\operatorname{Fix}(R_2)$ the above considerations yield

$$\dim\left(T_{\gamma(0)}W^u_S\cap\operatorname{Fix}R_S\right) \geq 1.$$

But as it has already been discussed before, Hypothesis 2.6 implies a transverse intersection of W^u_S and $\operatorname{Fix}(R_S)$. So we derive the desired contradiction. □

2.3. One-homoclinic orbits to the centre manifolds

The goal of the following analysis is the description of bifurcating homoclinic orbits to the centre-manifolds $W^c_{loc,\lambda}$ introduced in the last section. For that we will study the intersection of W^{cs}_λ and W^{cu}_λ in some cross section Σ to the primary homoclinic orbit Γ. The splitting of these manifolds will be described by Melnikov-like computations. We only consider one-homoclinic orbits in the following which means that we are only

concerned with the first intersections of $W_\lambda^{cs(cu)}$ with Σ. (Note that parts of these manifolds may visit Σ many times.)

Our approach is inspired by a technique known as Lin's method [66, 75, 81], see also Chapter 4. The original version of this method allows one to study the dynamics near orbits connecting hyperbolic equilibrium solutions by defining bifurcation equations for recurrent dynamics near the orbits. Since we deal here with a homoclinic orbit to a degenerate equilibrium we use a generalization of Lin's method, similar to the one developed in [57]. Although our procedure is comparable to [57] we include some technical details for the sake of self-containment of the forthcoming parts of the thesis. The consideration of one-homoclinic orbits here corresponds to the 'first step' of the original version of Lin's method. The spirit of the analysis is also similar to [83].

We first remind the reader that we have chosen $\gamma(0) \subset \mathrm{Fix}\,(R_1) \cap \mathrm{Fix}\,(R_2)$. At this point we introduce a cross-section Σ to Γ by decomposing

$$\mathbb{R}^{2n+2} = \mathrm{span}\{f(\gamma(0),0)\} \oplus Y^s \oplus Y^u \oplus Z$$

with $\mathrm{span}\{f(\gamma(0),0)\} \oplus Y^{s(u)} = T_{\gamma(0)} W^{s(u)}$ and setting

$$\Sigma := \gamma(0) + \{Y^s \oplus Y^u \oplus Z\}.$$

Again, we stress the fact that this decomposition is assumed to be orthogonal with respect to an R_i-invariant inner product. Note that Z is complementary to the sum of the tangent spaces of the stable and unstable manifolds of 0. Therefore Hypothesis 2.6 implies $\dim Z = 3$. Using Lin's method we will eventually detect one-homoclinic orbits by solving a bifurcation equation in Z.

Let us discuss how the symmetries of (2.1) are reflected in this decomposition. Recall that $\dim(\mathrm{Fix}\,(R_i)) = \dim(\mathrm{Fix}\,(-R_i)) = n+1$. Now, using $R_i W^s = W^u$, and therefore $R_i Y^s = Y^u$ for $i = 1, 2$ we obtain the equivalent of Lemma 2.4 and Lemma 2.5 in [57].

Lemma 2.3. *The space $Y^s \oplus Y^u$ contains $(n-1)$-dimensional subspaces of both $Fix(R_i)$ and $Fix(-R_i)$ for each $i = 1, 2$. The space Z contains a two-dimensional subspace Y_i of $Fix(R_i)$ and a one-dimensional subspace of $Fix(-R_i)$ for each $i = 1, 2$.*

Even more so, we have $Y_1 \neq Y_2$, because assuming $Y_1 = Y_2$ we can conclude $Z \subset \mathrm{Fix}\,(S)$. Within the invariant subspace $\mathrm{Fix}\,(S)$, however, Hypothesis 2.6 implies that Γ is a non-degenerate orbit homoclinic to the hyperbolic equilibrium 0. Since Z is complementary to the sum of the tangent spaces of the corresponding stable and unstable manifold we must have $\dim Z = 1$ in contradiction to the above.

An immediate consequence of this observation is the next lemma.

Lemma 2.4. *For Z there exists a decomposition into one-dimensional subspaces X_i*

$$Z = X_1 \oplus X_2 \oplus X_3, \tag{2.11}$$

where $X_1 \subset Fix(R_1) \cap Fix(-R_2)$, $X_2 \subset Fix(-R_1) \cap Fix(R_2)$, $X_3 \subset Fix(R_1) \cap Fix(R_2)$.

Proof. We first consider the situation in $\Sigma \cap \mathrm{Fix}\,(S)$. We recall again, that here the one-dimensional space $Z \cap \mathrm{Fix}\,(S)$ is complementary to the sum of the tangent spaces of the stable and unstable manifolds of 0. Since Γ is non-degenerate in $\mathrm{Fix}\,(S)$ we know from [81] that

$$(Z \cap \mathrm{Fix}\,(S)) \subset (\mathrm{Fix}\,(R_1) \cap \mathrm{Fix}\,(R_2)),$$

which shows the existence of X_3.
Now let $X_1 := Z \cap \mathrm{Fix}\,(-R_2)$. Then by Lemma 2.3 it holds $\dim X_1 = 1$. Moreover, by (2.3) we have $R_1 X_1 \subset X_1$ and thus, either $X_1 \subset \mathrm{Fix}\,(R_1)$ or $X_1 \subset \mathrm{Fix}\,(-R_1)$; and the second possibility is excluded because it would imply $X_1 \subset \mathrm{Fix}\,(S)$ in contradiction to $\dim Z \cap \mathrm{Fix}\,(S) = 1$ and $X_1 \cap X_3 = \{0\}$. In a similar manner we obtain the assertion for X_2. □

In a first step of Lin's method we look for one-homoclinic orbits to the origin. Now the non-hyperbolicity of the equilibrium comes into play in that we have to distinguish between two kinds of such orbits, namely *fast decaying* and *slowly decaying* solutions.

2.3.1. Fast decaying homoclinic orbits to the origin

Following Lin's method for connecting orbits between hyperbolic equilibria we would look for solutions $\gamma^{\pm}$ of (2.1) defined on $\mathbb{R}^{\pm}$ which start in Σ with a difference lying in a certain space and which approach 0 for $t \to \pm\infty$. In our case, however, 0 is degenerate for $\lambda = 0$. It turns out to be appropriate to detect only solutions, that approach 0 with some prescribed exponential rate, first.

Definition 2.1. Choose $\alpha \in (0, \mu)$ where $\mu \in \mathbb{R}^+$ is the leading non-zero eigenvalue of 0 as in Hypothesis 2.2. A solution $x(\cdot)$ of (2.1) and its orbit X are called *fast decaying* if

$$\sup\,\{e^{\alpha|t|}||x(t)|| : t \in \mathbb{R}\} < \infty.$$

Note that the primary homoclinic orbit Γ is fast decaying. For the detection of fast decaying homoclinic orbits we look for solutions $\gamma^{\pm}$ that fulfill

($\mathbf{P}_\gamma$)
- (i) The orbits of $\gamma^{\pm}$ are near Γ
- (ii) $\gamma^+(0), \gamma^-(0) \in \Sigma$
- (iii) $\sup\,\{e^{\pm\alpha t}||\gamma^{\pm}(t)|| : t \in \mathbb{R}^{\pm}\} < \infty$
- (iv) $\gamma^+(0) - \gamma^-(0) \in Z$

Such solutions will be detected as perturbations of Γ for which we introduce functions $v^{\pm}$ defined on $\mathbb{R}^{\pm}$ by

$$\gamma^{\pm}(t) = \gamma(t) + v^{\pm}(t), \quad t \in \mathbb{R}^{\pm}.$$

We will formulate an equivalent problem to (P_γ) for $v^\pm$. First, the functions have to solve the equation

$$\dot{v} = D_1 f(\gamma(t), 0)v + h(t, v, \lambda) \tag{2.12}$$

where $h(t, v, \lambda) = f(\gamma(t) + v, \lambda) - f(\gamma(t), 0) - D_1 f(\gamma(t), 0)v$. Note that $h(\cdot, 0, 0) \equiv 0$ and $D_2 h(\cdot, 0, 0) \equiv 0$. In order to satisfy the exponential rate for $\gamma^\pm$ we introduce spaces

$$\begin{aligned} V_\alpha^+ &:= \{v \in C^0([0, \infty), \mathbb{R}^{2n+2}) : \sup_{t \geq 0} e^{\alpha t} ||v(t)|| < \infty\} \\ V_\alpha^- &:= \{v \in C^0((-\infty, 0], \mathbb{R}^{2n+2}) : \sup_{t \leq 0} e^{-\alpha t} ||v(t)|| < \infty\}. \end{aligned}$$

The adopted version of (P_γ) then reads

($\mathbf{P}_v$)
- (i) $||v^\pm(t)||$ is small for all $t \in \mathbb{R}^\pm$
- (ii) $v^+(0)$, $v^-(0) \in Y^s \oplus Y^u \oplus Z$
- (iii) $v^+ \in V_\alpha^+$, $v^- \in V_\alpha^-$
- (iv) $v^+(0) - v^-(0) \in Z$

In order to find solutions of (2.12) that fulfill (P_v) we use the fact that the variational equation along the homoclinic orbit Γ

$$\dot{v} = D_1 f(\gamma(t), 0)v \tag{2.13}$$

possesses exponential trichotomies on $\mathbb{R}^\pm$, see [57]. This means, there exist projections $P_u^\pm(t)$, $P_s^\pm(t)$, $P_c^\pm(t)$ such that $id = P_u^\pm(t) + P_s^\pm(t) + P_c^\pm(t)$ $\forall\, t \in \mathbb{R}^\pm$ and

$$\Phi(t, s)P_i^\pm(s) = P_i^\pm(t)\Phi(t, s), \quad i = u, s, c,$$

where $\Phi(\cdot, \cdot)$ denotes the transition matrix of (2.13). Moreover, for $t \geq s \geq 0$ and for all α_c with $\mu > \alpha > \alpha_c > 0$ we have

$$\begin{aligned} ||\Phi(t, s)P_s^+(s)|| &\leq Ke^{-\alpha(t-s)}, \quad ||\Phi(s, t)P_u^+(t)|| \leq Ke^{-\alpha(t-s)}, \\ ||\Phi(t, s)P_c^+(s)|| &\leq Ke^{\alpha_c(t-s)}, \quad ||\Phi(s, t)P_c^+(t)|| \leq Ke^{\alpha_c(t-s)}. \end{aligned}$$

Using reversibility one can define $P_i^-(t)$ such that similar relations hold on $\mathbb{R}^-$. Of importance for us is that

$$\text{im } P_s^+(t) = T_{\gamma(t)} W_{\lambda=0}^s, \quad \text{im } P_u^-(t) = T_{\gamma(t)} W_{\lambda=0}^u, \tag{2.14}$$

and that we can choose

$$\ker P_s^+(0) = Z \oplus Y^u, \quad \ker P_u^-(0) = Z \oplus Y^s.$$

These results are proved in [39], see also [57].

Solutions of (2.12) satisfy the following fixed point problem

$$\begin{aligned} v^+(t) = \Phi(t,0)\eta^+ \quad &+ \quad \int_0^t \Phi(t,s)P_s^+(s)h(s,v^+,\lambda)ds \\ &\quad - \int_t^\infty \Phi(t,s)(id - P_s^+(s))h(s,v^+,\lambda)ds \\ v^-(t) = \Phi(t,0)\eta^- \quad &- \quad \int_t^0 \Phi(t,s)P_u^-(s)h(s,v^-,\lambda)ds \\ &\quad + \int_{-\infty}^t \Phi(t,s)(id - P_u^-(s))h(s,v^-,\lambda)ds, \end{aligned} \tag{2.15}$$

where $\eta^+ \in T_{\gamma(0)}W^s_{\lambda=0}$, $\eta^- \in T_{\gamma(0)}W^u_{\lambda=0}$. Expanding f in the definition of h we obtain the estimate

$$||h(t,v,\lambda)|| \leq c_1||v||^2 + c_2||\lambda||(||\gamma(t)|| + ||v||).$$

Thus, $v^\pm, \in V^\pm_\alpha$ implies $h(\cdot, v^\pm(\cdot), \lambda) \in V^\pm_\alpha$. Combining this with the exponential trichotomy we see that the right-hand side in (2.15) is a map

$$T_{\gamma(0)}W^{s(u)}(0) \times \mathbb{R} \times V^\pm_\alpha \to V^\pm_\alpha.$$

Therefore the exponentially bounded solution of (2.12) are exactly the solutions of (2.15), considered in $V^\pm_\alpha$. By the Implicit Function Theorem this problem can be solved around $(\eta^\pm, \lambda, v^\pm) = (0,0,0)$ for $v^\pm = v^\pm(\eta^\pm, \lambda)$. Now, regarding the requirements on $v^\pm(\eta^\pm,\lambda)(0)$ in (P_v) we decompose

$$\begin{aligned} v^+(\eta^+,\lambda)(0) &= \eta^+ + y_u(\eta^+,\lambda) + z^+(\eta^+,\lambda) \\ v^-(\eta^-,\lambda)(0) &= \eta^- + y_s(\eta^-,\lambda) + z^-(\eta^-,\lambda), \end{aligned}$$

with $y_{s(u)} \in Y^{s(u)}$, $z^\pm \in Z$. By (P_v) (iv) and (2.14) we must have

$$\eta^+ = y_s(\eta^-,\lambda), \quad \eta^- = y_u(\eta^+,\lambda),$$

which again can be solved for $\eta^\pm = \eta^\pm(\lambda)$. We thus obtain in complete analogy to Lemma 2.7 in [57]

Lemma 2.5. *For each λ sufficiently close to 0 the problem (P_γ) has a unique pair of solutions $(\gamma^+(\lambda), \gamma^-(\lambda))$.*

Remark 2.5. We see that the solution of (P_γ) is not affected by the change of dimension of the stable (unstable) manifold of the equilibrium 0 for $\lambda \neq 0$. This can be explained by the assumed exponential bound for the solutions, because for parameter values where 0 is hyperbolic we look for solutions of (P_γ) that are contained in the *strong stable (unstable) manifold* of 0. Therefore the change in the dimension of the whole stable (unstable) manifolds is not important.

We can detect fast decaying homoclinic orbits by solving the bifurcation equation

$$\xi^\infty(\lambda) := \gamma^+(\lambda)(0) - \gamma^-(\lambda)(0) = 0.$$

The uniqueness of the pair $(\gamma^+(\lambda), \gamma^-(\lambda))$ then immediately implies

$$R_i\gamma^+(\lambda)(0) = \gamma^-(\lambda)(0), \quad i = 1, 2.$$

Therefore $\xi^\infty(\lambda) \in \mathrm{Fix}\,(-R_i)$ for $i = 1, 2$ and since in Z

$$(\mathrm{Fix}\,(-R_1) \cap \mathrm{Fix}\,(-R_2)) = \{0\}$$

we conclude

Theorem 2.6. *For $|\lambda|$ sufficiently small there exists a unique fast decaying homoclinic orbit $\Gamma(\lambda)$ to 0 which is symmetric with respect to both involutions.*

Remark.

a) The geometric reason for this result is very clear. We have already established the fact that within $\mathrm{Fix}\,(S)$ the orbit Γ is non-degenerate. An application of Lemma 4 from [81] as in the proof of Lemma 2.2 then shows that the unstable manifold W^u_S of 0 intersects $\mathrm{Fix}\,(R_S)$ transversally. So there is no chance for destroying this homoclinic connection. In particular, no additional parameter is needed to control the existence of fast decaying homoclinic orbits.

b) There may exist additional homoclinic orbits to 0 which approach the fixed point with a smaller exponential rate and in fact such a smaller rate would be generic. Only the symmetries of (2.1) prevent Γ from switching to the lowest exponential rate available (reversible orbit flip bifurcation). We will deal with the existence of such orbits in the next part. ◇

2.3.2. Homoclinic orbits to $W^c_{loc,\lambda}$

In the second step of Lin's method for nonhyperbolic equilibria we determine one-homoclinic orbits to $W^c_{loc,\lambda}$. This time the loss of hyperbolicity near the equilibrium is overcome by looking for solutions of (2.1) on a finite time-interval. Let us introduce intervals $I^+ := [0, T]$ and $I^- := [-T, 0]$. Choosing a 'time' T we seek solutions $x^+ : I^+ \to \mathbb{R}^{2n+2}$ and $x^- : I^- \to \mathbb{R}^{2n+2}$ that satisfy

($\mathbf{P}_x$)
- (i) The orbits of $x^\pm$ are near Γ
- (ii) $x^+(0)$, $x^-(0) \in \Sigma$
- (iii) $x^+(0) \in W^{cs}_\lambda, x^-(0) \in W^{cu}_\lambda$
- (iv) $x^+(0) - x^-(0) \in Z$.

Provided T is chosen large enough we can formulate an equivalent demand to (P_x) (iii) by requiring

$(\widetilde{\mathbf{P}}_x)$ (iii) $x^+(T) \in W^{cs}_{loc,\lambda}, x^-(T) \in W^{cu}_{loc,\lambda}$

This time $x^\pm$ are described as perturbations of the solutions $\gamma^\pm(\lambda)$

$$x^\pm(t) = \gamma^\pm(\lambda)(t) + v^\pm(t);$$

which again leads to an equivalent problem for $v^\pm : I^\pm \to \mathbb{R}^{2n+2}$. So we determine solutions of

$$\dot{v} = D_1 f(\gamma^\pm(\lambda)(t), \lambda)v + h(t, v, \lambda) \tag{2.16}$$

on $I^\pm$ with

$$h(t, v, \lambda) = f(\gamma^\pm(\lambda)(t) + v, \lambda) - f(\gamma^\pm(\lambda)(t), \lambda) - D_1 f(\gamma^\pm(\lambda)(t), \lambda)v,$$

and we require the solutions of (2.16) to satisfy

$(\mathbf{P}^c_v)$
(i) $||v^\pm(t)||$ is small on $I^\pm$
(ii) $v^+(0), v^-(0) \in Y^s \oplus Y^u \oplus Z$
(iii) $v^+(T) \in W^{cs}_{loc,\lambda}, v^-(-T) \in W^{cu}_{loc,\lambda}$
(iv) $v^+(0) - v^-(0) \in Z$

Note that (P^c_v) (iii) uses the linear structure in $W^{cs(cu)}_{loc,\lambda}$ which is guaranteed in (2.5) for T sufficiently large.
The search for solutions of the above problem again relies on exponential trichotomies of the equation

$$\dot{v} = D_1 f(\gamma^\pm(\lambda)(t), \lambda)v. \tag{2.17}$$

Solutions of (2.16) are exactly the solutions of the fixed point equations

$$v^\pm(t) = \Phi^\pm(t, 0, \lambda)\eta^\pm + L^\pm(t, h(t, v^\pm, \lambda)), \quad t \in I^\pm \tag{2.18}$$

where $\Phi^\pm(t, s, \lambda)$ denote the transition matrices of (2.17) and the operators $L^\pm$ are defined for $t \in I^\pm$ by

$$\begin{aligned} L^+(t, g) &:= \int_0^t \Phi^+(t, s, \lambda)P^+_{cs}(s, \lambda)g(s)ds - \int_t^T \Phi^+(t, s, \lambda)(id - P^+_{cs}(s, \lambda))g(s)ds, \\ L^-(t, g) &:= -\int_t^0 \Phi^-(t, s, \lambda)P^-_{cu}(s, \lambda)g(s)ds + \int_{-T}^t \Phi^-(t, s, \lambda)(id - P^-_{cu}(s, \lambda))g(s)ds. \end{aligned}$$

The projections $P^\pm_{cs(cu)}$ are chosen in accordance with the exponential trichotomy of (2.17). Note that $L^\pm(t, g)$ solve the equations

$$\dot{v} = D_1 f(\gamma^\pm(\lambda)(t), \lambda)v + g(t),$$

with $g \in C^0(I^\pm, \mathbb{R}^{2n+2})$. Here it is essential that we deal with functions on finite intervals, which ensures that the solutions $L^\pm(t, g)$ are well-defined. Considering the right-hand side of (2.18) as map

$$T_{\gamma^\pm(\lambda)(0)} W^{cs(cu)} \times \mathbb{R} \times C^0(I^\pm, \mathbb{R}^{2n+2}) \to C^0(I^\pm, \mathbb{R}^{2n+2})$$

we can apply the Implicit Function Theorem near $(\eta^\pm, \lambda, v^\pm) = (0, 0, 0)$ and obtain solutions

$$v^\pm = v^\pm(\eta^\pm, \lambda), \tag{2.19}$$

where this time

$$\eta^+ \in (Y^s \oplus Y^u \oplus Z) \cap T_{\gamma^+(\lambda)(0)} W^{cs}_\lambda, \quad \eta^- \in (Y^s \oplus Y^u \oplus Z) \cap T_{\gamma^-(\lambda)(0)} W^{cu}_\lambda,$$

according to (P_v)(iii). Again we refer the reader to [57] for a more detailed exposition. In order to manage (P_v)(ii), (iv) we involve the space Y^c, as introduced in the proof of Lemma 2.2

$$\mathrm{span}\{f(\gamma(0), 0)\} \oplus Y^c = T_{\gamma(0)} W^{cs}_{\lambda=0} \cap T_{\gamma(0)} W^{cu}_{\lambda=0}$$

and use the refined decomposition

$$\mathbb{R}^{2n+2} = \mathrm{span}\{f(\gamma(0), 0)\} \oplus Y^s \oplus Y^u \oplus \widehat{Z} \oplus Y^c,$$

with $\widehat{Z} \oplus Y^c = Z$. Because of Lemma 2.2 we have $\dim Y^c = 2$, and we find that $R_i \widehat{Z} = \widehat{Z}$. We obtain a representation of $\Sigma \cap W^{cs(cu)}_\lambda$ as graphs of some functions

$$h^{cs(cu)}(\cdot, \lambda) : Y^c \oplus Y^{s(u)} \to Y^{u(s)} \oplus \widehat{Z},$$

which yields

$$\begin{aligned} \eta^+ &= y^+_c + y_s + D_1 h^{cs}(0, \lambda)(y^+_c, y_s) \\ \eta^- &= y^-_c + y_u + D_1 h^{cu}(0, \lambda)(y^-_c, y_u) \end{aligned}$$

with some $y^\pm_c \in Y^c$, $y_{s(u)} \in Y^{s(u)}$. Substituting this relation into (2.19) we obtain

$$v^+ = v^+(y^+_c, y_s, \lambda), \quad v^- = v^-(y^-_c, y_u, \lambda).$$

In a similar way as in the preceding subsection we decompose $v^\pm$ at $t = 0$ to find

$$\begin{aligned} v^+(y^+_c, y_s, \lambda)(0) &= y^+_c + y_s + y^+_u(y^+_c, y_s, \lambda) + z^+(y^+_c, y_s, \lambda) \\ v^-(y^-_c, y_u, \lambda)(0) &= y^-_c + y_u + y^-_s(y^-_c, y_u, \lambda) + z^-(y^-_c, y_u, \lambda). \end{aligned} \tag{2.20}$$

Again, (P_v)(iv) implies

$$y_s = y^-_s(y^-_c, y_u, \lambda), \quad y_u = y^+_u(y^+_c, y_s, \lambda), \tag{2.21}$$

and this system of equations can be solved for $y_s = y_s(y^+_c, y^-_c, \lambda)$, $y_u = y_u(y^+_c, y^-_c, \lambda)$. Putting things together we obtain in analogy to Lemma 3.5 in [57]

Lemma 2.7. *For λ sufficiently close to 0 and for sufficiently small $y_c^+, y_c^- \in Y^c$ there exists a unique pair $(x^+(y_c^+, y_c^-, \lambda), x^-(y_c^+, y_c^-, \lambda))$ of solutions of problem (P_x).*

For the detection of one-homoclinic orbits to $W^c_{loc,\lambda}$ it remains to solve

$$\xi(y_c^+, y_c^-, \lambda) := x^+(y_c^+, y_c^-, \lambda)(0) - x^-(y_c^+, y_c^-, \lambda)(0) = 0, \tag{2.22}$$

which can be written

$$\begin{aligned}\xi(y_c^+, y_c^-, \lambda) = (y_c^+ - y_c^-) \quad + \quad & (z^+(y_c^+, y_s(y_c^+, y_c^-, \lambda), \lambda) \\ & - \; z^-(y_c^-, y_u(y_c^+, y_c^-, \lambda), \lambda)) \,.\end{aligned} \tag{2.23}$$

Here we have used the representation (2.20) and the fact that because of Theorem 2.6 we have

$$\gamma^+(\lambda)(0) - \gamma^-(\lambda)(0) = 0, \quad \forall \lambda.$$

In order to solve (2.22) we must have $y_c^+ = y_c^- =: y_c$ since these are the Y^c-components of ξ. Introducing $\tilde{\xi}(y_c, \lambda) := \xi(y_c, y_c, \lambda)$ it therefore suffices to consider the bifurcation equation

$$\tilde{\xi}(y_c, \lambda) = 0. \tag{2.24}$$

We view $\tilde{\xi}$ as a map $\tilde{\xi} : Y^c \times \mathbb{R} \to \widehat{Z}$.

Our solution of (2.24) will to a large extend invoke the symmetries of (2.1). So we have to consider their consequences for the equation. Let us explore this point before we go on with the solution of (2.24).

We return to the presentation (2.19): $v^+ = v^+(\eta^+, \lambda)$, $v^- = v^-(\eta^-, \lambda)$. Due to the reversibility of the fixed point equation similar to (2.15) it holds that $R_i v^\pm(\eta^\pm, \lambda)(t) = v^\mp(\eta^\mp, \lambda)(-t)$ (as usual $i = 1, 2$). An immediate consequence for (2.21) is

$$\begin{aligned} R_i y_u^+(y_c^+, y_s, \lambda) &= y_s^-(R_i y_c^+, R_i y_s, \lambda), \\ R_i z^+(y_c^+, y_s, \lambda) &= z^-(R_i y_c^+, R_i y_s, \lambda). \end{aligned} \tag{2.25}$$

For the solutions of (2.21) we thus obtain

$$R_i y_u(y_c^+, y_c^-, \lambda) = y_s(R_i y_c^-, R_i y_c^+, \lambda). \tag{2.26}$$

These properties will be used below to detect symmetries in (2.24).

The last result of this part shows that we have a one-to-one correspondence between solutions (y_c, λ) of (2.24) with $y_c \in \mathrm{Fix}\,(R_i)$ and R_i-symmetric one-homoclinic orbits near the primary one Γ.

Lemma 2.8. *Suppose that the pair (y_c, λ) solves the bifurcation equation (2.24) and let $x(y_c, \lambda)(\cdot)$ denote the corresponding solution of (2.1) with orbit $\Xi(y_c, \lambda)$. Then $\Xi(y_c, \lambda)$ is R_i-symmetric if and only if $y_c \in Fix(R_i)$.*

Proof. For the proof we note first that $x(y_c,\lambda)(0) \in \mathrm{Fix}\,(R_i)$ is equivalent to

$$\begin{aligned} R_i\gamma^+(\lambda)(0) + R_i v^+(y_c, y_s(y_c,y_c,\lambda),\lambda)(0) \\ = \ \gamma^-(\lambda)(0) + v^-(y_c, y_u(y_c,y_c,\lambda),\lambda)(0). \end{aligned}$$

Now suppose $y_c \in \mathrm{Fix}\,(R_i)$. Since $R_i\gamma^+(\lambda)(0) = \gamma^-(\lambda)(0)$ by Theorem 2.6 we only have to consider the $v^{\pm}$-part. Here the above symmetries provide

$$\begin{aligned} R_i v^+(y_c, y_s(y_c,y_c,\lambda),\lambda)(0) &= v^-(R_i y_c, R_i y_s(y_c,y_c,\lambda),\lambda)(0) \\ &= v^-(R_i y_c, y_u(R_i y_c, R_i y_c,\lambda),\lambda)(0), \end{aligned}$$

and from $y_c \in \mathrm{Fix}\,(R_i)$ and the equivalence above we obtain $x(y_c,\lambda)(0) \in \mathrm{Fix}\,(R_i)$ and therefore the symmetry of the orbit.

On the other hand $v^+(y_c, y_s(y_c,y_c,\lambda),\lambda)(0) = v^-(y_c, y_u(y_c,y_c,\lambda),\lambda)(0)$ and therefore the only Y^c-component in $x(y_c,\lambda)(0)$ is y_c because of (2.20). Since the symmetry of $\Xi(y_c,\lambda)$ is equivalent to $x(y_c,\lambda)(0) \in \mathrm{Fix}\,(R_i)$ this requires $y_c \in \mathrm{Fix}\,(R_i)$. □

Geometry in Σ

Before we solve the bifurcation equation (2.24) we return to a discussion of geometric properties of the primary homoclinic orbit Γ. In Lemma 2.2 we have already shown that Γ results from a non-transverse intersection of $W^{cs}_{\lambda=0}$ and $W^{cu}_{\lambda=0}$. Now we investigate the relative position of these manifolds with respect to $\mathrm{Fix}\,(R_i)$. The following lemma shows that $W^{cs}_{\lambda=0}$ (and therefore also $W^{cu}_{\lambda=0}$) intersects both fixed spaces transversally.

Lemma 2.9. *Consider (2.1) under the Hypotheses 2.1 - 2.6. Then $W^{cs}_{\lambda=0} \pitchfork Fix(R_i)$ at $\gamma(0)$ where $i = 1, 2$.*

Proof. The proof is by contradiction, so let us assume that for instance $W^{cs}_{\lambda=0}$ intersects $\mathrm{Fix}\,(R_1)$ non-transversally, which implies

$$\dim\left(T_{\gamma(0)}W^{cs}_{\lambda=0} \cap \mathrm{Fix}\,(R_1)\right) \geq 2.$$

Because of Hypothesis 2.6 we therefore have $Y^c = T_{\gamma(0)}W^{cs}_{\lambda=0} \cap \mathrm{Fix}\,(R_1)$ and $\widehat{Z} \subset \mathrm{Fix}\,(-R_1) \cap \mathrm{Fix}\,(R_2)$. Applying the decomposition (2.11) we thus have $Y^c = X_1 \oplus X_3$ and $\widehat{Z} = X_2$. The idea of the proof is to show that for each $y_c \in X_3$ we have $\tilde{\xi}(y_c, 0) = 0$. Since $(y_c, 0) \in \mathrm{Fix}\,(S)$ this would amount to a family of homoclinic orbits to 0 in $\mathrm{Fix}\,(S)$ and as in the proof of Lemma 2.2 we derive a contradiction to the non-degeneracy Hypothesis 2.6.

We shall show first that

$$\tilde{\xi}(y_c, 0) = -\tilde{\xi}(R_2 y_c, 0). \tag{2.27}$$

The simple proof of this assertion uses the representation (2.23). We find that

$$\xi(y_c, y_c, 0) = z^+(y_c, y_s(y_c,y_c,0), 0) - z^-(y_c, y_u(y_c,y_c,0), 0)$$

and because of (2.25) we have

$$\begin{aligned}\xi(R_2y_c, R_2y_c, 0) &= z^+(R_2y_c, R_2y_u(y_c, y_c, 0), 0) - z^-(R_2y_c, R_2y_s(y_c, y_c, 0), 0)\\ &= z^-(y_c, y_u(y_c, y_c, 0), 0) - z^+(y_c, y_s(y_c, y_c, 0), 0),\end{aligned}$$

since $z^\pm \in \mathrm{Fix}\,(R_2)$. This proves (2.27).

From the symmetry (2.27) we immediately deduce that for $y_c \in \mathrm{Fix}\,(R_2)$ we have $\tilde{\xi}(y_c, 0) = 0$, i.e. we deduce that $\tilde{\xi}\big|_{X_3\times\{0\}} \equiv 0$. Then the application of Lemma 2.8 gives the R_1- and R_2-symmetry of the corresponding orbits, i.e. for the corresponding solutions $x(y_c, 0)(\cdot)$ we have $x(y_c, 0)(0) \in \mathrm{Fix}\,(R_1) \cap \mathrm{Fix}\,(R_2) \subset \mathrm{Fix}\,(S)$. By invariance of $\mathrm{Fix}\,(S)$ it holds $x(y_c, 0)(t) \in \mathrm{Fix}\,(S)\ \forall\, t \in \mathbb{R}$.

Hence, the above assumption implies the existence of a one-parameter family of one-homoclinic solutions in $\mathrm{Fix}\,(S)$ connecting $W^c_{loc,\lambda=0}$ - and thus the equilibrium 0 - to itself. Hypothesis 2.6, however, implies the non-degeneracy of Γ in $\mathrm{Fix}\,(S)$ which gives a contradiction. □

We recapitulate the result, namely that $T_{\gamma(0)}W^{cs}_{\lambda=0} \pitchfork \mathrm{Fix}\,(R_i)$, for $i = 1, 2$. By transversality this relation persists for λ small and we conclude that

$$\dim\left(T_{\gamma(0)}W^{cs}_{\lambda} \cap \mathrm{Fix}\,(R_i)\right) = 1 \text{ for } i = 1, 2. \tag{2.28}$$

In view of the decomposition (2.11) this results in $Y_c = X_1 \oplus X_2$ and $\widehat{Z} = X_3$. To see this choose $y \in Y_c \setminus \mathrm{Fix}\,(-R_1)$. By Lemma 2.3 such y exists. Then we have for $Y := \mathrm{span}(y + R_1y) \subset \mathrm{Fix}\,(R_1)$ that $R_2Y \subset Y$, and therefore we conclude that either $Y = X_1$ or $Y = X_3$. The latter possibility can be ruled out since we would find that in this case either $Y_c = X_1 \oplus X_3$ or $Y_c = X_2 \oplus X_3$ in contradiction to (2.28). We refer to Figure 2.3 for an impression of the geometric relations in Z. We also emphasize that the relative position of the manifolds $W^{cs(cu)}_\lambda$ is prescribed by the symmetries of the system to such an extent that no further parameter is needed for an unfolding.

For the solution of (2.24) we identify $\tilde{\xi} : X_1 \oplus X_2 \times \mathbb{R} \to \widehat{Z}$ with a map $\tilde{\xi}_\lambda : \mathbb{R} \times \mathbb{R} \to \mathbb{R}$. In a manner similar to the proof of Lemma 2.9 the symmetries of (2.1) yield in the present situation

$$\tilde{\xi}_\lambda(y_1, y_2) = -\tilde{\xi}_\lambda(-y_1, y_2), \quad \tilde{\xi}_\lambda(y_1, y_2) = -\tilde{\xi}_\lambda(y_1, -y_2);$$

note again that this is valid for all λ. In particular,

$$\tilde{\xi}_\lambda(0, \cdot) \equiv 0 \text{ and } \tilde{\xi}_\lambda(\cdot, 0) \equiv 0 \tag{2.29}$$

for all λ. Thus, we can write

$$\tilde{\xi}_\lambda(y_1, y_2) = y_1y_2 \cdot r_\lambda(y_1, y_2),$$

and in order to describe the solution set of (2.24) completely, we impose the following non-degeneracy condition

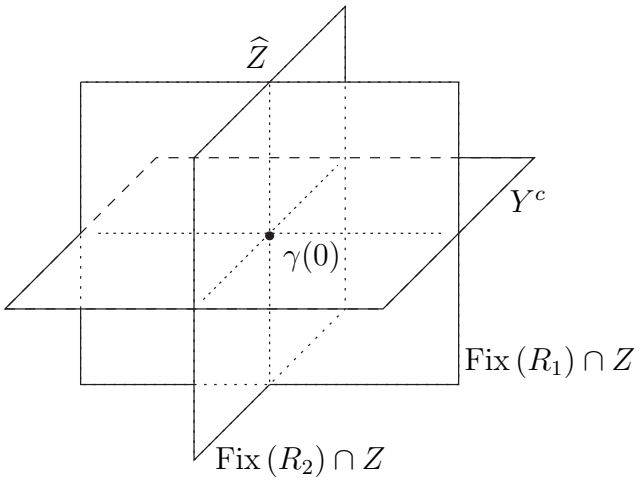

Figure 2.3.: Relative position of $T_{\gamma(0)}W^{cs}_\lambda = T_{\gamma(0)}W^{cu}_\lambda$ and the fixed spaces of the involutions R_i in Z

Hypothesis 2.7. $r_{\lambda=0}(0,0) \neq 0$.

This condition is equivalent to assuming $D^2\tilde{\xi}_{\lambda=0}(0,0)$ to be non-singular and it ensures that the zero level set of $\tilde{\xi}_\lambda$ is given in (2.29). Again applying Lemma 2.8 we find for each λ sufficiently small a curve of intersection points of W^{cs}_λ and W^{cu}_λ in $\mathrm{Fix}\,(R_1)$ and one in $\mathrm{Fix}\,(R_2)$. Let us summarize this in the next

Theorem 2.10. *Under the Hypotheses 2.1 - 2.7 we find curves $\mathcal{D}_1$ and $\mathcal{D}_2$ in Σ such that for each point of $\mathcal{D}_i$ the orbit through this point is an R_i-symmetric one-homoclinic orbit to $W^c_{loc,\lambda}$. The curves $\mathcal{D}_1, \mathcal{D}_2$ intersect in a unique point which corresponds to the fast decaying homoclinic orbit to 0, provided by Theorem 2.6. There exist no other one-homoclinic orbits than those described above.*

2.4. The bifurcation scenario for one-homoclinic orbits

In Theorem 2.10 we have seen that for each λ sufficiently small the intersection of W^{cs}_λ and W^{cu}_λ in Σ consists of two curves $\mathcal{D}_{1,2}$. To derive a complete description of the homoclinic bifurcation it remains to study the asymptotic behaviour of the corresponding homoclinic orbits. For this we project the solution set of (2.24) along the stable fibres of $W^c_{loc,\lambda}$ onto this manifold. For simplicity we return to the class of four-dimensional systems in this part, that is, we set $n = 1$ in (2.1). This allows a very convenient geometric arguing.

Let us introduce the projection method. Restricting to systems in $\mathbb{R}^4$ we have $\dim W^{cs}_\lambda = \dim W^{cu}_\lambda = 3$ and we can think of W^{cs}_λ as being foliated into one-dimensional fibres, i.e.

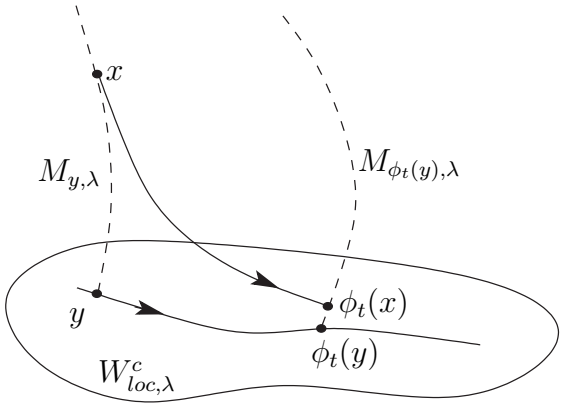

Figure 2.4.: Invariance of the stable fibres: The orbit through $x \in M_{y,\lambda}$ stays in the fibre with base point $\phi_t(y)$ for all $t \geq 0$.

from each $y \in W^c_{loc,\lambda}$ there originates a one-dimensional manifold $M_{y,\lambda} \subset W^{cs}_\lambda$, that is

$$W^{cs}_\lambda = \bigcup_{y \in W^c_{loc,\lambda}} M_{y,\lambda}.$$

In particular, $M_{0,\lambda}$ is nothing but the fast decaying homoclinic orbit $\Gamma(\lambda)$. We infer that for λ sufficiently small there exists a neighbourhood U of 0 (independent of λ) such that for each $y \in U$ the fibre $M_{y,\lambda}$ intersects Σ transversally which shows that the projection along the fibre is injective. Furthermore, this projection is smooth in both y and λ, see [79]. We thus conclude that the images of the curves $\mathcal{D}_i$ under the projection are smooth curves $\mathcal{C}_i$ in $W^c_{loc,\lambda}$.

Finally, the fibres enjoy an invariance property which is of fundamental importance for the following discussion. Choose $y \in W^c_{loc,\lambda}$ and let $\phi_t(y)$ denote the solution of (2.1) with $\phi_0(y) = y$. Then we have

$$\phi_t(M_{y,\lambda}) \subset M_{\phi_t(y),\lambda} \tag{2.30}$$

as long as $\phi_\tau(y) \in W^c_{loc,\lambda}$ for all $\tau \in [0,t]$. Hence, points in $M_{y,\lambda}$ follow the orbit through the base point y under the flow, see Figure 2.4. In particular, if $y \in W^c_{loc,\lambda}$ belongs to a stable manifold of an equilibrium or periodic orbit itself, then each point in $M_{y,\lambda}$ will be transported to this orbit under the flow.

For the discussion of one-homoclinic orbits to $W^c_{loc,\lambda}$ it suffices to consider the projection of $\mathcal{D}_{1,2}$ at $\lambda = 0$ since we can infer the images for λ sufficiently small from this by continuity. The above discussion immediately shows that the curves $\mathcal{C}_{1,2}$ intersect only in 0. We impose a final transversality condition concerning the projection.

Hypothesis 2.8. $\mathcal{C}_i \pitchfork \mathrm{Fix}\,(R_1)$ in $W^c_{loc,\lambda=0}$ for $i = 1, 2$.

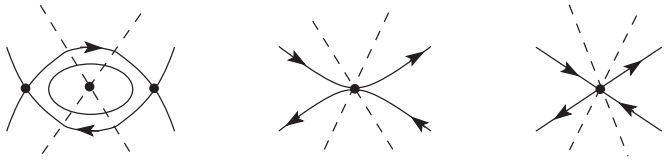

Figure 2.5.: Dynamics in $W^c_{loc,\lambda}$ together with the curves $\mathcal{C}_{1,2}$ (plotted dashed) needed for the detection of one-homoclinic orbits I: The eye case

Geometrically, we demand that $\mathcal{D}_{1,2}$ are projected on curves that are *not* tangent to the fixed space of the involution R_1. This is obviously a non-degeneracy condition which concerns the geometry within the centre stable manifold $W^{cs}_{\lambda=0}$. We postpone a detailed discussion of Hypothesis 2.8. In the following we demonstrate how Hypothesis 2.8 allows us to give a complete classification of bifurcating one-homoclinic orbits to $W^c_{loc,\lambda}$.

We have seen in Theorem 2.10 that the set of homoclinic orbits to $W^c_{loc,\lambda}$ does not depend on the local bifurcation of 0. Differences arise only now, when we investigate in detail which orbits in $W^c_{loc,\lambda}$ are connected by (large) homoclinic or heteroclinic orbits.

2.4.1. The eye case - the reversible homoclinic pitchfork bifurcation

Let us redraw Figure 2.1 including the curves $\mathcal{C}_{1,2}$ of points $x \in W^c_{loc,\lambda}$ whose fibres intersect Σ in points on one-homoclinic orbits to $W^c_{loc,\lambda}$. We then obtain Figure 2.5.

We can now discuss the type of orbits this bifurcation diagram yields. Let us start with $\lambda \geq 0$. Note first that Hypothesis 2.8 forbids intersection points of $\mathcal{C}_{1,2}$ with the stable and unstable manifolds of 0 in $W^c_{loc,\lambda}$ others than the origin, since these manifolds become tangent to $\mathrm{Fix}\,(R_1)$ as $\lambda \to 0$. Therefore the curves $\mathcal{C}_{1,2}$ only contain points whose orbits leave $W^c_{loc,\lambda}$ (apart from 0). And hence, there only exists the fast decaying one-homoclinic orbit to 0 whose existence has been established in Theorem 2.6.

For $\lambda < 0$ we find a large variety of one-homoclinic orbits. Again intersection points of $\mathcal{C}_i$ with bounded solutions in $W^c_{loc,\lambda}$ are of interest. First we observe from Figure 2.5 that both $\mathcal{C}_i$, $i = 1, 2$ intersect each periodic orbit in $W^c_{loc,\lambda}$ twice. Every such intersection point corresponds to a symmetric one-homoclinic orbit to a periodic orbit. Indeed, assume that $\mathcal{C}_i$ intersects the periodic orbit $\Gamma_p \subset W^c_{loc,\lambda}$. First, (2.30) shows that the corresponding solution that starts in Σ approaches Γ_p as $t \to \infty$. Moreover, considering a point $\Gamma_p \cap \mathcal{C}_i$ we know from the construction that this solution starts in $\mathrm{Fix}\,(R_i)$ which immediately shows that for $t \to -\infty$ it approaches $R_i\Gamma_p = \Gamma_p$.

Finally, we discuss the intersection points of $\mathcal{C}_i$ with the heteroclinic cycle in $W^c_{loc,\lambda}$. To these points there correspond solutions in W^{cs}_λ that approach the equilibria $\eta, R_2\eta$ as $t \to \infty$ by the invariance property (2.30). The intersections of the cycle with $\mathcal{C}_1$ give

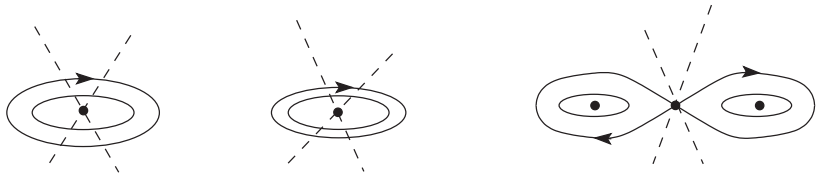

Figure 2.6.: Dynamics in $W^c_{loc,\lambda}$ together with the curves $\mathcal{C}_{1,2}$ (plotted dashed) needed for the detection of one-homoclinic orbits II: The figure-eight case.

rise to R_1-symmetric solutions which therefore approach $R_1\eta = \eta, R_2\eta$ as $t \to -\infty$, i.e. these solutions are homoclinic to the equilibria. This shows that a *reversible homoclinic pitchfork bifurcation*, as introduced in Section 1.3, occurs. Similarly, the intersection points of the cycle with $\mathcal{C}_2$ imply the existence of a (large) heteroclinic cycle near the primary homoclinic orbit Γ. It is important to note that Hypothesis (2.8) implies η, $R_2\eta \notin \mathcal{C}_i$. Therefore, the rate at which the detected homoclinic and heteroclinic orbits approach η, $R_2\eta$ is determined by the behaviour in $W^c_{loc,\lambda}$. We summarize the results as follows.

Theorem 2.11 (One-homoclinic orbits in the eye case). *Consider (2.1) under the Hypotheses 2.1 - 2.8 and assume moreover that the normal form for the local bifurcation of the equilibrium* 0 *is given by (2.8). Then for each* λ *sufficiently small there exists a fast decaying homoclinic orbit to the origin which is symmetric with respect to both* R_1 *and* R_2*.*

In addition for $\lambda < 0$ *every periodic orbit in* $W^c_{loc,\lambda}$ *is connected to itself by two pairs of* R_1*-symmetric and* R_2*-symmetric homoclinic orbits, respectively. Moreover, the equilibria* η *and* $R_2\eta$ *are connected to itself by* R_1*-symmetric homoclinic orbits, and furthermore there exists a symmetric heteroclinic cycle between* η, $R_2\eta$*.*

2.4.2. The figure-eight case

The procedure for the second type of the local pitchfork bifurcation is completely analogous to the one above. We start again by plotting the centre manifolds $W^c_{loc,\lambda}$ together with the curves $\mathcal{C}_i$ in Figure 2.6. (Recall that the behaviour in Σ was completely independent from the bifurcation of 0.)

We can analyse the intersection points of $\mathcal{C}_i$ with orbits in $W^c_{loc,\lambda}$ in a similar fashion. So for $\lambda \leq 0$ we see that each curve $\mathcal{C}_i$ intersects each periodic orbit surrounding the centre 0 two times. Hence, there exist two R_i-symmetric homoclinic orbits to each periodic orbit in $W^c_{loc,\lambda}$.

The analysis for $\lambda > 0$ requires a closer look at the figure-eight in $W^c_{loc,\lambda}$. It is important

that for $\lambda \to 0$ the stable and unstable manifold of the saddle 0 ($\lambda > 0$) become tangent to $\mathrm{Fix}\,(R_1)$. This is an immediate result of an analysis of the corresponding (Hamiltonian) normal form system (2.9). So for λ sufficiently small Hypothesis 2.8 prevents intersections of the curves $\mathcal{C}_i$ with the region bounded by the figure-eight. Therefore we only find intersections of $\mathcal{C}_i$ with periodic orbits that surround all three equilibria.

Theorem 2.12 (One-homoclinic orbits in the figure-eight case). *Consider (2.1) under the Hypotheses 2.1 - 2.8 and assume moreover that the normal form for the local bifurcation of the equilibrium* 0 *is given by (2.9). Then for each λ sufficiently small there exists a fast decaying homoclinic orbit to the origin which is symmetric with respect to both R_1 and R_2. No other one-homoclinic orbits to equilibria exist.*
In addition for $\lambda \leq 0$ every periodic orbit in $W^c_{loc,\lambda}$ is connected to itself by two pairs of R_1-symmetric and R_2-symmetric homoclinic orbits, respectively. For $\lambda > 0$ we find such two pairs of homoclinic orbits for the periodic orbits encircling all three equilibria.

2.4.3. Application to the model systems

We finally return to the umbilic systems (1.1) and demonstrate how the results obtained within the general frame apply to these systems and necessarily imply the occurrence of a reversible homoclinic pitchfork bifurcation. As usual we concentrate on the reversible hyperbolic umbilic f^-. Recall from Section 1.3 that a reversible homoclinic pitchfork bifurcation has been numerically detected for f^- at parameter values $\alpha > 0$, $\beta = -3\alpha^2$, i.e. on the bifurcation curve $\mathcal{B}_4$ in Figure A.1.

In order to verify the numerical results we obviously have to check the various hypotheses and non-degeneracy conditions imposed in Theorem 2.11. First we know from Section A.2 that the Hypotheses 2.1-2.5 are fulfilled for f^- at the above parameter values. Note that Hypothesis 2.4 requires to compute the normal form for the local bifurcation which has not been done explicitly in Section A.2. The results in that section, however, immediately show that the system falls within the eye case scenario. Furthermore, Hypothesis 2.6 is automatically fulfilled since we consider four-dimensional systems.

It would be more difficult to prove that f^- satisfies the non-degeneracy conditions in Hypotheses 2.7 and 2.8. Fortunately, we do not have to do this. In fact, these assumptions only exclude the existence of additional homoclinic orbits to $W^c_{loc,\lambda}$. More precisely, the bifurcation equation (2.24) is always solved if $y_1 = 0$ or $y_2 = 0$, which corresponds to the curves $\mathcal{D}_{1,2}$. If Hypothesis 2.7 is violated the solution set of this equation may contain additional curves and may vary with the parameter λ. Furthermore, Hypothesis 2.8 ensures that that the curves $\mathcal{C}_{1,2}$ do not intersect the additional equilibria η, $R_2\eta$ that are created in the local bifurcation. Thus, if Hypothesis 2.8 is violated, then additional 'orbit flip' homoclinic and heteroclinic orbits to η, $R_2\eta$ may exist. Nevertheless, we have

Corollary 2.13. *Consider f^- with parameter values in a suitable neighbourhood of the bifurcation curve $\mathcal{B}_4$ in Figure A.1. Then the statements of Theorem 2.11 apply to the orbit γ_{hom}, homoclinic to ξ_2. In particular, for parameter values $-(3+\varepsilon)\alpha^2 < \beta < -3\alpha^2$ and $\alpha > 0$, with $\varepsilon > 0$ sufficiently small, there exist two R_1-symmetric homoclinic orbits to the equilibria $\xi_{3,4}$, and these equilibria are connected by a further heteroclinic cycle.*

We remark once more that there may exist additional one-homoclinic orbits to orbits in a neighbourhood of ξ_2. Moreover, additional homoclinic and heteroclinic orbits to $\xi_{3,4}$ may be contained within the strong stable and strong unstable manifold of these equilibria and thus be subject to a reversible orbit flip bifurcation. Note, however, that the solutions computed in Section 1.3 are generic in that they do not lie in the strong (un)stable manifolds of $\xi_{3,4}$.

Remark 2.6. In the case of the reversible elliptic umbilic the above statements apply to the orbit γ_{hom} at parameter values $\alpha < 0$, $\beta = 3\alpha^2$.

2.5. Existence of two-homoclinic solutions

In this section we investigate the bifurcation of symmetric two-homoclinic orbits to $W^c_{loc,\lambda}$ from the primary homoclinic orbit Γ. Recall that a homoclinic orbit is called two-homoclinic if it is contained in a neighbourhood of the primary orbit Γ and makes exactly two windings, or, equivalently, if it intersects the cross section Σ for exactly two times.

Symmetric homoclinic orbits $W^c_{loc,\lambda}$ can again be detected by studying the intersection of $W^{cs(cu)}_\lambda$ with the fixed spaces of the involutions $\mathrm{Fix}\,(R_i)$. In general, there are two possibilities. Intersections can occur either near the equilibrium 0 or near the point $\gamma(0)$, that is, in Σ. In the former case orbits through such points of intersection is N-homoclinic with even N, whereas the latter case leads to N-homoclinic orbits with odd N. Furthermore, if points of intersections exist at all, then we would expect the intersection of $\mathrm{Fix}\,(R_i)$ and $W^{cs(cu)}_\lambda$ to be transverse. A simple count of dimensions reveals that thus one-parameter families of homoclinic orbits exist, just as in the results for one-homoclinic orbits, obtained above.

It is however, difficult, to prove the existence of intersection points of the manifold. Below we investigate this problem for the case of *two-homoclinic orbits* in the setting of this chapter. We will present a geometric approach and consequently consider only *four-dimensional systems*. Moreover, we restrict to an analysis in the case of the reversible homoclinic pitchfork bifurcation, i.e. we assume that the local bifurcation is given by the normal form (2.8). We study the existence of two-homoclinic orbits to $W^c_{loc,\lambda}$ for parameter values $\lambda < 0$ where three equilibria exist.

The difficulties in detecting N-homoclinic orbits stem from the fact that we have to analyse the behaviour of $W^{cs(cu)}_\lambda$ when these manifolds pass by the centre manifold

$W^c_{loc,\lambda}$. A description of this behaviour is achieved by combining results by Jones et. al. [52, 53], obtained in the frame of singularly perturbed systems, with results by Deng about the behaviour near nonhyperbolic equilibria [27].

2.5.1. The geometric setup

In this section we consider the system (2.1) with $x \in \mathbb{R}^4$ and under the assumptions of Theorem 2.11. This means in particular, that the local bifurcation of 0 is assumed to be of eye type. We study the existence of two-homoclinic orbits to $W^c_{loc,\lambda}$ for some fixed parameter value $\lambda < 0$ (sufficiently close to 0) where 0 is a saddle centre and the additional equilibria η, $R_2\eta$ are connected by a small heteroclinic cycle.

Two-homoclinic orbits are detected as intersections of $W^{cs(cu)}_\lambda$ with the fixed space $\mathrm{Fix}\,(R_2)$ near 0. For this we follow solutions starting in $W^{cu}_\lambda \cap \Sigma$ and investigate their intersection with the fixed spaces in some suitable three-dimensional section Σ_0 near 0. We study a Poincaré map $\mathcal{P} : \mathrm{dom}\,\mathcal{P} \subset \Sigma \to \Sigma_0$, where $\mathrm{dom}\,\mathcal{P}$ denotes the domain of $\mathcal{P}$. This set is characterized below.

Definition of $\mathcal{P}$

Let us first introduce the section Σ_0. For simplicity we choose suitable local coordinates in some neighbourhood $\widehat{U}$ of 0, such that the local centre stable and centre unstable manifold $W^{cs(cu)}_{loc,\lambda}$ are flattened out. So let us introduce coordinates $x = (x_s, x_u, y)$, in which

$$W^{cs}_{loc,\lambda} = \{x_u = 0\}, \quad W^{cu}_{loc,\lambda} = \{x_s = 0\}, \quad W^{c}_{loc,\lambda} = \{x_s = x_u = 0\}.$$

Moreover, in [27] Deng proves that it is always possible to choose *admissible variables* in which the local stable and unstable fibres are flattened out, as well. Hence, with no loss of generality we can for instance assume that the local stable fibre with base point y_0 is given by $M_{y_o,\lambda} = \{x_u = 0, y = y_0\}$ in $\widehat{U}$, see also [54]. The coordinates can be chosen such that the reversibility of the systems is preserved, and the involutions R_i now read for $y = (y_1, y_2)$

$$R_1 : (x_s, x_u, y_1, y_2) \to (x_u, x_s, y_1, -y_2), \quad R_2 : (x_s, x_u, y_1, y_2) \to (x_u, x_s, -y_1, y_2),$$

compare also with Section 2.2.1. In local coordinates equation (2.1) becomes

$$\begin{aligned} \dot{x}_s &= -\mu x_s + h_s(x_s, x_u, y, \lambda), \quad \dot{x}_u = \mu x_u + h_u(x_s, x_u, y, \lambda), \\ \dot{y} &= g(y, \lambda) + h_c(x_s, x_u, y, \lambda) \end{aligned} \tag{2.31}$$

with nonlinearities h_s, h_u, h_c whose derivatives vanish at 0, and which satisfy

$$h_s(0, x_u, y, \lambda) = h_u(x_s, 0, y, \lambda) = 0, \quad h_c(0, x_u, y, \lambda) = h_c(x_s, 0, y, \lambda) = 0,$$

see [27]. By $g(\cdot,\lambda)$ we denote the (normalized) vector field in $W^c_{loc,\lambda}$, as in equation (2.6). Note that in (2.31) we assume the positive eigenvalue μ of $D_1 f(0,0)$ to be independent of λ. Since we consider (2.1) with fixed $\lambda < 0$ below we do not have to worry about λ-dependence of terms in (2.31).

We introduce the section Σ_0 at 0 by setting

$$\Sigma_0 = \{x = (x_s, x_u, y) : \ x_s = x_u\}.$$

Note that Σ_0 contains both $\mathrm{Fix}\,(R_1)$ and $\mathrm{Fix}\,(R_2)$. In the notation of Section 2.3 we therefore have $\Sigma_0 = Z$. Furthermore, we find that $W^c_{loc,\lambda} \subset \Sigma_0$. A straightforward computation involving the local normal form (2.31) shows that orbits, which pass by the centre manifold $W^c_{loc,\lambda}$, intersect Σ_0 transversally. In Figure 2.7 we give an impression.

We now return to the situation within the cross section $\Sigma = \gamma(0) + Z$ to the primary orbit Γ. We consider the two-dimensional traces of the first intersection of $W^{cs(cu)}_\lambda$ with Σ. According to Lemma 2.2 these manifolds have a common tangent space, and since we deal with four-dimensional systems we have $T_{\gamma(0)}\,(W^{cs}_\lambda \cap \Sigma) = T_{\gamma(0)}\,(W^{cu}_\lambda \cap \Sigma) = Y^c$. We can therefore represent these traces as graphs of functions $h^{cs(cu)}_\lambda : Y^c \to \widehat{Z}$. Moreover, in Section 2.4 we have shown that we can identify points in $W^{cs(cu)}_\lambda$ with the base point of the respective (un)stable fibre. Now we can use this projection along fibres to obtain 'pictures' in $W^{cs(cu)}_\lambda \cap \Sigma$ of orbits in $W^c_{loc,\lambda}$, as for instance in Figure 2.8.

We are interested in orbits in W^{cu}_λ that start in Σ, intersect Σ_0 and return to Σ under the flow of the system. This motivates the next definition, see also [42]

Definition 2.2. The manifold W^{cu}_λ lies *inside* W^{cs}_λ at the point $(y_c, h^{cu}_\lambda(y_c)) \in W^{cu}_\lambda \cap \Sigma$, if $h^{cu}_\lambda(y_c) < h^{cs}_\lambda(y_c)$. If $h^{cu}_\lambda(y_c) > h^{cs}_\lambda(y_c)$, then W^{cu}_λ is said to lie *outside* W^{cs}_λ at the point $(y_c, h^{cu}_\lambda(y_c)) \in W^{cu}_\lambda \cap \Sigma$.

Let us now consider the solution $x_p(\cdot)$ through some point $p \in W^{cu}_\lambda \cap \Sigma$, such that $x_p(0) = p$, and assume that there exists a time $\tau \in \mathbb{R}^+$ such that $x(\tau) \in \Sigma_0$. If the orbit visits Σ_0 more than once, then take τ as the smallest time. The assignment $p \mapsto x_p(\tau)$, defines a map

$$\mathcal{P} : \mathrm{dom}\,\mathcal{P} \to \Sigma_0.$$

The above definition is related to the domain $\mathrm{dom}\,\mathcal{P}$ as the following general observation shows. We consider the part of W^{cs}_λ from Σ to $W^c_{loc,\lambda}$ and think of W^{cs}_λ and $W^c_{loc,\lambda}$ as being identified. This yields a closed manifold $\widetilde{W}^{cs}_\lambda$ in $\mathbb{R}^4$. Let us assume that $\widetilde{W}^{cs}_\lambda$ is not twisted. Since $\dim \widetilde{W}^{cs}_\lambda = 3$ it divides phase space, and therefore only those parts of $W^{cu}_\lambda \cap \Sigma$ that lie *inside* W^{cs}_λ intersect Σ_0 and return to Σ afterwards, see also Figure 2.7. On the other hand, if $\widetilde{W}^{cs}_\lambda$ is twisted then $\mathrm{dom}\,P$ consists of those parts of W^{cu}_λ that lie outside W^{cs}_λ.

This fact can be used to characterize $\mathrm{dom}\,\mathcal{P}$ in our situation. For that we return to the bifurcation equation for one-homoclinic orbits (2.24). Recall that with $y_c = (y_1, y_2)$ the

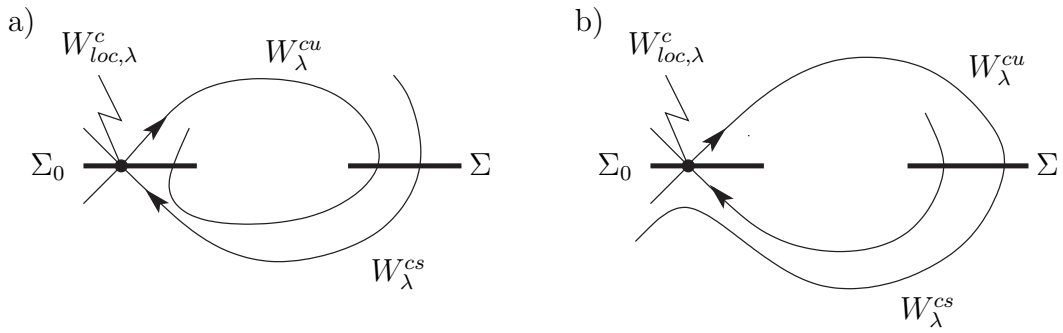

Figure 2.7.: Schematic description of the domain of $\mathcal{P}$: If $\widetilde{W}^{cs}_\lambda$ is not twisted, then the part of W^{cu}_λ that starts *inside* W^{cs}_λ in Σ will intersect Σ_0 and eventually return to Σ (panel a)). Points outside W^{cs}_λ are not transported back to Σ (panel b)). Two dimensions are missing in this picture.

equation could be written as

$$\tilde{\xi}_\lambda(y_1, y_2) = y_1 y_2 \cdot r_\lambda(y_1, y_2) = 0,$$

where y_i represent the $\mathrm{Fix}\,(R_i)$-coordinate of y_c in Y^c. Moreover, using the graph representation of $W^{cs(cu)}_\lambda \cap \Sigma$ introduced above, we can also write $\tilde{\xi}_\lambda(y_1, y_2) = h^{cu}_\lambda(y_c) - h^{cs}_\lambda(y_c)$. Therefore the sign of $\tilde{\xi}_\lambda$ determines the domain of $\mathcal{P}$. Since $r_{\lambda=0}(0,0) \neq 0$ by Hypothesis 2.7, the domain must consist of two opposite quadrants in Y^c, see Figure 2.8.

We have to distinguish two different possibilities, which are illustrated in Figure 2.8. In this figure we show a plot of $W^{cu}_\lambda \cap \Sigma$. For simplicity we have flattened out this manifold. Furthermore, a picture of the heteroclinic cycle in $W^c_{loc,\lambda}$ is achieved by a projection along unstable fibres. (Recall that we are concerned with the case $\lambda < 0$ such that three equilibria exist in $W^c_{loc,\lambda}$.) Of particular importance to us are the unstable fibres of the equilibria η, $R_2\eta$. The corresponding intersection points in Σ are indicated by dots, denoted p_η, Sp_η in Figure 2.8. As we have seen, Hypothesis 2.8 prevents that homoclinic orbits to η, $R_2\eta$ exist, which are contained in the strong unstable manifold of these equilibria. Therefore, the unstable fibres of the equilibria do not lie in $\mathrm{Fix}\,(R_i)$ in Σ. We conclude that either both p_η, Sp_η or none of the points are contained in $\mathrm{dom}\,\mathcal{P}$. In the following we restrict to the latter possibility. In this case we can prove the existence of R_2-symmetric two-homoclinic orbits to $W^c_{loc,\lambda}$. Hence, let us assume

Hypothesis 2.9. Let p_η, Sp_η denote the points in which the unstable fibres of η, $R_2\eta$ intersect Σ. Then $p_\eta, Sp_\eta \notin \mathrm{dom}\,\mathcal{P}$.

The Poincaré map $\mathcal{P}$ is used for proving the existence of two-homoclinic orbits to $W^c_{loc,\lambda}$ in the following way : In Figure 2.8, consider the upper point p_u where the projection of the heteroclinic cycle intersects $\mathrm{Fix}\,(R_2)$, i.e. the line $y_1 = 0$, in Σ. The point p_u is

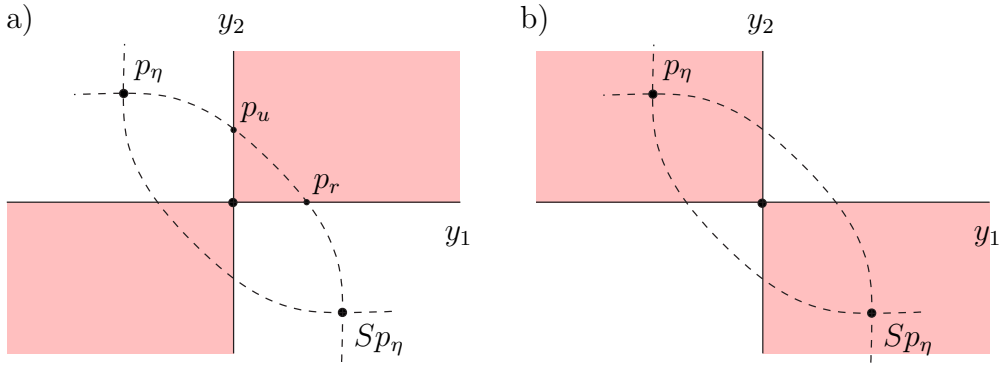

Figure 2.8.: Illustration of the two possibilities of $\operatorname{dom}\mathcal{P}$ in Σ (filled with grey). The heteroclinic cycle in $W^c_{loc,\lambda}$ is projected along unstable fibres onto W^{cu}_λ. The points, where the unstable fibres of η, $R_2\eta$ intersect Σ are denoted by p_η, Sp_η. Thus, the situation in panel a) corresponds to Hypothesis 2.9.

contained in the unstable manifold of the equilibrium η. Since $p_u \in \operatorname{Fix}(R_2)$ a solution through p_u is therefore asymptotic to $R_2\eta$ as time $t \to \infty$. We will show that in a neighbourhood of p_u in $\operatorname{dom}\mathcal{P}$ there exist points whose $\mathcal{P}$-image is arbitrarily close to $R_2\eta$ in Σ. In a similar way, we find points in a neighbourhood of $p_r \in \operatorname{Fix}(R_1)$ which are mapped in a neighbourhood of η by $\mathcal{P}$. (Note that the orbit through p_r is homoclinic to η.) Thus, the $\mathcal{P}$-images of curves in $\operatorname{dom}\mathcal{P}$ that connect such points near p_u with those near p_r necessarily have to intersect $\operatorname{Fix}(R_2)$ in Σ_0, see Figure 2.9 below. We thus conclude that there exists a one-parameter family of R_2-symmetric homoclinic orbits to $W^c_{loc,\lambda}$.
In the next part we establish the existence of suitable points near p_u, p_r by a careful study of the Poincarè map $\mathcal{P}$.

2.5.2. Analysis of the Poincaré map $\mathcal{P}$

Consider a point $p \in \operatorname{dom}\mathcal{P}$. We follow the solution x_p of (2.1) with $x_p(0) = p$ until it intersects Σ_0 at some time τ_p. The corresponding trajectory is divided into two parts. The second part describes the behaviour of x_p in a neighbourhood of $W^c_{loc,\lambda}$, the first one the behaviour outside this neighbourhood. For that let us introduce a box

$$B := \{(x_s, x_u, y) : |x_s| \le \delta_1, |x_u| \le \delta_1, ||y|| < \delta_2\}$$

where the δ_i are chosen such that $B \subset \widehat{U}$.
The difficult task lies in describing the behaviour of solutions in B. Here it is of advantage that we are only interested in solutions that start close to W^{cs}_λ in Σ. Let us first analyse, how such solutions enter the box B. Consider the flight from Σ to B. For all $p \in \Sigma$ the

orbit through p will enter B through the side $B_s := \{x_s = \delta_1\}$ of B. In particular, if $p \in W^{cs}_\lambda \cap \Sigma$, then there exists a time τ such that $x_p(\tau) = (\delta_1, 0, y_p)$. A straightforward computation, using again (2.31), shows that the orbit intersects the side B_s transversally at $x_p(\tau)$. Thus, B_s is a cross section to the flow and the corresponding map from Σ to B_s is a diffeomorphism and we obtain as a result.

Lemma 2.14. *If $p \in \Sigma$ is sufficiently close to W^{cs}_λ, then the orbit through p enters B in some point $(x_s, x_u, y) = (\delta_1, \varepsilon, y_p)$. Moreover, $\varepsilon \to 0$ as $d(p, W^{cs}_\lambda) \to 0$, where $d(\cdot,\cdot)$ denotes the standard metric.*

The behaviour of solutions that enter B in points $(\delta_1, \epsilon, y_p)$ is described by the following lemma which is used in the proof of an 'exchange lemma with exponentially small error' in [52]. In this lemma let $\tilde{\mu}$ be a constant close to but smaller than μ.

Lemma 2.15 ([52]). *Let $(x_s, x_u, y)(\cdot)$ be a solution of (2.31). As long as the trajectory stays in B, there exist constants $c_s, c_u, c, K > 0$ such that, for $s \le t$*

1) $|x_s(t)| \le c_s |x_s(s)| e^{-\tilde{\mu}(t-s)}$

2) $|x_u(t)| \ge c_u |x_u(s)| e^{\tilde{\mu}(t-s)}$

3) $\int_s^t |x_s(\tau)| \cdot |x_u(\tau)|\, d\tau \le K e^{c(s-t)}$

Of concern to us is the following interpretation, which can be found in a similar version in [42, 53].

Lemma 2.16. *Let $x_{cs}(\cdot)$ be a solution in $W^{cs}_{loc,\lambda}$ through $x_{cs}(0) = (\delta_1, 0, y_0)$ and assume that the solution through y_0 in $W^c_{loc,\lambda}$ is bounded. For each $\tau > 0$ there exists a $\Delta_0 > 0$ such that for all $\Delta \in (0, \Delta_0)$ the solution through (δ_1, Δ, y_0) stays in B for all $t \in [0, \tau]$. If τ is chosen large enough, there is a time interval where both x_s and x_u are exponentially small. In this case a solution leaves B at time τ through point $(\epsilon, \delta_1, z_1)$ with ϵ exponentially small.*

During the time interval where x_s and x_u are exponentially small the solution follows the flow in the centre manifold $W^c_{loc,\lambda}$ closely. Hence, the behaviour in $W^c_{loc,\lambda}$ determines where the solution intersects the cross section Σ_0. This geometric consideration can be put on rigorous footing using general results by Deng [27] about the behaviour near nonhyperbolic equilibria. Observe that the solution in Lemma 2.16 can be characterized by a *Shilnikov problem* in that it fulfills

$$x_s(0) = \delta_1, \quad x_u(\tau) = \delta_1, \quad y(0) = y_0. \tag{2.32}$$

In [27] Deng shows that given the *Shilnikov data* $(\tau, \delta_1, \delta_1, y_0)$ there exists a unique solution $(x_s, x_u, y)(t; \tau, \delta_1, \delta_1, y_0)$ of the Shilnikov problem (2.32). Moreover, he obtains *exponential expansions* for the solution. Let D^i denote the i-th derivative in all arguments of some function. We quote from Lemma 3.1 in [27]:

Lemma 2.17. *Let $(x_s, x_u, y)(\cdot)$ denote the (unique) solution of the above Shilnikov problem. Denote by y_c the solution in $W^c_{loc,\lambda}$ with $y_c(0) = y_0$, and assume that this solution is bounded. Then there exists $\tilde{\mu} \in (0, \mu)$ and $K > 0$, such that for all $t \in [0, \tau]$ and $i = 0, 1, 2, \ldots$*

1) $|D^i x_s(t)| \leq K e^{-\tilde{\mu} t}$

2) $|D^i x_u(t)| \leq K e^{\tilde{\mu}(t-\tau)}$

3) $y(t) = y_c(t) + R(t)$, where $|D^i R(t)| \leq K e^{-\tilde{\mu}\tau}$.

Note that the first two estimates are similar to Lemma 2.15 above.

We can summarize the results of this technical part as follows. Let us once more consider a solution $(x_s, x_u, y)(\cdot)$ which enters B sufficiently close to $W^{cs}_{loc,\lambda}$. The time τ this solutions spends in B can be controlled by the distance to $W^{cs}_{loc,\lambda}$. In particular, this distance determines at what time $\hat{\tau} \approx \tau/2$ the solution intersects Σ_0. During its passage through B there is a time interval where both x_s and x_u are exponentially small, and y follows its reference solution y_c in $W^c_{loc,\lambda}$ exponentially closely according to points 1)-3) in Lemma 2.17. With regard to our original problem concerning the Poincaré map we conclude that the solution intersects Σ_0 in an exponentially small neighbourhood of the position of the reference solution y_c, see estimate 3) in Lemma 2.17.

We are finally in position to prove the existence of points near p_u, p_r whose $\mathcal{P}$-image lies in a neighbourhood of $R_2\eta$ and η, respectively.

Lemma 2.18. *For each $\varepsilon > 0$ there exist points p_1, p_2 (depending on ε) in the same quadrant of $\operatorname{dom}\mathcal{P}$, such that $d(\mathcal{P}p_1, \eta) < \varepsilon$, $d(\mathcal{P}p_2, R_2\eta) < \varepsilon$ in Σ_0. As before $d(\cdot,\cdot)$ denotes the usual metric.*

Proof. Let us describe how to find points p_1. For that we follow the solution through the distinguished point $p_r \in W^{cs}_\lambda$ in Σ, see again Figure 2.8. This point enters the box B at some point $(x_s, x_u, y) = (\delta_1, 0, y_r)$. Since the local stable fibres are flattened out in $\widehat{U} \supset B$, the centre manifold solution y_c with $y_c(0) = y_r$ describes the heteroclinic orbit Γ_h from $R_2\eta$ to η. We consider solutions through points $(x_s, x_u, y) = (\delta_1, \Delta, y_c(s))$, with $s \in (-1, 1)$. If $\Delta = 0$ all of these points lie on stable fibres of the orbit Γ_h. By the above computations we thus find that, given an ε-neighbourhood U of η, there exists a Δ such that every orbit through points $(\delta_1, \Delta, y_c(s))$ intersects Σ_0 in U.

It remains to show that there exists a point in $\operatorname{dom}\mathcal{P}$ that enters B at a point of the form $(\delta_1, \Delta, y_c(s))$. This can be achieved by following solutions through these points backward to the cross section Σ. If $\Delta = 0$ the solutions intersect Σ in some curve which is contained in $W^{cs}_\lambda \cap \Sigma$ and transversally intersects $W^{cu}_\lambda \cap \Sigma$ in p_r. Applying Lemma 2.14 we conclude that for $\Delta > 0$ small the 'backward image' of $\{(\delta_1, \Delta, y_c(s)), s \in (-1, 1)\}$ also intersects W^{cu}_λ at some point p_1 which belongs to $\operatorname{dom}\mathcal{P}$ and whose $\mathcal{P}$-image is ε-close to η, by construction.

The existence of p_2 is proved similarly using the distinguished point p_u. □

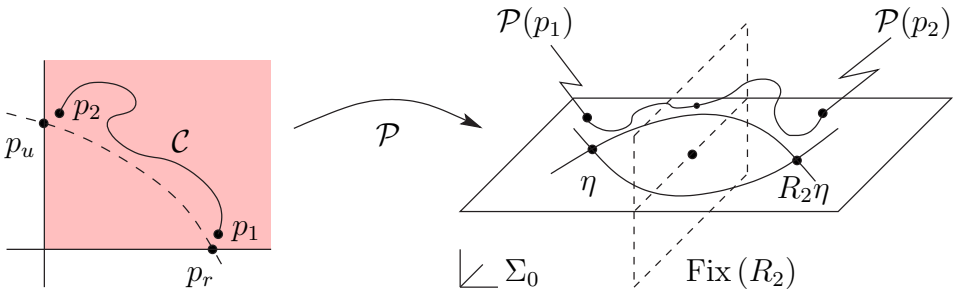

Figure 2.9.: Existence of two-homoclinic orbits to $W^c_{loc,\lambda}$. The left part shows a quadrant of $\operatorname{dom}\mathcal{P}$ in Σ. The $\mathcal{P}$-image of curves through p_1 and p_2 must intersect $\operatorname{Fix}(R_2)$ in Σ_0, as shown in the right part. The intersection point represents a two-homoclinic orbit.

Let us now choose $\varepsilon > 0$ sufficiently small and take points p_1, p_2 according to the above lemma. We can connect these points by some curve $\mathcal{C}$ in $\operatorname{dom}\mathcal{P}$. By continuity, $\mathcal{P}(\mathcal{C})$ is a curve in Σ_0 with end points $\mathcal{P}(p_i)$ on different sides of $\operatorname{Fix}(R_2)$. Therefore $\mathcal{P}(\mathcal{C})$ has to intersect $\operatorname{Fix}(R_2)$ in Σ_0, giving rise to a R_2-symmetric homoclinic orbit to $W^c_{loc,\lambda}$, see Figure 2.9. Since $\mathcal{C}$ can be chosen arbitrarily we obtain

Theorem 2.19. *Consider (2.1) with $\lambda < 0$, under the assumptions of Theorem 2.11 and Hypothesis 2.9. There exists a one-parameter family of R_2-symmetric two-homoclinic orbits to $W^c_{loc,\lambda}$.*

By choosing a special curve $\mathcal{C}$ we can prove the existence of further connecting orbits between η, $R_2\eta$. Indeed, we find parts of the unstable manifold of η, $R_2\eta$ in $\operatorname{dom}\mathcal{P}$. These parts stem from the projected heteroclinic cycle in W^{cu}_{λ}, see for instance Figure 2.8 again. We can take $\mathcal{C}$ to be the part between p_u and p_r in Figure 2.8 and conclude by the same argument as above that an orbit in the unstable manifold of η ($R_2\eta$) intersects $\operatorname{Fix}(R_2)$ near 0.

Theorem 2.20. *In the setting of Theorem 2.19 above there exists a two-heteroclinic cycle between the equilibria η, $R_2\eta$.*

Remark 2.7. It should be clear that the approach does not allow us to prove the existence of R_1-symmetric two-homoclinic orbits, since $\eta, R_2\eta \in \operatorname{Fix}(R_1)$. Hence, we cannot control whether curves starting near η and ending near $R_2\eta$ intersect $\operatorname{Fix}(R_1)$. We remark further, that also in the case where Hypothesis 2.9 is violated (panel b) in Figure 2.8) the presented method cannot be used to obtain existence results for two-homoclinic orbits. The interested reader may easily be convinced of this fact by applying the geometric idea to this case.

2.5.3. Bifurcation of N-homoclinic solutions in the umbilic systems

Let us finally return to the umbilic systems (1.1) and present some numerical results about N-homoclinic orbits. Again we concentrate on the reversible hyperbolic umbilic f^-. According to Corollary 2.13 a reversible homoclinic pitchfork bifurcation occurs for this system at parameter values $\alpha > 0$, $\beta = -3\alpha^2$. Hence, parameter values $\beta < -3\alpha^2$ are of interest in the following. Unfortunately, we cannot prove that the theory applies to f^-, since it is almost impossible to check whether the technical, but fundamental Hypothesis 2.9 is fulfilled. Nevertheless, we present results of numerical computations below.

We can compute N-homoclinic (and N-heteroclinic) orbits to equilibria of f^- using a homoclinic branch-switching method, developed by Oldeman et. al. in [70]. This branch-switching uses continuation methods to 'switch' from a given one-homoclinic solution to N-homoclinic solutions nearby. The computational scheme is based on ideas from Lin's method. The branch-switching is implemented in AUTO/HomCont.

We apply the method for investigating whether additional homoclinic and heteroclinic orbits to the equilibria $\xi_{3,4}$ of f^- exist. We use the homoclinic orbits and heteroclinic orbits which emerge in the reversible homoclinic pitchfork bifurcation of γ_{hom} as starting solutions. Note that the branch-switching can only be applied to homoclinic orbits. However, we have already described that the treatment of homoclinic and heteroclinic orbits to $\xi_{3,4}$ can be unified by a $\mathbb{Z}_2$-symmetry reduction of the system. For the computation of heteroclinic orbits, we therefore have to consider the reduced system (A.7).

We have applied the method to f^- with parameter values $\alpha = 1$, $\beta = -3.5$. Here we have computed N-homoclinic solutions to ξ_3 for $N = 2, 3, 4$. Precisely one N-homoclinic solution for each N could be computed. Plots of the x_1-and x_3-component of the solutions are presented in Figure 2.10. We see that these orbits first follow the one-homoclinic solution to ξ_3 until they come close to $\mathrm{Fix}\,(S)$ $(x_1 = 0)$ and then follow γ_{hom} before they return to ξ_3. Therefore the orbits are not N-homoclinic orbits in the classic sense, since they are composed of two homoclinic solutions to different equilibria. But along the lines of this chapter it is perfectly justified to view them as N-homoclinic orbits to the centre manifolds.

We could not compute further heteroclinic orbits between $\xi_{3,4}$. This, however, does not exclude the existence of such orbits since numerical difficulties have been encountered because of the loss of smoothness in the point $y_1 = y_2 = 0$ in the reduced system (A.7).

Finally, we point out one aspect that could not be covered by the general analysis, which has been performed for a fixed value of the parameter $\lambda < 0$: A continuation of the N-homoclinic orbits up to the critical parameter values suggests that these orbits emerge in the reversible homoclinic pitchfork bifurcation of γ_{hom}. In particular, no N-homoclinic solutions can be computed for parameter values $\beta > -3\alpha^2$, where only ξ_2 exists.

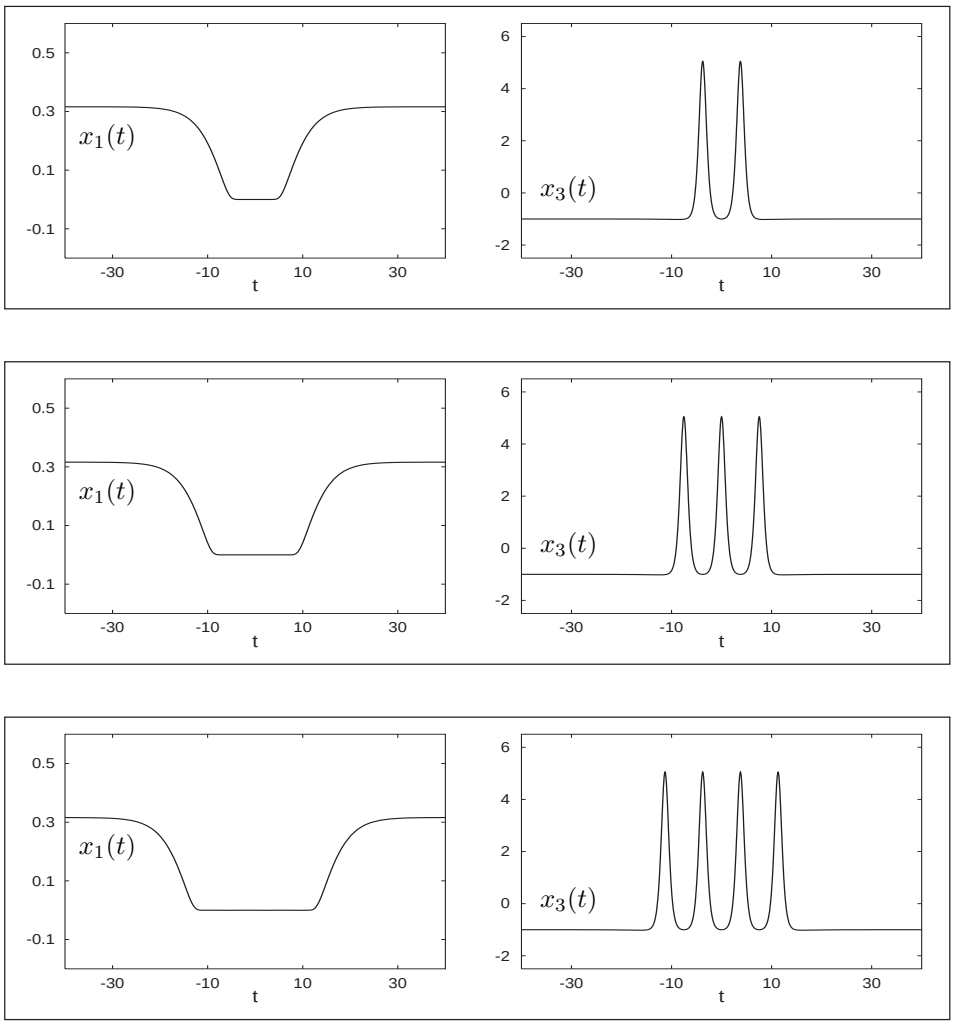

Figure 2.10.: Plots of 2-, 3-, and 4-homoclinic solutions created in the reversible homoclinic pitchfork bifurcation of γ_{hom}. The solutions have been computed at $\alpha = 1$, $\beta = -3.5$. The x_1- and x_3-components of the solutions are shown.

CHAPTER 3

Homoclinic orbits to degenerate equilibria - other cases

3.1. Introduction

In this part we continue the study of homoclinic orbits to degenerate equilibria. In the main part we generalize the studies of Chapter 2 to the class of purely reversible systems. Our analysis proceeds along similar lines as before. There are, however, differences. In the case of a purely reversible system a second parameter is needed for controlling the existence of fast decaying homoclinic orbits to 0, such that the homoclinic bifurcation is of codimension-two. In addition, the generic local bifurcation of the equilibrium is either a reversible saddle-centre bifurcation or transcritical bifurcation. We consider the case of the transcritical bifurcation, since we are interested in the transition of real saddle to saddle centre for the equilibrium, associated to the homoclinic orbit.

In the analysis we concentrate on the bifurcation of one-homoclinic orbits. For the detection of one-homoclinic orbits to $W^c_{loc,\lambda}$ we do not employ Lin's method, but rely on a geometric reasoning. Consequently, we restrict the analysis to four-dimensional systems in this chapter. We achieve a complete description of one-homoclinic orbits to $W^c_{loc,\lambda}$ in Theorem 3.3, see also Figure 3.3.

Of particular interest to us is the analysis of one-homoclinic orbits to 0, because of an application to solitary wave solutions of PDE models, that we have in mind (see below). If the origin is a saddle centre, homoclinic orbits to this equilibrium are of codimension-one, whereas they are structurally stable when 0 is hyperbolic. We show that homoclinic orbits to the saddle 0 are generically destroyed either by developing an algebraically decaying tail or through a fold, depending on the sign of the second perturbation parameter.

After the analysis of the bifurcation in purely reversible systems we consider systems

with an additional $\mathbb{Z}_2$-symmetry in Section 3.4. Finally, the important class of reversible Hamiltonian systems is studied in Section 3.5.

In the final Section 3.6 we apply the theory to a problem for solitary waves, which concerns the transition from *embedded solitons* to *gap solitons*. Details are provided in Section 3.6, where the general results are also shown to match numerical computations on examples from water-wave theory and nonlinear optics.

The chapter is based on the joint paper [87] with Alan Champneys.

3.2. The setting

In this part we consider four-dimensional ODEs

$$\dot{x} = f(x, \lambda), \quad x \in \mathbb{R}^4, \ \lambda \in \mathbb{R}^l \tag{3.1}$$

and assume them to be R-reversible.

Hypothesis 3.1. There exists a (linear) involution $R : \mathbb{R}^4 \to \mathbb{R}^4$ such that

$$f(Rx, \lambda) + Rf(x, \lambda) = 0, \quad \forall x, \lambda.$$

Moreover, we have $\dim(\mathrm{Fix}\,(R)) = 2$.

Turning to equilibria of (3.1) we assume that the origin is an equilibrium of (3.1) which is degenerate for $\lambda = 0$, that is

Hypothesis 3.2. $f(0, \lambda) = 0 \ \forall \lambda$, and $\sigma(D_1 f(0, 0)) = \{0\} \cup \{\pm\mu\}$ with 0 being a non-semisimple eigenvalue and $\mu \in \mathbb{R}^+$.

This hypothesis assumes the existence of an equilibrium in 0 for all λ and therefore prevents a local saddle-centre bifurcation of 0. Instead we will find that Hypothesis 3.2 generically results in a transcritical bifurcation of the equilibrium. We have already explained above that this bifurcation is of interest to us, since it leads to a transition of 0 from real saddle to saddle centre. We also remark that Hypothesis 3.2 is again generically met in one-parameter families of reversible ODEs.

Our final assumption concerns the existence of a homoclinic orbit Γ.

Hypothesis 3.3. At $\lambda = 0$ equation (3.1) possesses an orbit $\Gamma = \{\gamma(t) : t \in \mathbb{R}\}$ homoclinic to 0, i.e. $\gamma(t) \to 0$ as $t \to \pm\infty$. Furthermore, Γ is R-symmetric and fast decaying, i.e. we have $R\Gamma = \Gamma$, and choosing α such that $0 < \alpha < \mu$ we have $||\gamma(t)||e^{\alpha t} \to 0$ as $t \to \infty$.

In the following we study bifurcations of one-homoclinic orbits from the primary orbit Γ. The procedure runs completely along the lines of Chapter 2. Via centre manifold theory

we first analyse the local bifurcation of the 0-equilibrium, thereby introducing centre stable and centre unstable manifolds. We then study the intersection of these manifolds and detect one-homoclinic orbits to the centre manifolds. Afterwards the asymptotic behaviour of these orbits is described by a projection along stable fibres.

To shorten the presentation we have now chosen to perform an analysis that consists of purely geometrical considerations. The analytical machinery developed in the last chapter can be applied to this problem in precisely the same way as above and yields the same results. This is demonstrated in an earlier preprint version [86] of the article [87]. In particular, [86] shows that, similar to the last section, the results can be generalized to higher-dimensional systems. Hence, our choice of considering four-dimensional systems only is not restrictive.

3.3. Bifurcation of one-homoclinic orbits in the general case

3.3.1. Bifurcation of the equilibrium

For the analysis of the local bifurcation we again turn to the extended system

$$\begin{aligned} \dot{x} &= f(x,\lambda) \\ \dot{\lambda} &= 0 \end{aligned}$$

with equilibrium $(x,\lambda) = (0,0)$. As before this allows to introduce an $l+2$-dimensional centre manifold $\mathfrak{W}^c_{loc}$ and $l+3$-dimensional centre (un)stable manifolds $\mathfrak{W}^{cs(cu)}_{loc}$. These manifolds are foliated into $\{\lambda = const.\}$-slices which we again denote by $W^c_{loc,\lambda}$ and $W^{cs(cu)}_{loc,\lambda}$, respectively.

In accordance with the reversibility we can choose $W^{cs}_{loc,\lambda} = RW^{cu}_{loc,\lambda}$ and set $W^c_{loc,\lambda} = W^{cs}_{loc,\lambda} \cap W^{cu}_{loc,\lambda}$, see [49]. We can also extend the local manifolds $W^{cs(cu)}_{loc,\lambda}$ along the orbit Γ to derive global centre (un)stable manifolds. Again the global versions are denoted by the same symbols without *loc*-index. We note that the symmetries of the local manifolds are preserved such that $RW^{cs}_{\lambda} = W^{cu}_{\lambda}$.

By the Centre Manifold Theorem [82, 37] we can follow the evolution of small bifurcating solutions of (3.1) in a family of planar reversible vector fields on $W^c_{loc,\lambda}$. We use again the fact that the local bifurcation is completely described by the normal form of the 0-equilibrium. Introducing (y_1,y_2)-coordinates in $W^c_{loc,\lambda}$ the involution R can be assumed to act as $R:(y_1,y_2)\mapsto(y_1,-y_2)$ and an appropriate reversible normal form is given in [65, 64] by

$$\begin{aligned} \dot{y}_1 &= y_2 \\ \dot{y}_2 &= \textstyle\sum_{k\geq 1} a_k(\lambda) y_1^k. \end{aligned}$$

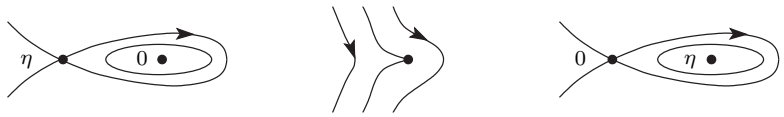

$\lambda_1 < 0$ $\lambda_1 = 0$ $\lambda_1 > 0$

Figure 3.1.: Phase portraits for the normal form (3.2) of the reversible transcritical bifurcation in $W^c_{loc,\lambda}$.

Note that by Hypothesis 3.2 we have $a_1(0) = 0$ and we can ensure to deal with a generic bifurcation by imposing

Hypothesis 3.4. $a_2(0) \neq 0$.

With no loss of generality the normal form for the problem then reads

$$\begin{aligned} \dot{y}_1 &= y_2 \\ \dot{y}_2 &= \lambda_1 y_1 + y_1^2. \end{aligned} \tag{3.2}$$

Being Hamiltonian, the system (3.2) is easily analysed. We find the familiar phase portrait of the reversible transcritical bifurcation, see Figure 3.1. The origin is a centre for $\lambda_1 < 0$ and a saddle for $\lambda_1 > 0$. In addition, for $\lambda_1 > 0$ it is connected to itself by a (small) homoclinic orbit Υ. If $\lambda_1 \neq 0$ there exists a second equilibrium $\eta = (-\lambda_1, 0)$. The properties of η are the same as those of the 0-equilibrium except for the fact that one has to reverse the sign of λ_1.

3.3.2. Detection of one-homoclinic orbits

We now go on and investigate the bifurcation of one-homoclinic orbits to $W^c_{loc,\lambda}$ from Γ. We study the intersection of W^{cs}_λ and W^{cu}_λ in some cross-section Σ to Γ. Of course these manifolds may visit Σ many times. As in the first part of Chapter 2 our analysis now concerns only those pieces of the manifolds that visit Σ for the first time, since we are interested in one-homoclinic orbits. In a second step we analyse the asymptotic behaviour of these homoclinic orbits in detail by performing the *projection along stable fibres*. Fast decaying homoclinic orbits to the origin again play a distinguished role here. A discussion of their bifurcation reveals the problem to be of codimension two.

Since Γ is symmetric we have $\Gamma \cap \mathrm{Fix}\,(R) \neq \emptyset$. Thus, we can choose $\gamma(0) \in \mathrm{Fix}\,(R)$ and we introduce a cross-section Σ to Γ at $\gamma(0)$

$$\Sigma = \gamma(0) + Z,$$

where we can choose the space Z such that $RZ = Z$. This implies in particular that $\mathrm{Fix}\,(R) \subset Z$.

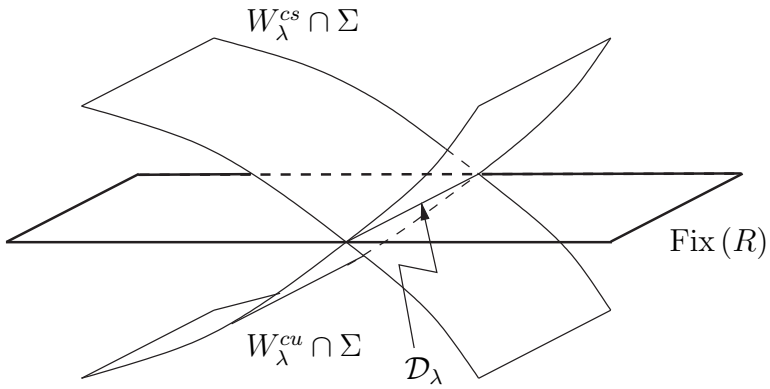

Figure 3.2.: Position of the traces of $W^{cs(cu)}_\lambda$ in Σ under Hypothesis 3.5

Recall that both W^{cs}_λ and W^{cu}_λ are $l+3$-dimensional. A simple count of dimensions shows that these manifolds can intersect transversally along orbits. The following transversality condition is crucial for our analysis.

Hypothesis 3.5. At $\gamma(0)$ we have $W^{cs}_{\lambda=0} \pitchfork W^{cu}_{\lambda=0}$.

We claim that from Hypothesis 3.5 we can gather all the information we need. First note that by standard arguments the transverse intersection of the manifolds will persist for λ sufficiently close to 0. Now, the traces of W^{cs}_λ and W^{cu}_λ in the cross section Σ are both two-dimensional. Their transverse intersection will therefore be a one-dimensional object, i.e. some curve $\mathcal{D}_\lambda$ in Σ. Furthermore, Hypothesis 3.5 implies that the traces of both $W^{cs}_{\lambda=0}$ and $W^{cu}_{\lambda=0}$ intersect Fix (R) transversally in Σ. Indeed, assuming this was not the case would amount to $(T_{\gamma(0)}W^{cs}_{\lambda=0} \cap Z) \subset \text{Fix}\,(R)$. But because of $RW^{cs}_\lambda = W^{cu}_\lambda$ this would yield $T_{\gamma(0)}W^{cs}_{\lambda=0} = T_{\gamma(0)}W^{cu}_{\lambda=0}$ in contradiction to Hypothesis 3.5. Repeating the arguments above we see that both W^{cs}_λ and W^{cu}_λ intersect Fix (R) in Σ in some curve. Hence, $\mathcal{D}_\lambda \subset \text{Fix}\,(R)$, see Figure 3.2 for an illustration. We formulate this result as a first lemma.

Lemma 3.1. *Under Hypotheses 3.1-3.5 equation (3.1) possesses a one-parameter family of symmetric homoclinic orbits to the manifolds $W^c_{loc,\lambda}$ for λ sufficiently small. This family of orbits intersects Σ in a smooth curve $\mathcal{D}_\lambda \subset Fix(R)$.*

Because of Hypothesis 3.5 the set of one-homoclinic orbits to $W^c_{loc,\lambda}$ does not depend on λ. But the structure within this set, for instance the number and type of homoclinic orbits to equilibria, will change. Fast decaying orbits again play a distinguished role here. To see this we use the invariant foliation of W^{cs}_λ into stable fibres, introduced in Section 2.4. We denote the fibre with base point $y \in W^c_{loc,\lambda}$ again by $M_{y,\lambda}$.

Let us first consider the stable fibre $M_{0,\lambda}$ of the origin. By the invariance property (2.30) of the foliation this fibre is invariant itself. It is therefore the *strong stable* manifold of

the 0-equilibrium (which coincides with the stable manifold for $\lambda_1 \leq 0$). Thus, a fast decaying homoclinic orbit exists if and only if $M_{0,\lambda}$ intersects W^{cu}_λ (or, equivalently, if it intersects $\mathrm{Fix}\,(R)$) in Σ. Indeed, a solution in the fibre would be homoclinic to 0 because of its symmetry established in Lemma 3.1 and would satisfies the exponential bound of Hypothesis 3.3, since it is contained in the strong (un)stable manifold of 0.

In order to consider a generic situation for the bifurcation of fast decaying orbits we impose a transversality condition with regard to the stable fibre $M_{0,\lambda}$. For this define

$$\mathfrak{M}_0 := \bigcup_{\lambda \text{ small}} M_{0,\lambda}, \qquad \mathfrak{W}^{cu} := \bigcup_{\lambda \text{ small}} W^{cu}_\lambda.$$

(Note that $\mathfrak{W}^{cu}$ is nothing but the extended version of the local manifold introduced in Section 3.3.1.) We demand the following.

Hypothesis 3.6. $\mathfrak{M}_0 \pitchfork \mathfrak{W}^{cu}$ in $\gamma(0)$ at $\lambda = 0$.

Let us discuss the consequences of Hypothesis 3.6. We can consider the intersection of $\mathfrak{M}_0$ and $\mathfrak{W}^{cu}$ in $\Sigma \times \mathbb{R}^l$ (recall that $\lambda \in \mathbb{R}^l$ in (3.1)). By counting dimensions one easily sees that Hypothesis 3.6 implies this intersection to be $(l-1)$-dimensional. Thus, we can consider (3.1) with parameters $(\lambda_1, \lambda_2) \in \mathbb{R}^2$. In a suitable unfolding fast decaying homoclinic orbits then exist on some curve in parameter space. With no loss of generality we can assume this curve to be the λ_1-axis.

Lemma 3.2. *Under Hypothesis 3.6 we can choose parameters $(\lambda_1, \lambda_2) \in \mathbb{R}^2$ such that the local bifurcation of the 0-equilibrium is described by (3.2) and such that (3.1) possesses a fast decaying homoclinic orbit if and only if $\lambda_2 = 0$.*

In order to investigate whether additional homoclinic orbits to 0 exist we follow the procedure in Section 2.4 and project the curve $\mathcal{D}_\lambda$ along stable fibres from Σ onto $W^c_{loc,\lambda}$. As before, this projection is injective and smooth. Thus, the image of $\mathcal{D}_\lambda$ under the projection is some curve $\mathcal{C}_\lambda$ which intersects the origin for $\lambda = 0$. Similar to Section 2.4 we impose the following transversality condition upon this curve.

Hypothesis 3.7. $\mathcal{C}_{\lambda=0} \pitchfork \mathrm{Fix}\,(R)$

In consequence we obtain the bifurcation diagram in Figure 3.3. This diagram shows the local behaviour in $W^c_{loc.\lambda}$ together with the curve $\mathcal{C}_\lambda$ in dependence of the parameters (λ_1, λ_2). We recall that λ_1 has been chosen to control the local bifurcation of 0. The parameter λ_2 has been introduced to unfold the bifurcation of fast decaying homoclinic orbits. Such orbits exist if $\mathcal{C}_\lambda$ intersects the origin. Hence, λ_2 controls the position of $\mathcal{C}_\lambda$ in $W^c_{loc,\lambda}$. Since the stable fibres depend smoothly on λ and because of Hypothesis 3.6, the curve $\mathcal{C}_\lambda$ moves linearly to lowest order with respect to λ_2.

Again, points of intersection of $\mathcal{C}_\lambda$ with bounded orbits in $W^c_{loc,\lambda}$ are of interest. First note that all homoclinic orbits to $W^c_{loc,\lambda}$ are R-symmetric by Lemma 3.1. Hence, the

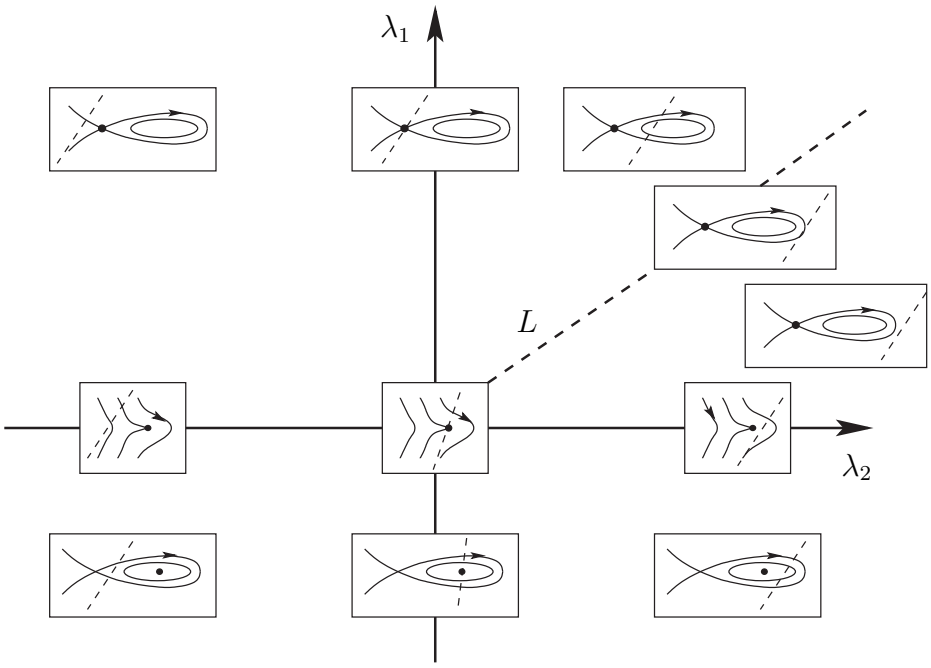

Figure 3.3.: Bifurcation diagram for one-homoclinic orbits near Γ. The dashed line in each small box shows the curve $\mathcal{C}_\lambda$. On the curve L a saddle-node bifurcation of slowly decaying homoclinic orbits to 0 occurs. A similar curve exists for homoclinic orbits to η but is not shown in the diagram.

invariance (2.30) of the foliation of W^{cs}_λ implies that points of intersection of $\mathcal{C}_\lambda$ with periodic orbits in $W^c_{loc,\lambda}$ correspond to homoclinic orbits to these periodic orbits. Similarly, there exists a fast decaying homoclinic orbit if and only if $0 \in \mathcal{C}_\lambda$ (this has already been observed above!). But homoclinic orbits to equilibria also exist, if $\mathcal{C}_\lambda$ intersects orbits in $W^c_{loc,\lambda}$ which are themselves asymptotic to an equilibrium. For instance, points of intersection of $\mathcal{C}_\lambda$ with the (small) homoclinic orbit Υ yield (large) homoclinic orbits to equilibria. We note that for such orbits the asymptotic behaviour is essentially governed by the corresponding solution within $W^c_{loc,\lambda}$.

It is now straightforward to discuss the bifurcation diagram in Figure 3.3. Let us first focus on homoclinic orbits to the origin. We first consider the situation for $\lambda_1 < 0$. Here, 0 is a saddle centre and we find that $\mathcal{C}_\lambda$ intersects the origin if and only if $\lambda_2 = 0$. This intersection corresponds to a fast decaying homoclinic orbit. For $\lambda_2 \neq 0$ the curve $\mathcal{C}_\lambda$ only intersects periodic orbits near 0, which represents homoclinic orbits to these periodic orbits. We conclude that for $\lambda_2 \neq 0$ no homoclinic orbits to the origin exist. This result is also compatible with the fact that symmetric homoclinic orbits to a saddle centre are of codimension-one in the class of reversible systems.

For $\lambda_1 = 0$ we find homoclinic orbits when $\lambda_2 \leq 0$. In fact, for $\lambda_2 = 0$ this is implied

by Hypothesis 3.2, while for $\lambda_2 < 0$ we see that $\mathcal{C}_\lambda$ intersects the curve of points which are asymptotic to the origin within $W^c_{loc,\lambda}$ as $t \to \infty$. This intersection represents an algebraically decaying homoclinic solution to 0. An elementary calculation for the normal form (3.2) shows that this solution will eventually decay like $1/t^2$ for $t \to \pm\infty$.

Let us now discuss the bifurcations when $\lambda_1 > 0$. Here the origin is a real saddle and for $\lambda_2 = 0$ there exists a fast decaying homoclinic orbit to this saddle. This orbit lies in the strong (un)stable manifold of 0 and one would expect a reversible orbit flip bifurcation when the parameters are varied, [74]. Indeed, we find this in Figure 3.3. For $\lambda_2 < 0$ the curve $\mathcal{C}_\lambda$ intersects the stable manifold of 0 (in $W^c_{loc,\lambda}$) which shows the existence of a slowly decaying homoclinic orbit. For $\lambda_2 > 0$ sufficiently small we actually find two points of intersection of $\mathcal{C}_\lambda$ with the small homoclinic orbit Υ in $W^c_{loc,\lambda}$. (Note that this is a consequence of Hypothesis 3.7.) Therefore two slowly decaying homoclinic orbits to the origin exist. However, a closer examination shows that the upper point of intersection corresponds to an orbit which first follows Γ for some time, but when the orbit is close to the centre manifold, it does not approach the 0-equilibrium directly but runs along Υ. We therefore not view this orbit as being one-homoclinic to 0 since it comprises a gluing between Γ and Υ. Doing so, we find agreement with general results concerning the reversible orbit flip bifurcation derived in [74] which show that generically only a single one-homoclinic orbit exists.

Finally, another interesting bifurcation occurs when λ_2 is increased further. We find a curve L on which the two points of intersection of $\mathcal{C}_\lambda$ with Υ merge and vanish. This scenario corresponds to a saddle-node bifurcation of symmetric homoclinic orbits as was analysed in [9, 59]. Such a bifurcation occurs when a homoclinic orbit becomes degenerate, i.e. when the tangent spaces of the stable and unstable manifold of 0 have another common direction along the orbit (in the four-dimensional case they thus agree). For λ_2 large enough there exists no homoclinic orbit to 0. Let us give some explanation concerning the properties of the curve L: First of all we recall that the motion of $\mathcal{C}$ in $W^c_{loc,\lambda}$ is linear in λ_2. On the other hand, it is an easy calculation using the normal form (3.2) that the size of the small homoclinic orbit Υ varies linear in λ_1. Therefore, we conclude that L is the graph of some function $\lambda_1 = a\lambda_2 + o(\lambda_2)$ with $a > 0$, $\lambda_2 \geq 0$. We summarize the results in a theorem.

Theorem 3.3 (One-homoclinic orbits to 0 in the general case). *Consider (3.1) under the Hypotheses 3.1 - 3.7 with parameters $\lambda = (\lambda_1, \lambda_2)$ chosen in accordance with the normal form (3.2) and with Lemma 3.2. Then fast decaying homoclinic orbits to 0 exist if and only if $\lambda_2 = 0$. For $\lambda_1 < 0$ no other one-homoclinic orbits exist.*

In the case $\lambda_1 = 0$ we find one homoclinic orbit to the 0-equilibrium if $\lambda_2 \leq 0$ which is algebraically decaying for $\lambda_2 < 0$.

For $\lambda_1 > 0$, $\lambda_2 \leq 0$ we find one homoclinic orbit to the 0-equilibrium. For $\lambda_2 > 0$ there exist two homoclinic orbits which coalesce in a saddle-node bifurcation on some curve $L := \{(\lambda_2, \lambda_1) : \lambda_2 \geq 0,\ \lambda_1 = a\lambda_2 + o(\lambda_2)\}$, with some $a > 0$.

An equivalent theorem describes homoclinic orbits to η, the second equilibrium in $W^c_{loc,\lambda}$. The reason for this is the symmetry of the bifurcation diagram in Figure 3.3 and the symmetry in $W^c_{loc,\lambda}$, where the properties of 0 and η are exchanged if the sign of λ_1 is reversed. We leave further details to the reader.

Let us finally discuss how homoclinic orbits to periodic orbits in $W^c_{loc,\lambda}$ bifurcate from the primary orbit Γ. If $\lambda_1 < 0$, $\lambda_2 = 0$ there exists a homoclinic orbit to the saddle centre equilibrium 0, and every periodic orbit in $W^c_{loc,\lambda}$ is connected to itself by two homoclinic orbits. For $\lambda_2 \neq 0$ there exists a critical amplitude A, depending linearly on λ_2, such that we only find homoclinic orbits to periodic orbits with an amplitude greater than A. The range of λ_2 for which homoclinic orbits to periodic orbits exist is bounded by the saddle-node curve for homoclinic orbits to η and by the reversible orbit flip curve for homoclinic orbits to η. Similar statements apply to parameter values $\lambda_1 > 0$ if the roles of the equilibria 0 and η are again exchanged.

3.4. Cases with $\mathbb{Z}_2$-symmetry

In this section we consider the situation under the additional assumption that (3.1) is $\mathbb{Z}_2$-symmetric with respect to some involution S (commuting with R), that is we have

$$Sf(x,\lambda) = f(Sx,\lambda), \quad \forall (x,\lambda). \tag{3.3}$$

Since the composition $Q := R \circ S$ gives another reversibility, this is equivalent to considering systems that are reversible with respect to two involutions. Hence, this is the situation we have encountered in Chapter 2. We will see, however, that the location of the invariant subspace $\mathrm{Fix}\,(S)$ is crucial for the bifurcation results. And of course, we will consider cases that differ from the ones studied in Chapter 2.

3.4.1. Odd symmetry

We deal with (3.1) under Hypotheses 3.1 - 3.3 and assume additionally

Hypothesis 3.8. f is odd-symmetric, that is $f(x,\lambda) = -f(-x,\lambda)$ for all (x,λ).

Equivalently we could have required f to be reversible with respect to $Q := -R$, as well. We remark that since $S = -id$ we have $\mathrm{Fix}\,(S) = \{0\}$.

Hypothesis 3.8 has consequences for the local bifurcation of the equilibrium 0. Now we have to consider systems (and therefore normal forms) in $W^c_{loc,\lambda}$ that are reversible with respect to the involutions R and $-R$. Therefore the local behaviour is the same as in Chapter 2, and is governed by the general normal form (2.7). Under Hypothesis 2.4 we consequently obtain the two normal forms (2.8), (2.9) for the local bifurcation of 0, which differ in the sign of the cubic term and which give rise to a reversible pitchfork bifurcation of eye type and of figure-eight type, respectively.

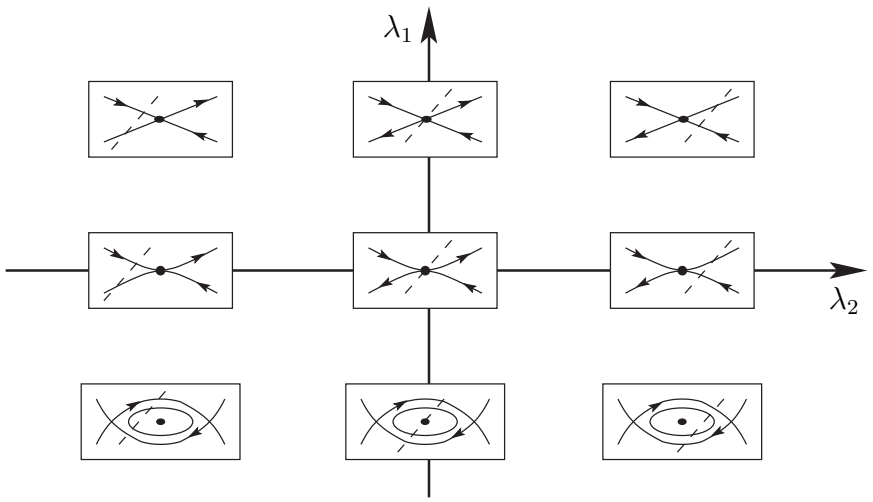

Figure 3.4.: Bifurcation diagram for one-homoclinic orbits near Γ in case of the normal form (2.8). The dashed line in each box shows the curve $\mathcal{C}_\lambda$.

We can now proceed with the analysis of bifurcations from Γ as in Section 3.3.2. But for that two things are important. First, Hypothesis 3.8 implies that $-\Gamma$ is another fast decaying homoclinic orbit to the origin at $\lambda = 0$. Second, we again impose Hypothesis 3.5, which by symmetry also holds for points on $-\Gamma$. Thus, we can deal with the orbit Γ alone and infer all results for $-\Gamma$ using the $\mathbb{Z}_2$-symmetry of (3.1).

For the orbit Γ the analysis of the last section can be performed again. Lemma 3.1 thus shows the existence of a manifold of homoclinic orbits to $W^c_{loc,\lambda}$ of which all orbits are R-symmetric. Projecting along stable fibres in this case we also get a curve $\mathcal{C}_\lambda$ for which the non-degeneracy Hypothesis 3.7 is assumed to hold. Doing so, we derive two bifurcation scenarios, depending on which normal form describes the bifurcation of 0. The corresponding diagrams are given in Figure 3.4 and 3.5.

As before, these diagrams allow us to give a complete description of the homoclinic orbits to $W^c_{loc,\lambda}$. Exclusively considering homoclinic orbits to 0 and we obtain the following theorem.

Theorem 3.4. *Consider (3.1) under the Hypotheses 3.1 - 3.8 with parameters $\lambda = (\lambda_1, \lambda_2)$ chosen in accordance with the normal form (2.8), (2.9) and Lemma 3.2. Then fast decaying homoclinic orbits to the origin near Γ exist if and only if $\lambda_2 = 0$. For $\lambda_1 < 0$ no other one-homoclinic orbits exist.*

In case the normal form for the local bifurcation is given by (2.8) then there exist additional homoclinic orbits for all $\lambda_1 \geq 0$, $\lambda_2 \neq 0$ which are algebraically decaying when $\lambda_1 = 0$.

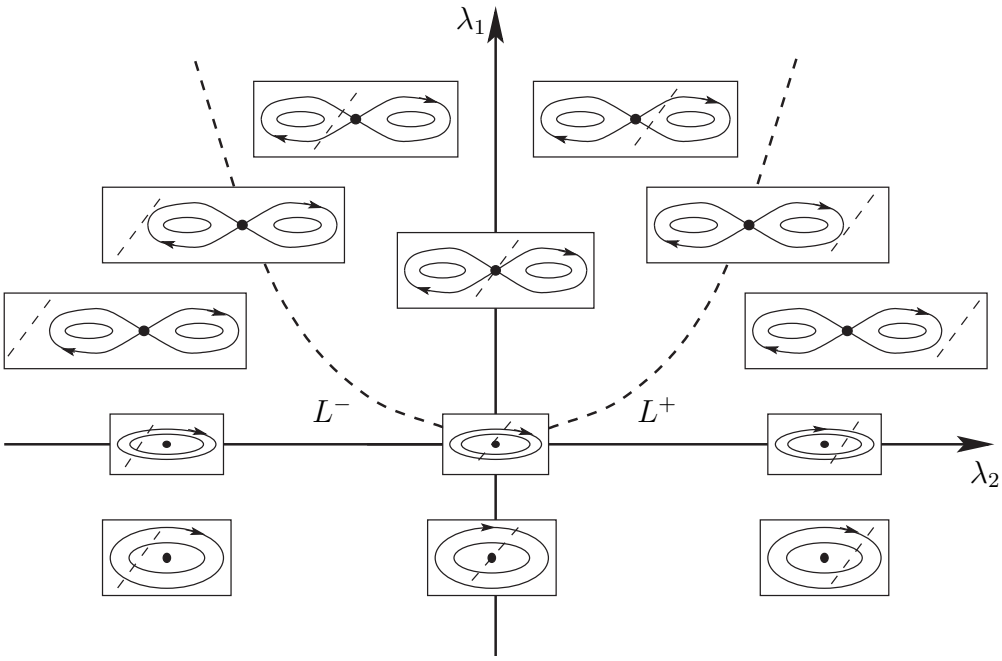

Figure 3.5.: Bifurcation diagram for one-homoclinic orbits near Γ in case of the normal form (2.9). The dashed line in each box shows the curve $\mathcal{C}_\lambda$.

When the local bifurcation is described by (2.9) then additional orbits only exist for $\lambda_1 > 0$. *For* $|\lambda_2|$ *sufficiently small there exist two homoclinic orbits which coalesce in a saddle-node bifurcation at some curve* $L = L^+ \cup L^-$ *given by* $\lambda_1 = a\lambda_2^2 + o(\lambda_2^2)$, *with some* $a > 0$.

By symmetry the assertions are also valid near $-\Gamma$.

Remark 3.1. For the figure-eight case we need again Hypothesis 3.7 to derive the bifurcation diagram. Furthermore, for the normal form (2.9) the size of the figure-eight depends quadratically on λ_1. More precisely, let $v_{1,2} := (\pm v, 0)$ denote the two points of the figure-eight $\Upsilon_1 \cup \Upsilon_2$ which have the largest respectively smallest y_1-component. Then we find that $v^2 = 2\lambda_1$. This explains the shape of the 'saddle-node-curves' $L^\pm$ in Figure 3.5.

3.4.2. $\mathbb{Z}_2$-symmetry with $W^c_{loc,\lambda} \subset \mathsf{Fix}\,(S)$

We are now interested in the case when the fixed space of S is non-trivial. That is we consider (3.1) under Hypotheses 3.1 - 3.3 and assume in addition that

Hypothesis 3.9. There exists an involution $S : \mathbb{R}^4 \to \mathbb{R}^4$ commuting with R and with $\dim(\mathrm{Fix}\,(S)) = 2$, such that (3.3) is fulfilled.

As remarked before, the map $Q := S \circ R$ induces another reversing symmetry for (3.1). We remark that, within $\mathrm{Fix}\,(S)$, the involutions Q and R agree.

In Chapter 2 we have considered the situation where $\Gamma \subset \mathrm{Fix}\,(S)$. We now deal with the other possibility, namely that the symmetry affects the local bifurcation. Denoting the centre eigenspace of $D_1 f(0,0)$ by E^c, let us assume that

Hypothesis 3.10. $E^c \subset \mathrm{Fix}\,(S)$.

Under Hypothesis 3.9 we can derive a bifurcation diagram for one-homoclinic orbits near Γ in precisely the same manner as before. First, we see that within $W^c_{loc,\lambda} \subset \mathrm{Fix}\,(S)$ the vector field is reversible with respect to *one* involution. Therefore the equilibrium 0 generically bifurcates in a transcritical bifurcation as in Section 3.3 above. The corresponding normal form for the local bifurcation is given by (3.2) and the local bifurcation diagram is shown in Figure 3.1.

For the homoclinic orbit Γ Hypothesis 3.10 yields that $Q\Gamma \neq \Gamma$, i.e. Γ is *not* symmetric with respect to Q. Indeed, assuming that Γ was Q-symmetric we would have $\gamma(0) \in \mathrm{Fix}\,(R) \cap \mathrm{Fix}\,(Q)$, i.e. $\gamma(0) \in \mathrm{Fix}\,(S)$. But this results in $\Gamma \subset \mathrm{Fix}\,(S)$, which is forbidden by Hypothesis 3.10. We therefore conclude that $Q\Gamma$ is a second homoclinic orbit of (3.1).

Precisely as in Section 3.4.1 we can now consider each orbit separately and then immediately apply the results of Section 3.3.2. Thus the bifurcation diagram for one-homoclinic orbits in Figure 3.3 is valid for both Γ and $Q\Gamma$. So, we obtain the next theorem.

Corollary 3.5. *Consider (3.1) under Hypotheses 3.1 - 3.7, and Hypotheses 3.9, 3.10. Then $Q\Gamma$ is a second homoclinic orbit to 0 at $\lambda = 0$ and Theorem 3.3 applies to both orbits Γ and $Q\Gamma$.*

Remark 3.2. A completely analogous result is valid when the local bifurcation of $x = 0$ is described by the normal forms (2.8) or (2.9). This case is non-generic in our general setup. It could, however, arise when we assume an additional symmetry within the subspace $\mathrm{Fix}\,(S)$. Then the bifurcation of one-homoclinic orbits from Γ is described by Theorem 3.4.

3.5. Reversible Hamiltonian systems

We now turn to systems that are both reversible and Hamiltonian. This class of systems is of particular importance in applications since many mechanical or optical problems lead to the study of ODEs that are both reversible and Hamiltonian. (We also encounter this in the examples treated below.)

We show below that the basic transversality condition, Hypothesis 3.5, cannot be satisfied in the class of Hamiltonian systems, i.e. such systems are non-generic in the sense

of this chapter. It is nevertheless possible to prove that the previously obtained results about bifurcating symmetric orbits are necessarily valid in Hamiltonian systems. (There may, however, bifurcate non-symmetric orbits, which is not the case in generic reversible systems.) Therefore, in applying the theory to a specific reversible Hamiltonian system, we do not have to check whether Hypothesis 3.5 is fulfilled, which usually is a serious obstacle.

So let us consider (3.1) under Hypotheses 3.1 - 3.3 and demand in addition that

Hypothesis 3.11. There exists a function $H : \mathbb{R}^4 \times \mathbb{R}^2 \to \mathbb{R}$ such that (3.1) can be written as

$$\dot{x} = J \cdot \nabla H(x, \lambda), \tag{3.4}$$

where

$$J = \begin{pmatrix} 0 & I \\ -I & 0 \end{pmatrix}$$

denotes the standard symplectic structure on $\mathbb{R}^4$.

A well-known property of (3.4) is that the Hamilton function H is a first integral for the equation, i.e. it is constant along orbits of the system. It is this conservative character of the equation which is of relevance for the following analysis. We also note that the reversibility of (3.4) is reflected by the fact that $H \circ R = H$.

Proceeding as usual we find that the local bifurcation of 0 in $W^c_{loc,\lambda}$ is described by the normal form (3.2). The determination of homoclinic orbits to $W^c_{loc,\lambda}$, however, is difficult. Similar to the situation in Chapter 2 the property of (3.4) being Hamiltonian imposes additional restrictions for $W^{cs(cu)}_\lambda$ and does not allow our basic Hypothesis 3.5 to be fulfilled. To see this note that the cross-section Σ is smoothly foliated by level-sets $\mathcal{H}_h$ of the Hamiltonian H. Each of these intersects the space $\mathrm{Fix}\,(R)$ transversally and with no loss of generality we can assume them to be straightened out, i.e. $\mathcal{H}_h \subset T\mathcal{H}_0$. (Here we assume that the equilibrium is contained in the zero level set $\mathcal{H}_0$ of H.)

In addition, Lemma 3.2 implies that for $\lambda_1 < 0$, $\lambda_2 = 0$ there exists a homoclinic orbit to the saddle centre 0. Let us consider the consequences. Restricted to the centre manifold the Hamilton function H has a local extremum, say minimum. If $H(0) = 0$ this implies that all points in $W^{cs(cu)}$ take non-negative values of H which in turn implies that the traces of $W^{cs(cu)}$ in Σ lie 'on one side' of the trace of $\mathcal{H}_0$ in Σ. This observation shows that the tangent spaces of both manifolds at $\gamma(0)$ are contained in the tangent space of $\mathcal{H}_0$; see [62] for a rigorous proof and Figure 3.6 for an illustration. Clearly, the same relations must be found for $\lambda = 0$ such that we obtain the next lemma.

Lemma 3.6. *Consider (3.4) under Hypotheses 3.1 - 3.3. Then*

$$T_{\gamma(0)} W^{cs}_{\lambda=0} = T_{\gamma(0)} W^{cu}_{\lambda=0}$$

and $T_{\gamma(0)} W^{cs}_{\lambda=0} \pitchfork \mathit{Fix}(R)$.

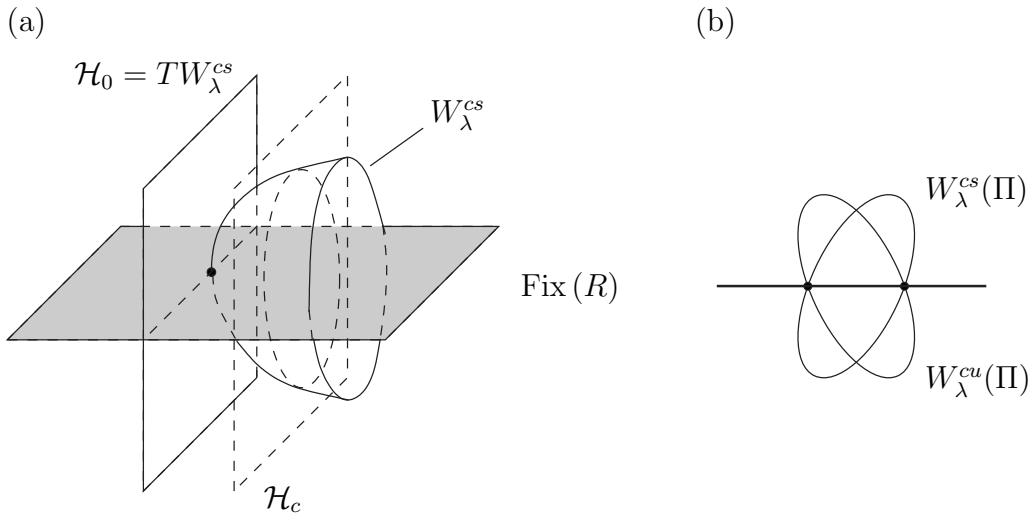

Figure 3.6.: Situation in Σ in the Hamiltonian case: For parameter values where a homoclinic orbit to a saddle centre equilibrium exists the trace of W^{cs}_λ is tangent to the zero level set $\mathcal{H}_0$ of the Hamiltonian and intersects Fix (R) transversally. (By reversibility the same statement is valid for W^{cu}_λ.) Panel (a) of the picture shows a sketch of the intersection the stable and unstable manifold of a periodic orbit Π in some level set $\mathcal{H}_c$ of H in Σ. Note that in addition to the intersection points in Fix (R) these manifolds generically intersect in two further points giving rise to a pair of non-symmetric solutions as in (b).

Because of the non-transverse intersection of $W^{cs}_{\lambda=0}$ and $W^{cu}_{\lambda=0}$ we expect that both R-symmetric and non-symmetric solutions bifurcate from Γ, compare again with Figure 3.6. In the following we concentrate on the bifurcation of symmetric orbits.

The existence of symmetric homoclinic orbits can be discussed in the same way as before. Lemma 3.6 implies the existence of a manifold of homoclinic orbits to $W^c_{loc,\lambda}$ which intersects the cross-section Σ in some curve $\mathcal{D}_\lambda$. Hence, we are in precisely the same situation as in Section 3.3.2 and immediately obtain the final theorem.

Theorem 3.7. *Consider the Hamiltonian system (3.4) under Hypotheses 3.1 - 3.3, and Hypotheses 3.6, 3.7. Then the existence of R-symmetric homoclinic orbits near Γ is described by Theorem 3.3.*

Remark 3.3. In the same way one can discuss the different cases in Section 3.4 under the additional hypotheses that the systems are Hamiltonian. One then finds that the main theorems in the corresponding sections describe the existence of symmetric homoclinic orbits near the primary orbit Γ.

3.6. Three numerical examples

We shall illustrate our theoretical results with numerical computations for three examples, belonging to the class of reversible Hamiltonian systems. First, we deal with a reversible fourth-order equation arising in a water-wave problem which is part of the general family of 5th-order KdV models. Afterwards, we study two problems from nonlinear optics involving reversible and $\mathbb{Z}_2$-symmetric systems. For the numerical investigations we have used the methods for homoclinic continuation implemented in AUTO/HomCont [32]. Let us provide some information on the underlying physical problems before we turn to the specific problems.

3.6.1. Embedded and gap solitons

There has been much interest in recent years in the existence of localised coherent structures in nonlinear media, especially in optics. A particularly important class of localised structure are solitary waves, or 'solitons'. In situations governed by higher-order or multi-component partial differential equation (PDE) models in 1+1 dimensions, the spectrum of linearized waves generally has at least two branches. If these branches do not fill out the entire possible spectrum of wave frequencies, then one has the possibility of a gap in the linear spectrum where exponentially localised solutions can exist, so called *gap solitons* [31]. Such solutions can be linearly stable solutions of the PDE in that they are attractors for a range of initial data. They are also typically structurally stable, in that they exist for a range of frequency and other parameter values.

In contrast, an *embedded soliton* (ES) is a solitary wave which exists despite having its internal frequency in resonance with linear waves. Specifically, they occur in a two-component model when the dispersion relation has only one branch. Generally, such solitons should not exist , one finding instead (delocalized) quasi-solitons or 'generalized solitary waves' with non-vanishing oscillatory tails (radiation component) [7]. However, at some special values of the internal frequency, the amplitude of the tail may exactly vanish, giving rise to an isolated soliton embedded into the continuous spectrum. Hence, at these discrete values embedded solitons exist as *codimension-one* solutions [93, 18]. Another interesting feature of ESs is that they may at best be only linearly neutrally stable, being subject to a weak one-sided algebraic instability, see e.g. [93, 71]. That is, if one makes an energy increasing perturbation then via the shedding of radiation, the initial condition relaxes algebraically back to the solitary wave. In contrast, energy decreasing perturbations cause the solitary wave to decay algebraically away. The existence of embedded solitons has been established in a number of physical models including generalized 5th-order Korteweg-de Vries (KdV) equations [56, 14, 15, 95], coupled KdV equations [36], in nonlinear Schrödinger (NLS) equations with higher-order derivatives [12, 35] and in various coupled NLS-type equations arising in nonlinear optics [93, 17, 19].

In the usual way, soliton solutions in each of these example PDEs reduce to homoclinic orbits of ordinary differential equations (ODEs) via a travelling-wave or steady-state reduction. The ODEs typically have the structure of being fourth-order, reversible and Hamiltonian. The parameter region that supports embedded solitons corresponds to when the origin (the trivial equilibrium) in such an ODE system is a saddle centre. Here, one two-dimensional component gives rise to the imaginary eigenvalues $\pm i\omega$ (corresponding to a continuous branch in the linear spectrum of the PDE system), and the other to real eigenvalues $\pm\mu$ (corresponding to a gap in the linear spectrum). In contrast, the gap soliton parameter region is where the eigenvalues of the origin are purely real.

Hence, our general studies so far describe precisely what happens as we trace a path of embedded solitons up to a parameter value $\omega = 0$ at which it passes over into being a gap soliton. Indeed, within the unfolding (3.1) of the degenerate situation at $\lambda = 0$ we find this process on the curve $\lambda_2 = 0$ where fast decaying homoclinic orbit exists and where 0 changes its type from a saddle centre (for $\lambda_1 < 0$) to a real saddle ($\lambda_1 > 0$). Bifurcating homoclinic orbits to the invariant manifolds $W^c_{loc,\lambda}$ represent additional solitary waves (homoclinic orbits to equilibria) or generalized solitary waves (homoclinic orbits to periodic orbits). Of particular importance in the following examples are solitary waves that decay to 0.

3.6.2. A fifth-order KdV equation

In this section we illustrate the results of Section 3.3 with numerical studies for a fourth-order equation arising in water-wave theory. We are concerned with the existence of solitary wave solutions for the following fifth-order long-wave equation for gravity-capillary water waves,

$$\mathfrak{r}_\tau + \frac{2}{15}\,\mathfrak{r}_{xxxxx} - b\,\mathfrak{r}_{xxx} + 3\,\mathfrak{r}\mathfrak{r}_x + 2\,\mathfrak{r}_x\mathfrak{r}_{xx} + \mathfrak{r}\mathfrak{r}_{xxx} = 0.$$

Which is an example of a general family of 5th-order KdV equations, see [56, 95]. Making the travelling wave ansatz $r(x - a\tau) = \mathfrak{r}(\tau, x)$, introducing $t := x - a\tau$ and integrating the resulting ODE once, we obtain a fourth-order equation for r

$$\frac{2}{15}r^{iv} - br'' + ar + \frac{3}{2}r^2 - \frac{1}{2}(r')^2 + [rr']' = 0, \tag{3.5}$$

where a prime denotes differentiation with respect to t. Homoclinic orbits to the origin of (3.5) were intensively studied in [15], using a combination of analytical and numerical techniques.

Here we are interested in the situation for $a = 0$ and $b = 2$, since for these parameter values the fundamental Hypotheses 3.1 - 3.3 are fulfilled. First note, that for all parameter values a, b equation (3.5) is reversible with respect to

$$R : (r, r', r'', r''') \mapsto (r, -r', r'', -r''').$$

Note also, that one can introduce variables such that (3.5) may be written as a Hamiltonian system; see [15] for details. Moreover, the origin is an equilibrium for all a, b which is easily seen to possess a double non-semisimple eigenvalue 0 and a pair of real eigenvalues if $a = 0$, $b > 0$. Increasing the parameter a through 0, the equilibrium undergoes a transcritical bifurcation described by the normal form (3.2). The equilibrium turns from a saddle centre ($a < 0$) into a real saddle ($a > 0$). In particular, for $a > 0$ a small homoclinic orbit emerges which corresponds to the famous Korteweg-de Vries solitary wave (after an appropriate rescaling of the system).

Finally, in [15] the following explicit homoclinic solution

$$r_h(t) = 3\left(b + \frac{1}{2}\right)\operatorname{sech}^2\left(\frac{\sqrt{3}}{2}(2b+1)t\right)$$

of (3.5) is found for parameter values $a = 3/5 \cdot (2b+1)(b-2)$, $b \geq -1/2$. In particular, r_h exists for $a = 0$ and $b = 2$ where it is a fast decaying homoclinic solution. So the results of Sections 3.3 and 3.5 should apply to this situation.

In fact, numerical studies in [15] already revealed the orbit flip bifurcation of the primary homoclinic orbit for $a > 0$. Also the existence of the curve L, where the saddle-node bifurcation of homoclinic orbits occurs, could be numerically verified. This curve can be approximated by taking different values of $a > 0$, b for which r_h exists and performing a numerical continuation of the homoclinic solution with decreasing b and fixed a. For example, for $a = 0.1$ we can continue the starting solution with decreasing b until we find a limit point at $b^* = 1.83226$. In Figure 3.7 we present the bifurcation diagram together with corresponding plots of solutions at the indicated points. We have found comparable results for all tested parameter values.

The results in Figure 3.7 show excellent agreement with the general theory. Indeed, we find that in the reversible orbit flip bifurcation two homoclinic orbits emerge, of which one is composed of the fast decaying solution and the (small) 'KdV'-homoclinic orbit, see panel b) in Figure 3.7. The two homoclinic orbits coalesce in a saddle-node bifurcation, and we find that the corresponding bifurcation curve L is essentially linear.

Also the existence of an algebraically decaying solution for $a = 0$, $b > 2$ can be verified numerically. In Figure 3.7 such a solution is shown for parameter values $a = 0$, $b = 2.5$. Another illustration is given in Figure 3.8 where we compare this solution to the exponentially decaying solution at $a = 0.1$, $b = 2.5$. The plots in part c) of this figure indicate that the solution for $a = 0$ decays with a quadratic rate in accordance to results of Section 3.3.

So, for equation (3.5) we can compute everything that has been predicted by the theory. We remark that for this example we have not made use of the reversible symmetry of the equation (which is possible in AUTO). Nevertheless, all solutions found have been symmetric under time-reversal which suggests that only symmetric one-homoclinic solutions bifurcate from the primary homoclinic orbit. This is of interest since the results in Section 3.5 did not concern non-symmetric solutions.

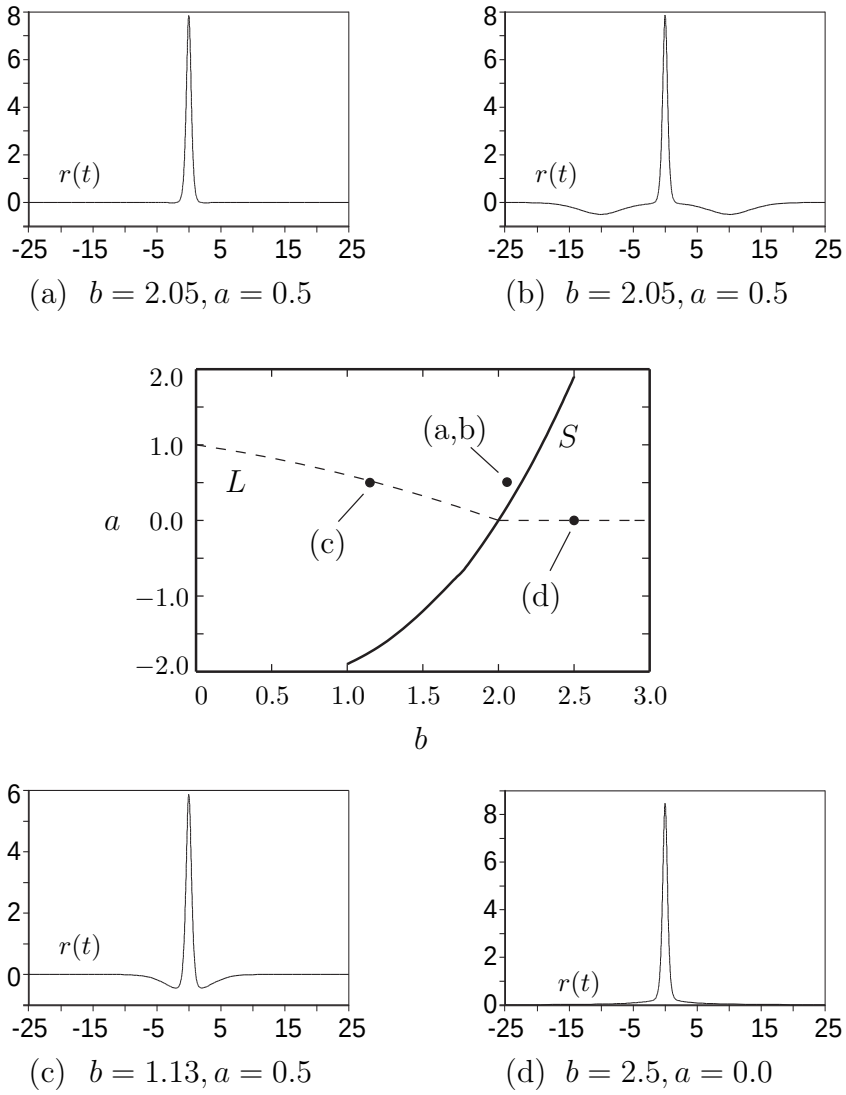

Figure 3.7.: Bifurcation diagram for (3.5) as computed with AUTO. On the solid curve S the analytically known solution r_h exists. For $a > 0$ this curve describes a reversible orbit flip. After decreasing b two homoclinic solutions can be found. In a) the slow decaying solution after the orbit flip is shown. In b) we show a plot of the second solution which is composed of the primary orbit and the small 'KdV' homoclinic solution. These two orbits coalesce in a saddle-node bifurcation on the curve L to the left of S (see panel c)). For parameter values $b > 2$, $a = 0$, represented by the dashed line to the right of S, computations with AUTO show the existence of an algebraically decaying homoclinic solution as depicted in d) see also Figure 3.8.

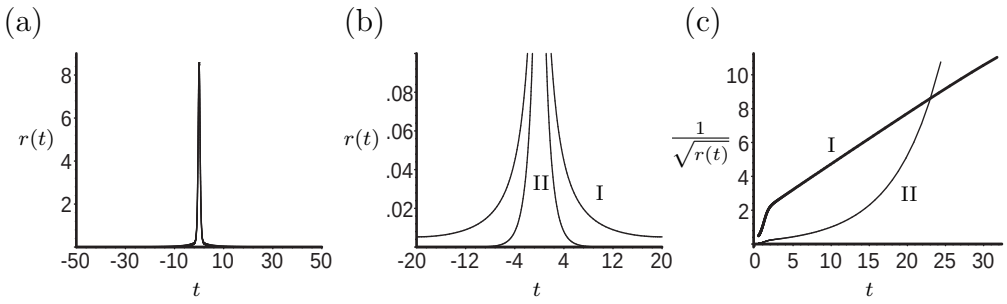

Figure 3.8.: Comparison of the solutions for $a = 0$, $b = 2.5$, (I), and $a = 0.1$, $b = 2.5$, (II). Panels (a) and (b) show plots of the solutions. In (c) the reciprocal of the square-root of the solutions is plotted. Here the linearity of (I) as $t \to \infty$ reveals the quadratic rate of decay for the solution whereas (II) decays at some higher (exponential) rate. Note that the solution (II) in (c) is multiplied by a factor 1/10 in order to view it on the same set of axes.

Note that we do not attempt to prove any of the results for (3.5) rigorously. This would amount to proving that the equation fulfills the non-degeneracy conditions imposed for the general analysis. In particular regarding Hypothesis 3.7 this is a major difficulty. But since we find perfect agreement of the numerical and the theoretical results we could argue the other way around and claim that (3.5) is a generic Hamiltonian system in the sense of this chapter. So our analysis can explain the numerical results obtained for the equation.

3.6.3. Two examples from nonlinear optics

In connection with the general results of Section 3.4.1 and 3.4.2 we study two examples which possess an additional $\mathbb{Z}_2$-symmetry. Both deal with the existence of embedded solitons in nonlinear optical media.

An extended massive Thirring model

We first consider an extended massive Thirring model that describes solitons in an optical media equipped with Bragg-grating, see [20] and references therein. The model is described by the following systems of complex PDEs

$$\begin{aligned} iu_t + iu_x + Du_{xx} + (\sigma|u|^2 + |v|^2)u + v &= 0 \\ iv_t - iv_x + Dv_{xx} + (\sigma|v|^2 + |u|^2)v + u &= 0. \end{aligned}$$

Looking for steady state solutions via $u(x,t) = e^{i\chi t}U(x)$, $v(x,t) = e^{-i\chi t}U(x)$ we can perform scalings and assume with no loss of generality that $\sigma = 0$ and $U = V^*$, where

V^* denotes the complex conjugate of V. Doing so, we obtain the single complex ODE

$$DU'' + iU' + \chi U + U|U|^2 + U^* = 0, \tag{3.6}$$

which is reversible with respect to

$$R : (U, U') \mapsto (U^*, -(U')^*)$$

and has odd symmetry

$$S : (U, U') \mapsto -(U, U').$$

We note again that one can write (3.6) as a Hamiltonian system in $\mathbb{R}^4$.

For $|\chi| < 1$ the origin is a saddle centre equilibrium of (3.6) and at $\chi = -1$ it undergoes a reversible pitchfork bifurcation of figure-eight-type to become a real saddle itself.

In [17] it was found numerically that there are three curves in the (D, χ)-plane at which embedded solitons exist. Each of these curves can be extended to parameter values $\chi < -1$, so that there exist three points in the parameter plane around which the results of Section 3.4.1 apply, see Figure 3.9. (Note that because of the odd symmetry of (3.6) embedded solitons, i.e. homoclinic orbits, come in pairs. But obviously it suffices to consider one of the two orbits for our purposes.) We restrict attention to one of the points and choose the point $(D^*, \chi^*) = (1.5, -1)$ with the largest D-value for our computations.

In accordance with Theorem 3.4 we can detect a reversible orbit flip bifurcation of the primary homoclinic orbit and two curves where a saddle-node bifurcation of homoclinic orbits occur. In Figure 3.10 the bifurcation diagram including plots of the real parts of the corresponding homoclinic solutions is shown. In the computations we have explicitly used the reversing symmetry of (3.6). As for example (3.5) above we find that the reversible orbit flip bifurcation of the primary orbit also gives rise to a solution which is composed of the fast decaying solution and a small homoclinic solution in the centre manifold. Note, however, that for (3.6) there are two different small homoclinic solutions and which one is chosen depends on whether D is decreased or increased.

We remark that for this example the computations have to be performed very close to the critical parameter values to find agreement with the general bifurcation results concerning the shape of the "saddle-node curves". On the other hand, in order to illustrate the different types of bifurcating solutions it is necessary to compute the solutions in Figure 3.10 for larger parameter values. This explains why the bifurcation diagram in this figure is only schematic for $\chi < -1.00005$.

A second-harmonic-generation system

We end this section with computations for the system in connection to which the term embedded solitons was used first. In [93] solitary waves appearing in an optical medium

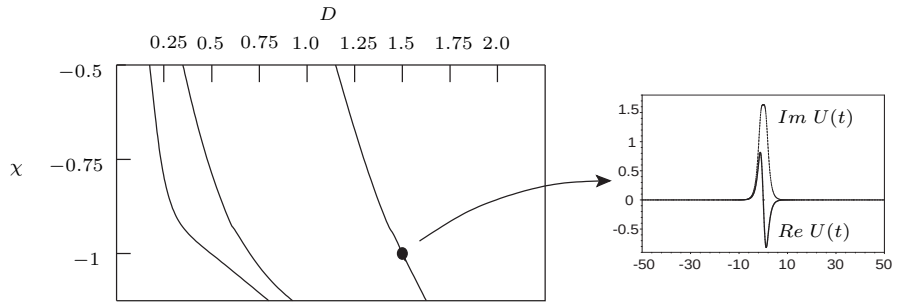

Figure 3.9.: The three curves in the (D, χ)-parameter plane at which homoclinic solutions of (3.6) were computed in [17] to cross the boundary of the region for which the origin is a saddle centre ($|\chi| < 1$). The indicated solution at $(D^*, \chi^*) := (1.5, -1)$ is the one whose unfolding is computed in Figure 3.10.

with competing quadratic and cubic nonlinearities were studied. The model is given by

$$\begin{aligned} iu_z + \tfrac{1}{2}u_{tt} + u^*v + \gamma_1\left(|u|^2 + 2|v|^2\right)u = 0 \\ iv_z + \tfrac{1}{2}\delta v_{tt} + qv + \tfrac{1}{2}u^2 + 2\gamma_2\left(|v|^2 + 2|u|^2\right)v = 0, \end{aligned}$$

where u and v are the amplitudes of complex wave vectors corresponding to the fundamental and second-harmonic fields. Seeking stationary solutions in the form $u = U(t)\exp(ikz)$, $v = V(t)\exp(2ikz)$, with real k we are led to the system of ODEs for U, V

$$\begin{aligned} \tfrac{1}{2}U'' - kU + UV + \gamma_1\left(|U|^2 + 2|V|^2\right)U = 0 \\ -\tfrac{1}{2}\delta V'' + (q-2k)V + \tfrac{1}{2}U^2 + 2\gamma_2\left(|V|^2 + 2|U|^2\right)V = 0. \end{aligned} \tag{3.7}$$

Embedded soliton solution of (3.7) have been found for $\delta > 0$ and $\gamma_{1,2} < 0$ in [93], and for $\delta < 0$, $\gamma_{1,2} > 0$ in [18]. We shall follow the latter paper here and search for parameter values $\delta < 0$ where our theory applies. In the following we fix the parameters $\gamma_1 = \gamma_2 = 0.05$, $k = 1$ and consider (3.7) as a system depending on the two parameters δ, q.

Let us first discuss the symmetries of (3.7). The system is reversible with respect to

$$R : (U, U', V, V') \mapsto (U, -U', V, -V')$$

and $\mathbb{Z}_2$-symmetric with respect to

$$S : (U, U', V, V') \mapsto (-U, -U', V, V').$$

The origin is an equilibrium for all parameter-values. We are interested in the situation at $q = 2$ since on this line the equilibrium has a zero eigenvalue and a pair of real eigenvalues.

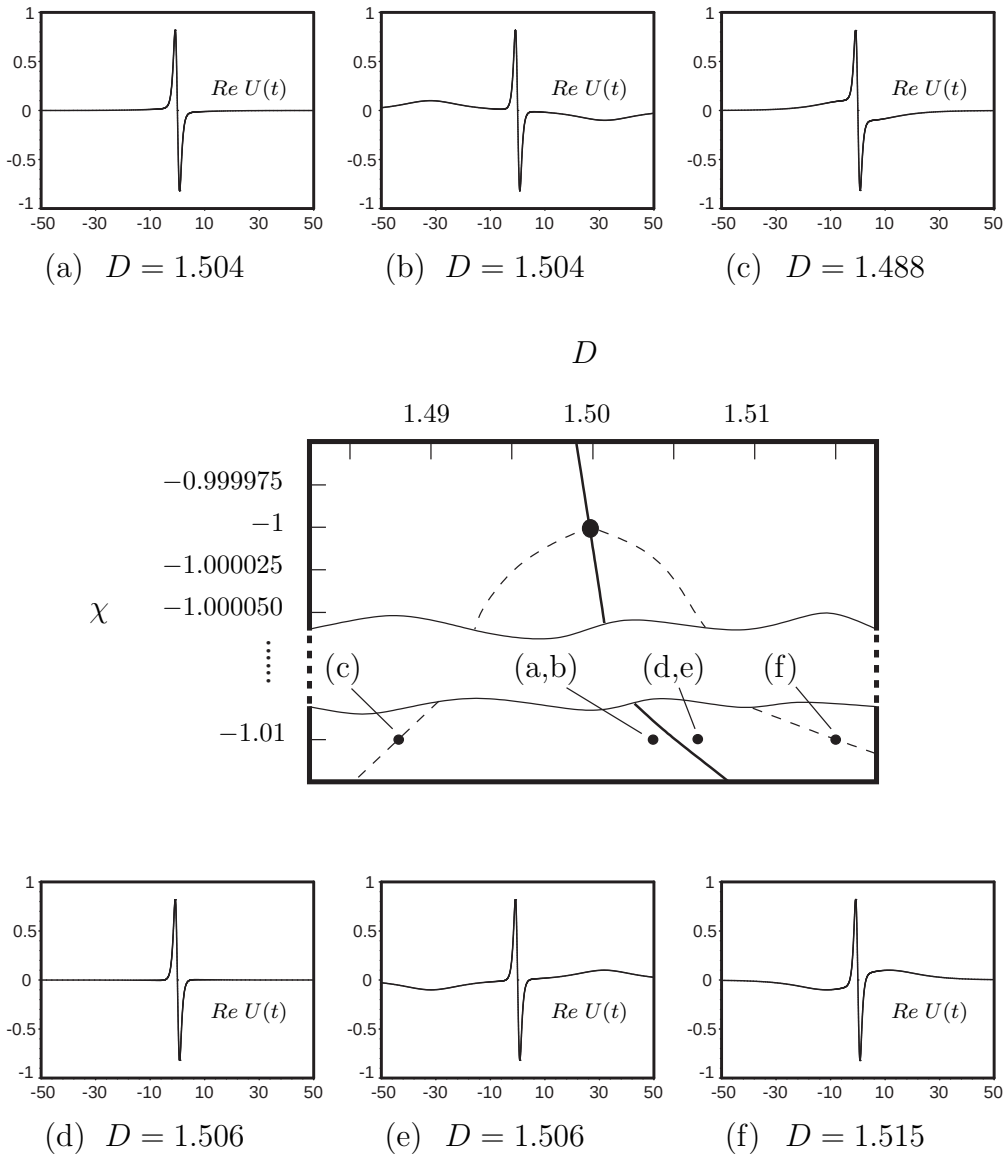

Figure 3.10.: Bifurcation of one-homoclinic orbits of (3.6) near (D^*, χ^*), computed using AUTO. On the solid curve, the fast decaying homoclinic orbit exists and for $\chi < -1$ this defines an orbit flip bifurcation. On the dashed curves saddle-node bifurcations of homoclinic orbits were detected. The solutions in the sub-panels were all computed for $\chi = -1.01$ and the given values of D. Only the real parts of the solutions are shown.

Moreover, it is easy to compute that the centre eigenspace of the linearization at this equilibrium is contained in $\mathrm{Fix}\,(S)$. According to Section 3.4.2 we would therefore expect a transcritical bifurcation of the equilibrium. Equation (3.7), however, is non-generic since we find that the local bifurcation is governed by the normal form (2.9). This means that the equilibrium undergoes a pitchfork bifurcation of figure-eight type. Nevertheless, our general studies still apply to this system. As it has been observed after Corollary 3.5 we just have to adapt the results of Section 3.4.1 in this case.

In [18] curves (in the (δ, q)-parameter plane) of R-symmetric embedded soliton solutions were found for $k = 0.3$. In a similar manner we find a curve of such solutions for $k = 1$. This curve can be extended to parameter values $q < 2$ where the origin is a real saddle, see Figure 3.11. The critical parameter value is given by $(\delta^*, q^*) = (-2.6425, 2)$. Now we can go again through computations similar to the last example. The results are comprised in the bifurcation diagram in Figure 3.11. We have again incorporated plots of solutions of (3.7) for several parameter values. For the purpose of illustrating the different types of homoclinic solutions we only show the V-component of the solutions.

The computations in this section show an excellent agreement to the general results obtained above, and thus our general approach seems to be appropriate to explain the bifurcation of solitary waves in the examples. A logical next step lies in investigating bifurcations of N-homoclinic orbits, which represent N-pulse solitary waves of the physical system. This could be achieved similar to Section 2.5. In that section, however, the difficulties in the analysis already have become apparent. The investigations are therefore beyond the scope of this paper. A discussion is postponed to Chapter 5.

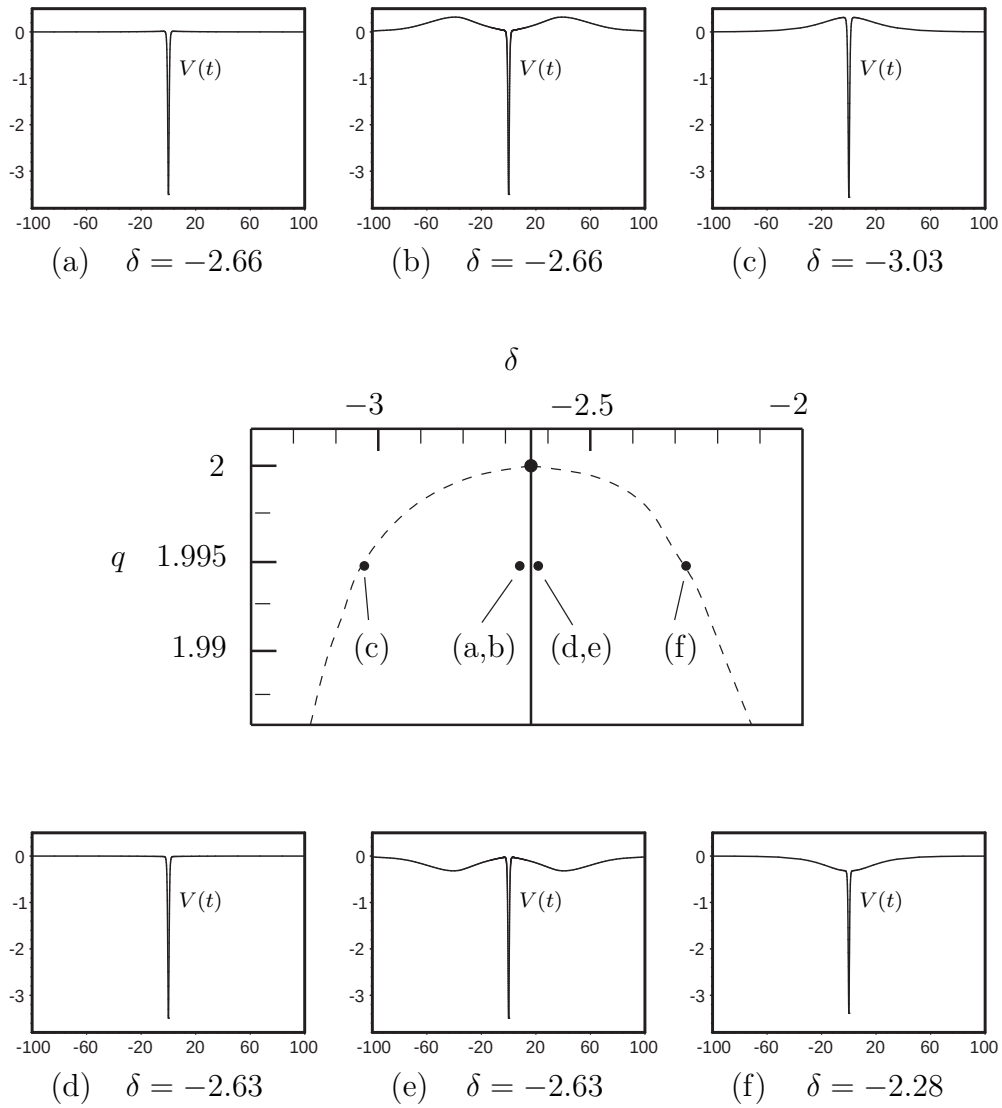

Figure 3.11.: Bifurcation diagram for one-homoclinic orbits of (3.7) near (δ^*, q^*). The fast decaying homoclinic orbit exists at the solid curve whereas at the dashed curves the saddle-node bifurcation of homoclinic orbits occurs. The corresponding solutions have been computed for $q = 1.995$ and the given values of δ. Plots show the V-components of the solutions.

CHAPTER 4

Broom bifurcation of a bellows configuration

4.1. Introduction

We now turn to the homoclinic bifurcation in reversible systems, that is caused by a change in the type of the associated equilibrium from real saddle to complex saddle focus. We are interested in bifurcations from a homoclinic bellows configuration of two symmetric homoclinic orbits. Of particular concern is the emergence of N-homoclinic orbits near the bellows configuration.

A symmetric equilibrium undergoes the above transition through some critical parameter value, at which its leading eigenvalues are real, double, and non-semisimple. The unfolding of this situation requires one parameter. We assume the two homoclinic orbits in the bellows configuration to be generic, such that also the homoclinic bifurcation is of codimension-one. As in Chapters 2 and 3 we study the bifurcation in the corresponding unfolded family.

In Section 4.2 we discuss the problem's setting in detail. In particular, we state the non-degeneracy conditions for the homoclinic orbits and we derive a linear normal form for the equilibrium, which associates a precise meaning to the parameter in the unfolding. Afterwards, in Section 4.3 we derive bifurcation equations for N-homoclinic orbits near the bellows configuration. This section extensively uses general results by Sandstede [75]. The bifurcation scenario is described in Section 4.4 where the equations are solved. We prove the existence of infinitely many N-homoclinic orbits near the bellows configuration if the equilibrium is a complex saddle focus, whereas there are no N-homoclinic orbits if it is a real saddle (Theorem 4.6). The homoclinic orbits in the saddle focus region follow both orbits in the bellows configuration.

4.2. Basic assumptions

Let us consider a system of ODEs

$$\dot{x} = f(x, \lambda), \quad x \in \mathbb{R}^{2n}, \text{ with } n > 1, \ \lambda \in \mathbb{R} \tag{4.1}$$

such that the following hypotheses are fulfilled.

Hypothesis 4.1. The system is R-reversible.

Hypothesis 4.2. At $\lambda = 0$ there exists an equilibrium in 0, i.e. $f(0,0) = 0$. In addition, $\sigma(D_1 f(0,0)) = \{\pm 1\} \cup \sigma^{ss} \cup \sigma^{uu}$, with $\mu = 1$ as a double non-semisimple eigenvalue and $|\Re(\tilde{\mu})| > \mu_0 > 1 \ \forall \tilde{\mu} \in \sigma^{ss} \cup \sigma^{uu}$ for some $\mu_0 \in \mathbb{R}$.

Remark 4.1. The assumption, that the leading eigenvalues of 0 are precisely ± 1 is not restrictive. This can always be achieved by a suitable time scaling. We have made the assumption only to simplify later computations.

Hypothesis 4.3. At $\lambda = 0$ there exist two R-symmetric homoclinic orbits Γ_1, $\Gamma_2 \neq \Gamma_1$ to 0. Let $\Gamma_i = \{\gamma_i(t) : t \in \mathbb{R}\}$, such that $\gamma_i(0) \in \mathrm{Fix}\,(R)$ for $i = 1, 2$. The orbits Γ_i form a bellows configuration. This means that

$$\begin{aligned} \lim_{t\to\infty} \frac{\dot{\gamma}_1(t)}{||\dot{\gamma}_1(t)||} &= \lim_{t\to\infty} \frac{\dot{\gamma}_2(t)}{||\dot{\gamma}_2(t)||} =: \mathfrak{e}^+, \\ \lim_{t\to-\infty} \frac{\dot{\gamma}_1(t)}{||\dot{\gamma}_1(t)||} &= \lim_{t\to-\infty} \frac{\dot{\gamma}_2(t)}{||\dot{\gamma}_2(t)||} =: \mathfrak{e}^-. \end{aligned}$$

Note that $\mathfrak{e}^+ = R\mathfrak{e}^-$, due to the symmetry of Γ_i.

We make further assumptions that ensure the bifurcation of Γ_i to be at least-degenerate as possible. First note that due to Hypothesis 4.2 the equilibrium is hyperbolic, and therefore no local bifurcation occurs in perturbations of $f(0,0)$. In particular, we find a symmetric hyperbolic equilibrium for all λ sufficiently close to 0. We can assume this equilibrium to be independent of λ, such that $f(0,\lambda) = 0$ for all λ. Since the spectrum of $D_1 f(0,\lambda)$ is symmetric to the origin in the complex plane, Hypothesis 4.2 thus describes a codimension-one situation in the class of reversible systems.

We demand that the family $f(\cdot,\lambda)$ is chosen such that λ unfolds the linearization at 0. This can be made precise by consideration of a normal form of $D_1 f(0,0)$.

A linear normal form near the equilibrium

Consider the linearization $D_1 f(0,0) =: A$ of the equilibrium 0 in (4.1). By the Jordan normal form theorem we can assume that

$$A = \begin{pmatrix} 1 & 1 & 0 & 0 & 0 & 0 \\ 0 & 1 & 0 & 0 & 0 & 0 \\ 0 & 0 & -1 & 1 & 0 & 0 \\ 0 & 0 & 0 & -1 & 0 & 0 \\ 0 & 0 & 0 & 0 & A_{uu} & 0 \\ 0 & 0 & 0 & 0 & 0 & A_{ss} \end{pmatrix}, \tag{4.2}$$

where A_{uu} and A_{ss} denote the strong unstable and strong stable part of A. We have the following result about a normal form of A.

Lemma 4.1. *Let $A(\cdot) : \mathbb{R} \to \mathcal{L}(\mathbb{R}^{2n})$ be a smooth family of matrices and suppose that $A(0) = A$, as in (4.2). Moreover, suppose that the family is reversible with respect to some involution R, that is, $RA(\lambda) + A(\lambda)R = 0$ for all λ sufficiently close to 0. Then there exists a smooth family of linear transformations $T(\cdot) : \mathbb{R} \to \mathcal{L}(\mathbb{R}^{2n})$, such that*

$$T(\lambda)A(\lambda)T(\lambda)^{-1} = \begin{pmatrix} 1 & 1 & 0 & 0 & 0 & 0 \\ a(\lambda) & 1 & 0 & 0 & 0 & 0 \\ 0 & 0 & -1 & 1 & 0 & 0 \\ 0 & 0 & a(\lambda) & -1 & 0 & 0 \\ 0 & 0 & 0 & 0 & A_{uu}(\lambda) & 0 \\ 0 & 0 & 0 & 0 & 0 & A_{ss}(\lambda) \end{pmatrix}, \tag{4.3}$$

with $a(0) = 0$, and $A_{ss(uu)}(\cdot)$ as $(n-2) \times (n-2)$-matrices, that contain the strong (un)stable spectrum of $A(\cdot)$.

Proof. Consider the SN-decomposition of $A(0) =: S(0) + N(0)$, where $S(0)$ denotes the semisimple and $N(0)$ the nilpotent part of $A(0)$, respectively. By the linear version of the normal form theorem for vector fields (see for instance [82] and [49]) we can find transformations $T(\lambda)$, smooth in λ, such that for

$$\widetilde{A}(\lambda) := T(\lambda)A(\lambda)T(\lambda)^{-1}$$

it holds $\widetilde{A}(\lambda)S(0) = S(0)\widetilde{A}(\lambda)$. Moreover $T(\lambda)$ can be chosen to commute with R such that $\widetilde{A}(\lambda)$ is also R-reversible. A simple calculation reveals that (4.3) is the only possible form for an R-reversible matrix that commutes with $S(0)$. □

Let us return to our specific problem. By the above lemma we can assume $D_1 f(0,\lambda)$ to be of the form (4.3). In order to unfold $D_1 f(0,0)$ completely we demand

Hypothesis 4.4. $a'(0) \neq 0$.

The sign of $a'(0)$ determines on which side of the parameter line the equilibrium has real eigenvalues. Thus, choosing $a'(0) > 0$ we can with no loss of generality assume that $a(\lambda) = \lambda$. In this case we find $\sigma(D_1 f(0,\lambda)) = \{\pm 1 \pm \sqrt{\lambda}\} \cup \sigma^{ss} \cup \sigma^{uu}$. (Note that also $\sigma^{ss(uu)}$ varies smoothly with λ. These strong spectra are not of concern for our analysis.)

Remark 4.2. For deriving a linear normal form near 0 only a local transformation is needed. This transformation can be globalized in the usual way by some cut-off function. It is important to note that the reversibility of the system can be preserved in this process.

A generic bellows configuration

We now turn to the homoclinic orbits Γ_i. We are interested in bifurcations from the bellows structure that are caused only by the change in the eigenvalues of 0. Therefore, we have to exclude the occurrence of several codimension-one bifurcations of the Γ_i. We need to introduce some notation first.

In the following we use the convention that the index i takes values $i = 1, 2$. Let $W^{s(u)}(0)$ denote the (un)stable manifold of 0. One of the assumptions concerns bounded solutions of the *formal adjoint* to the variational equation along Γ_i

$$\dot{x} = -D_1 f(\gamma_i(t), 0)^T \, x. \tag{4.4}$$

It is well known [75] that the dimension of the space of bounded solutions of (4.4) is related to the dimension of $T_{\gamma_i(t)} W^u(0) \cap T_{\gamma_i(t)} W^s(0)$, see below.

Hypothesis 4.5. The orbits Γ_i satisfy the following.

(i) The orbits are non-degenerate, i.e.

$$\dim \left(T_{\gamma_i(t)} W^u(0) \cap T_{\gamma_i(t)} W^s(0) \right) = 1 \text{ for all } t.$$

(ii) Define $\mathfrak{e}^+$ as in Hypothesis 4.3, and denote by $\mathfrak{e}^s$ the (normalized) eigenvector of $D_1 f(0,0)$ to the eigenvalue -1. Then $\mathfrak{e}^+ = \mathfrak{e}^s$.

(iii) Because of (i) equation (4.4) possess a unique bounded solution Ψ_i, up to multiples [75]. We assume that Ψ_i approaches 0 at an exponential rate greater than $-\mu_0$ as $t \to -\infty$ (see Hypothesis 4.2 for the definition of μ_0).

Let us comment on this. As a whole, Hypothesis 4.5 contributes to the fact that the Γ_i are of codimension-zero. (Note that we need one further non-degeneracy condition below.) It has already been remarked that the non-degeneracy (i) of the orbits leads to a transverse intersection of $W^u(0)$ and $\mathrm{Fix}\,(R)$ at the points $\gamma_i(0)$. Therefore homoclinic orbits $\Gamma_{i,\lambda}$ to 0 exist for all λ sufficiently close to 0. Part (ii) excludes that Γ_i approaches 0 with some exponential rate greater than μ_0. This assumption is also generic. Indeed,

if (ii) was violated, one would find a bifurcation of Γ_i similar to the reversible orbit flip [74]. Note that the classic orbit flip bifurcation concerns homoclinic orbits that are contained in the strong (un)stable manifold of equilibria with *simple* leading eigenvalues. We therefore have to adapt the standard assumption to our case. Similarly, part (iii) is an adapted version of the usual assumption to prevent an inclination flip bifurcation of Γ_i, see also [60] for an analogous hypothesis in the case of a discrete system. Both assumptions (ii), (iii) are needed for estimating terms in the bifurcation equations for N-homoclinic orbits.

We conclude that two smooth families of homoclinic orbits $\Gamma_{i,\lambda}$, $i = 1, 2$, parameterized by λ, exist by the above hypothesis. In particular, for fixed λ the orbits $\Gamma_{1,\lambda}$ and $\Gamma_{2,\lambda}$ also form a bellows configuration. (Below we apply the notation of Hypothesis 4.3 at $\lambda = 0$ and write Γ_i instead of $\Gamma_{i,0}$.)

4.3. Deriving bifurcation equations

For the analysis of bifurcating homoclinic orbits from the bellows configuration we use Lin's method. Since 0 is a hyperbolic equilibrium we can apply the original version of the method, which is due to Lin [66] and which has been substantially improved later by Sandstede [75]. (Note that some authors refer to the method as 'homoclinic Lyapunov-Schmidt reduction' [97].) The geometric idea of the method is to obtain certain types of solutions near a homoclinic orbit Γ, or more generally a heteroclinic cycle, by gluing together pieces of orbits which themselves can be viewed as copies of Γ. For that a cross section Σ to Γ is introduced. Lin's methods yields the existence of discontinuous 'orbits', built from sequences of solutions of (4.1), with the discontinuities or 'gaps' lying in some lower dimensional space of Σ. The closing of these gaps defines bifurcation equations for detecting solutions near Γ.

In the following we apply Lin's method to the investigation of bifurcating N-homoclinic orbits near the bellows configuration $\Gamma_1 \cup \Gamma_2$. We set up the problem and derive bifurcation equations for N-homoclinic orbits near the bellows. This procedure relies on general results concerning Lin's method, which are quoted from the literature. The main source is [75], but we also refer to [59, 76, 77, 74, 81] for other examples in which Lin's method is employed.

Let us equip $\mathbb{R}^{2n}$ with an inner product, such that R is orthogonal. We introduce cross sections $\Sigma_i = \gamma_i(0) + W_i$, transverse to Γ_i, see Figure 4.1. By choosing W_i orthogonal to $\dot\gamma_i(0)$ we ensure that $W_i = \mathrm{Fix}\,(R) + W_i^-$, where W_i^- denotes an $(n-1)$-dimensional subspace of $\mathrm{Fix}\,(-R)$. Besides, let Z_i be the subspace in Σ_i, orthogonal to $T_{\gamma_i(0)}W^u(0) + T_{\gamma_i(0)}W^s(0)$,

$$Z_i = \left(T_{\gamma_i(0)}W^u(0) + T_{\gamma_i(0)}W^s(0)\right)^\perp .$$

Because of Hypothesis 4.5, (i), Z_i is one-dimensional; moreover, $Z_i \subset \mathrm{Fix}\,(-R)$. We will derive bifurcation equations in Z_i.

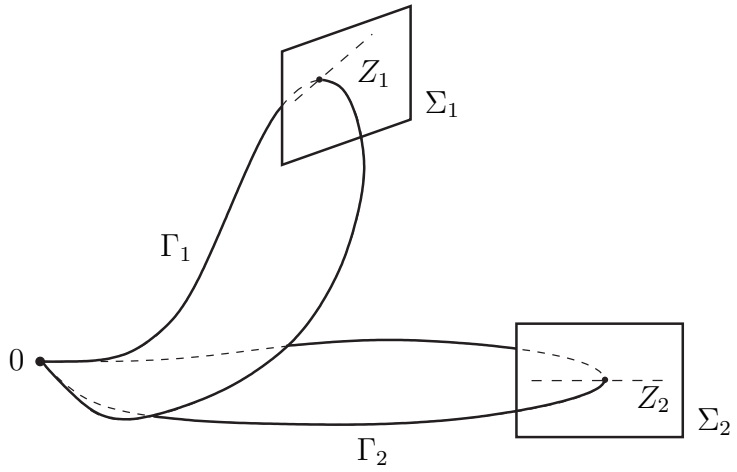

Figure 4.1.: Setup of Lin's method for studying bifurcations from the bellows configuration $\Gamma_1 \cup \Gamma_2$

We are interested in solutions that follow the orbits Γ_i with some given itinerary. So let us introduce a sequence $\kappa = (\kappa_j) \in \{1, 2\}^{\mathbb{Z}}$ of indices κ_j. We look for a sequence (x_j) of solutions of (4.1), such that x_j starts in $\Sigma_{\kappa_{j-1}}$ at $t = 0$, follows $\Gamma_{\kappa_{j-1}}$ to a neighbourhood of 0 and returns along Γ_{κ_j} to Σ_{κ_j} at the time $2\omega_j$. Moreover, the gap

$$\Xi_j := x_{j+1}(0) - x_j(2\omega_j)$$

should lie in the space Z_{κ_j}, see Figure 4.2. The solutions x_j can be characterized by the sequence of 'times' (ω_j). Indeed, since 0 is a hyperbolic equilibrium, and since the orbits Γ_i are non-degenerate we obtain from [75].

Theorem 4.2 ([75], Lemma 3.9). *Choose $\kappa = (\kappa_j)_{j\in\mathbb{Z}}$. For each λ and for each $\omega := (\omega_j)_{j\in\mathbb{Z}}$, with $\omega_j \in \mathbb{R}^+$ sufficiently large for all j, there is a unique sequence (x_j) of solutions $x_j : [0, 2\omega_j] \to \mathbb{R}^{2n}$ of (4.1), that fulfill*

(i) $x_j(0) \in \Sigma_{\kappa_{j-1}}$, $x_j(2\omega_j) \in \Sigma_{\kappa_j}$

(ii) The orbit X_j of x_j is contained in a neighbourhood of $\Gamma_1 \cup \Gamma_2$.

(iii) $\Xi_j(\lambda, \omega) := x_{j+1}(0) - x_j(2\omega_j) \in Z_{\kappa_j}$.

Remark 4.3. It is important that Theorem 4.2 remains true if we have $\omega_j = \infty$ for some $j \in \mathbb{Z}$ [75]. In this case x_j is contained in the stable or unstable manifold of the equilibrium, and the sequence ω is not continued. Hence, N-homoclinic orbits, if they exist, can be described by finite sequences (ω_j) of length $N + 1$ with $\omega_1 = \omega_{n+1} = \infty$, and $N - 1$ times ω_j for the flight from $\Sigma_{\kappa_{j-1}}$ to Σ_{κ_j}, $j = 2, \ldots, N$.

In order to find a solution of (4.1) we have to glue together the pieces x_j in Z_{κ_j} and consequently derive a set of *bifurcation equations*

$$\Xi(\lambda, \omega) := (\Xi_j(\lambda, \omega))_{j\in\mathbb{Z}} = 0. \tag{4.5}$$

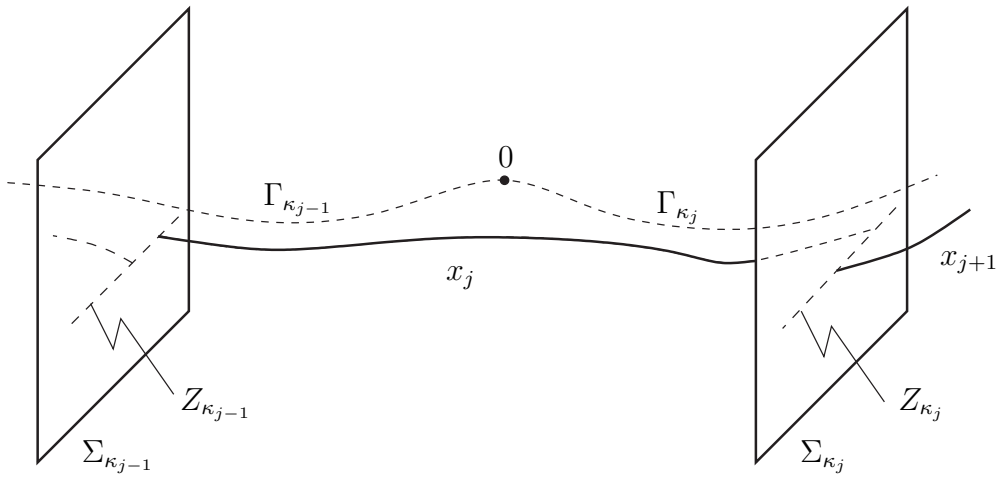

Figure 4.2.: Illustration of solutions x_j in Theorem 4.2.

Note that in the case of an N-homoclinic orbit (4.5) reduces to a set of N equations.

Estimates for $\Xi_j(\lambda, \omega)$

We follow the general analysis in [75] and express $\Xi_j(\lambda, \omega)$ as

$$\Xi_j(\lambda, \omega) = \xi_\infty(\lambda) + \xi_j(\lambda, \omega).$$

Here ξ_∞ measures the splitting of $W^{s(u)}(0)$ in Σ under variation of λ, and ξ_j reflects the influence of taking a finite 'time of passage' from $\Sigma_{\kappa_{j-1}}$ to Σ_{κ_j}.
Since Γ_i exists robustly in the family $\Gamma_{i,\lambda}$, we immediately conclude

$$\xi_\infty(\lambda) = 0 \text{ for all } \lambda.$$

It remains to compute $\xi_j(\lambda, \omega)$, for which we introduce some further notation first. Let us consider the variational equation along $\Gamma_{i,\lambda}$

$$\dot{x} = D_1 f(\gamma_{i,\lambda}(t), \lambda)\, x.$$

The formal adjoint equation is given by

$$\dot{x} = -D_1 f(\gamma_{i,\lambda}(t), \lambda)^T\, x \tag{4.6}$$

and because of the non-degeneracy of $\Gamma_{i,\lambda}$ for λ small enough, equation (4.6) has a unique bounded solution $\Psi_{i,\lambda}$, compare with above and [75]. Moreover, $\Psi_{i,\lambda}(0) \in Z_i$ and with this at hand we cite the following result, again taken from [75].

Theorem 4.3 ([75], Satz 3). *Choose λ and ω as in Theorem 4.2. Then the gaps Ξ_j can be expressed as*

$$\begin{aligned}\Xi_j(\lambda,\omega) &= \langle \Psi_{\kappa_j,\lambda}(-\omega_j), \gamma_{\kappa_{j-1},\lambda}(\omega_j)\rangle \\ &\quad -\langle \Psi_{\kappa_j,\lambda}(\omega_{j+1}), \gamma_{\kappa_{j+1},\lambda}(-\omega_{j+1})\rangle + \mathcal{R}(\lambda,\omega)\end{aligned}$$

In this theorem $\mathcal{R}(\lambda,\omega)$ denotes terms of higher order for which estimates are given in [75]. Note that $\mathcal{R}(\lambda,\omega)$ is differentiable.

The inner product terms in the above formula concern points in a neighbourhood of 0. For estimating these terms we use a general lemma that describes the behaviour of solutions in the stable manifold of 0. Its assertion closely resembles that of Lemma 1.5 in [75] and of Lemma 2.2 in [97]. We also refer to the latter paper for a proof since it proceeds along the same lines as the one given there.

Lemma 4.4. *Consider the differential equation*

$$\dot{y} = B(\lambda)y + F(y,\lambda), \qquad y \in \mathbb{R}^n, \lambda \in \mathbb{R}^l$$

where B is a family of linear operators and F is smooth with $F(0,\lambda) = 0$, $D_1F(0,\lambda) = 0$. Suppose that the spectrum of $B(\lambda)$ can be decomposed into $\sigma(B(\lambda)) = \sigma^{ss}(\lambda) \cup \sigma^s(\lambda)$ such that for all λ

$$Re\ \sigma^{ss}(\lambda) < -\beta^{ss} < Re\ \sigma^s(\lambda) < -\beta^s < 0$$

with numbers $\beta^s, \beta^{ss} \in \mathbb{R}^+$ satisfying $\beta^{ss} < 2\beta^s$, independent of λ. Suppose that the corresponding spectral projections $P^{s(ss)}$ are smooth in λ and set $B_s(\lambda) := B(\lambda)P^s$. For small initial values $y_0(\lambda)$, depending smoothly on λ, let $y(\cdot,\lambda)$ denote the solution with $y(0,\lambda) = y_0(\lambda)$. Then there exists a vector $v(\lambda)$ such that

$$||y(t,\lambda) - e^{B_s(\lambda)t}v(\lambda)|| \le ce^{-\beta^{ss}t} \text{ for all } t > 0.$$

The vector v depends smoothly on λ.

A similar result applies to solutions of (4.6), see for instance Lemma 1.8 in [75]. We apply this result for estimating the inner product terms in Theorem 4.3. Recall that $\sigma(D_1 f(0,\lambda)) = \{\pm 1 \pm \sqrt{\lambda}\} \cup \sigma^{ss} \cup \sigma^{uu}$. Observing Hypothesis 4.5 it is straightforward to compute

$$\begin{aligned}\langle \Psi_{\kappa_j,\lambda}(-\omega_j), \gamma_{\kappa_{j-1},\lambda}(\omega_j)\rangle = \Bigg\langle &\begin{pmatrix} e^{-\omega_j}\cosh\sqrt{\lambda}\,\omega_j & -e^{-\omega_j}/\sqrt{\lambda}\cdot\sinh\sqrt{\lambda}\,\omega_j \\ -e^{-\omega_j}\sqrt{\lambda}\sinh\sqrt{\lambda}\,\omega_j & e^{-\omega_j}\cosh\sqrt{\lambda}\,\omega_j \end{pmatrix} v(\lambda), \\ &\begin{pmatrix} e^{-\omega_j}\cosh\sqrt{\lambda}\,\omega_j & e^{-\omega_j}\sqrt{\lambda}\sinh\sqrt{\lambda}\,\omega_j \\ e^{-\omega_j}/\sqrt{\lambda}\cdot\sinh\sqrt{\lambda}\,\omega_j & e^{-\omega_j}\cosh\sqrt{\lambda}\,\omega_j \end{pmatrix} w(\lambda), \Bigg\rangle + \widetilde{R}(\lambda,\omega_j)\end{aligned} \tag{4.7}$$

with v, w differentiable in λ and with $\widetilde{R}$ as terms of higher order in ω_j, see below for details. As it is written, this formula only makes sense for $\lambda > 0$. We can, however,

permit complex arguments for the functions appearing in (4.7). Then this formula describes the leading terms in ξ_j.

We will make a final assumption about these leading terms. Computing the above inner product at $\lambda = 0$, we find terms

$$\langle \Psi_{\kappa_j}(-\omega_j), \gamma_{\kappa_{j-1}}(\omega_j)\rangle = e^{-2\omega_j}(\langle v(0), w(0)\rangle + 2\omega_j) + \widetilde{R}(\lambda, \omega_j).$$

Moreover, the term $\langle v(\lambda), w(\lambda)\rangle$ contributes to the coefficient for the leading terms in (4.7) for all λ. We assume

Hypothesis 4.6. The vectors $v(0)$ and $w(0)$ are not orthogonal.

Let us comment on this. Assume that this assumption is violated such that the leading term in (4.7) is zero. In this case we can introduce a second parameter to unfold this leading term. In particular, one then finds a curve in the region $\lambda > 0$ where 0 is a real saddle such that the leading term in ξ_j, i.e. the coefficient in front of $e^{(-1+\sqrt{\lambda})\omega_j}$, vanishes on the curve. This corresponds to an orbit flip bifurcation, since it means that the orbit does not approach the equilibrium at the lowest possible speed. Hence, Hypothesis 4.6 prevents an orbit flip in the unfolded family.

4.4. Existence of N-homoclinic orbits

Let us consider Theorem 4.2 with an N-tuple $\kappa = \{\kappa_1, \dots, \kappa_N\}$ and an $(N+1)$-tuple $\omega = \{\infty, \omega_2, \dots, \omega_N, \infty\}$. The tuples uniquely determine a sequence (x_j), $j = 1, \dots, N$ of solutions that satisfy (i)-(iii) in Theorem 4.2. The sequence describes an N-homoclinic solution if it solves (4.5).

We focus on *symmetric* homoclinic orbits. Here the number of equations in (4.5) can be reduced further. Let us exploit this point. We call the above N-tuple κ symmetric, if $\kappa_{N+1-j} = \kappa_j$ for all $j = 1, \dots, N$. Similarly, we call ω symmetric if $\omega_{N+2-j} = \omega_j$ for $j = 2, \dots N$. Finally, R-symmetry of a sequence of solutions of (i)-(iii) in Theorem 4.2 means that $Rx_j(t) = x_{N+1-j}(-t)$. Note that an R-symmetric solutions of (4.1) necessarily is an R-symmetric sequence of solutions.

As a consequence of the uniqueness in Theorem 4.2 we obtain

Lemma 4.5. *Consider the unique sequence of solutions (x_j) from Theorem 4.2, associated to κ and ω as above. This sequence is R-symmetric if and only if both κ and ω are symmetric. Moreover, the gaps ξ_j satisfy $\xi_{N+1-j}(\lambda, \omega) = \xi_j(\lambda, \omega)$ in that case.*

Proof. It is clear that R-symmetric sequences are necessarily described by symmetric tuples κ, ω. The proof that symmetry of κ, ω is sufficient for the symmetry of (x_j) is completely analogous to the proof of Lemma 3.1 in [74], see also [81]. The idea is to represent the corresponding R-images by solutions $(\tilde{x}_j)$ of (i)-(iii) in Theorem 4.2.

Straightforward considerations show that $(\tilde{x}_j)$ correspond to the same tuples κ, ω, and thus uniqueness in Theorem 4.2 implies equality. The gap property is a simple consequence. □

Hence, for the detection of symmetric N-homoclinic orbits it suffices to choose a symmetric tuple κ and to solve the system

$$\xi_j(\lambda, \omega) = 0, \quad j = 1, 2, \ldots, [N/2] \tag{4.8}$$

with symmetric ω. (By $[N/2]$ we denote the largest integer smaller than $N/2$.)
In the following we discuss the existence of symmetric N-homoclinic orbits for different signs of λ. We assume that κ and ω are symmetric and look for solutions of (4.8). We first consider values of λ where 0 is a real saddle.

The case $\lambda \geq 0$

If $\lambda > 0$ we can simplify the inner product terms, such that for $j = 1, \ldots, [N/2]$ the gap ξ_j can be written as

$$\begin{aligned} \xi_j(\lambda, \omega) &= c_1(\lambda) e^{-2\omega_j} \sinh(2\sqrt{\lambda}\, \omega_j + d(\lambda)) \\ &\quad + c_2(\lambda) e^{-2\omega_{j+1}} \sinh(2\sqrt{\lambda}\, \omega_{j+1} + d(\lambda)) + o(e^{-2(1-\sqrt{\lambda})\omega_j}) + o(e^{-2(1-\sqrt{\lambda})\omega_{j+1}}) \end{aligned}$$

with functions $c_{1,2}$, d that are smooth in λ and bounded away from 0, because of Hypothesis 4.6. The functions $c_{1,2}$, d are related to the vectors $v(\lambda)$, $w(\lambda)$, such that smoothness is a consequence of Lemma 4.4.
It is easy to see that the equation has no solution apart from the trivial one. Recall that $\omega_1 = \infty$. Thus, $\xi_1(\lambda, \omega) = 0$ implies $\omega_2 = \infty$. The same argument yields $\omega_i = \infty$ for all $i = 2, \ldots, N-1$. We conclude that no symmetric N-homoclinic orbits exist, if the equilibrium 0 is a real saddle. Moreover, the argument does not need the symmetry of κ and ω and hence we conclude that no N-homoclinic orbits exist at all if $\lambda > 0$.
The same argument shows the non-existence of N-homoclinic orbits for $\lambda = 0$. Here we compute

$$\xi_j(0, \omega) = c_1(0) e^{-2\omega_j}(\omega_j + d(0)) + c_2(0) e^{-2\omega_{j+1}}(\omega_{j+1} + d(0)) + o(e^{-2\omega_j}) + o(e^{-2\omega_{j+1}}),$$

again with non-zero coefficients $c_{1,2}$, and $d \in \mathbb{R}$.

The case $\lambda < 0$

We can detect a plethora of N-homoclinic orbits if $\lambda < 0$. Here the gap ξ_j reads

$$\begin{aligned} \xi_j(\lambda, \omega) &= c_1(\lambda) e^{-2\omega_j} \sin(2\sqrt{|\lambda|}\, \omega_j + d(\lambda)) \\ &\quad + c_2(\lambda) e^{-2\omega_{j+1}} \sin(2\sqrt{|\lambda|}\, \omega_{j+1} + d(\lambda)) + o(e^{-2\omega_j}) + o(e^{-2\omega_{j+1}}), \end{aligned} \tag{4.9}$$

for $j = 1, \dots, [N/2]$. We note that similar formulas in the saddle focus region have been derived in [76, 77].

This system can be solved in the same way as in [76]: We chose a real number w, such that $\omega_j \geq w$ for all $j = 2, \dots, [N/2]$ and introduce variables

$$r = e^{-2w}, \quad a_j = e^{-2(\omega_j - w)}, \quad j = 2, \dots, [N/2] + 1.$$

Then (4.9) becomes

$$\begin{aligned} c_1(\lambda) r a_j \sin\left(\sqrt{|\lambda|}\ln(r a_j) + d(\lambda)\right) \\ + c_2(\lambda) r a_{j+1} \sin\left(\sqrt{|\lambda|}\ln(r a_{j+1}) + d(\lambda)\right) = o(r a_j). \end{aligned}$$

We can divide through r and choose in particular

$$r = e^{-2k\pi/\sqrt{|\lambda|}}, k \in \mathbb{N}.$$

Using the periodicity of $\sin(\cdot)$ we see that the r drops out in the sin-terms, such that we are left with

$$\begin{aligned} c_1(\lambda) a_j \sin\left(\sqrt{|\lambda|}\ln(a_j) + d(\lambda)\right) \\ + c_2(\lambda) a_{j+1} \sin\left(\sqrt{|\lambda|}\ln(a_{j+1}) + d(\lambda)\right) = O(r a_j). \end{aligned}$$

Now, letting $r \to 0$ and recalling that $\omega_1 = \infty$ we obtain the system

$$\begin{aligned} c_2(\lambda) a_2 \sin\left(\sqrt{|\lambda|}\ln(a_2) + d(\lambda)\right) &= 0 \\ c_1(\lambda) a_j \sin\left(\sqrt{|\lambda|}\ln(a_j) + d(\lambda)\right) & \\ + c_2(\lambda) a_{j+1} \sin\left(\sqrt{|\lambda|}\ln(a_{j+1}) + d(\lambda)\right) &= 0, \quad j = 2, \dots, [N/2]. \end{aligned} \tag{4.10}$$

Obviously, this system can be solved for infinitely many sequences (a_i). Moreover, the Jacobian of the left hand side is a upper-triangular matrix with non-zero diagonal-entries. Hence, it is regular and we can apply the implicit function theorem at an arbitrary solution sequence $(a_j)^*$ of (4.10). This yields the existence of infinitely many values of $r_k = e^{-2k\pi/\sqrt{|\lambda|}}$ such that the sequences ω that correspond to $(a_j)^*$, r_k solve (4.9). We conclude that infinitely many symmetric homoclinic orbits exist for each choice of itinerary κ.

Let us discuss the result. The special choice of symmetric sequences $\kappa^1 := (1, 1, \dots, 1)$ and $\kappa^2 := (2, 2, \dots, 2)$ shows that for each N there exist infinitely many N-homoclinic orbits in a neighbourhood of each one of the primary orbits Γ_i. This agrees with the well known results in [41, 76]. But, of course, we find additional homoclinic orbits that are composed of parts of both Γ_1 and Γ_2.

Furthermore, the computations also give some information about the fate of N-homoclinic orbits as $\lambda \to 0 - 0$. Choose a fixed $\lambda < 0$ and assume that the sequence $\omega \in \mathbb{R}^{N+1}$ describes the N-homoclinic solution x. Now, if the orbit is continued with respect to λ we find that $\omega_j \to \infty$ for $j = 2, \ldots, N$. Thus, the orbit approaches the primary homoclinic bellows $\Gamma_1 \cup \Gamma_2$.

We summarize the results about the existence of N-homoclinic orbits in a final theorem.

Theorem 4.6. *Consider (4.1) under Hypothesis 4.1-4.6. Then for $\lambda \geq 0$ there exist no additional homoclinic orbits near the bellows configuration $\Gamma_1 \cup \Gamma_2$. If $\lambda < 0$, then for each symmetric sequence $\kappa \in \{1, 2\}^N$ of arbitrary length N, there exist infinitely many symmetric homoclinic orbits that follow the bellows configuration according to κ.*

4.5. Application to the umbilic systems

Let us finally return to the systems (1.1) and discuss some consequences of the above results for them. We concentrate on f^- with parameter values $\alpha > 0$, $\beta = -4\alpha^2$. Our results suggest that a plethora of homoclinic and heteroclinic orbits emerges at these parameter values.

First recall from Section 1.4 that we have to consider the reduced system (A.7) in orbit space. Here the heteroclinic cycle $\{\gamma_{het}, R_1\gamma_{het}\}$ and the homoclinic orbits to $\xi_{3,4}$ are represented by a homoclinic bellows configuration. Second, we note that we cannot prove that f^- fulfills the assumptions for the general analysis. In particular, it is not clear whether the orbits are non-degenerate. But the robust existence of the orbits, established numerically, strongly suggests this.

Therefore, according to Theorem 4.6 there should emerge N-homoclinic orbits near the bellows for $\beta < -4\alpha^2$. We have shown one of them in Figure 1.4. This orbit is represented by a three-homoclinic orbit in the reduced system, which alternately follows the primary orbits.

We finally remark that there are even more orbits that form a bellows configuration with $\{\gamma_{het}, R_1\gamma_{het}\}$. For instance, also the large heteroclinic cycle in Figure 1.3 and each N-homoclinic orbit in Figure 2.10 can be continued to parameter values $\beta = -4\alpha^2$. All of these orbits are in bellows configuration with $\{\gamma_{het}, R_1\gamma_{het}\}$. Therefore the arguments using Theorem 4.6 can be repeated for each of these bellows.

CHAPTER 5

Discussion

Let us conclude this thesis by discussing a few open problems and interesting directions for future research in connection with the studies undertaken here. Let us begin with some general remarks.

This thesis concerns homoclinic bifurcations in reversible systems that are caused by a change in the type of the associated equilibrium. We have discussed the bifurcation caused by a saddle / saddle centre transition and - in a concise way - the bifurcation caused by a saddle / saddle focus transition. Our analysis has by no means answered all questions about these bifurcations and a few interesting problems are discussed below. However, let us first look at two further possible bifurcations of the equilibrium that lead to an interesting behaviour near an associated homoclinic orbit.

Consider the case of a homoclinic orbit to a complex saddle focus, for simplicity in $\mathbb{R}^4$. We have studied what happens, if the orbit is continued in a one-parameter family and the complex eigenvalues of the equilibrium meet on the real axis. Another possibility for the eigenvalues is to meet on the imaginary axis, such that the equilibrium becomes a centre. This process is known as a reversible 1:1-resonance [50] or Hamiltonian-Hopf bifurcation [85]. Iooss and Peroueme show in [50] that the local bifurcation is essentially governed by a normal form of the system. In the so-called *subcritical* case of the local bifurcation they prove the existence of two symmetric homoclinic orbits in the parameter region where the equilibrium is hyperbolic. The size of these orbits shrinks to 0 when the equilibrium becomes a centre. This effect has been observed in a number of examples, for instance also in the umbilic systems [58]. Note however, that there is a second possibility. In [6] a class of systems is studied where the homoclinic orbit persists up to parameter values of the reversible 1:1-resonance. At the resonance the orbit decays algebraically to the centre, and it is accompanied by an infinite number of algebraically decaying N-homoclinic orbits.

Another study of the effect of a local codimension-one bifurcation on a symmetric homoclinic orbits can be found in the literature. Assume the existence of a homoclinic orbit

to a saddle centre. We have seen that in two-parameter families of reversible ODEs such orbits typically exist along curves in parameter space. Our studies have dealt with the bifurcation when along such a curve the equilibrium becomes a real saddle. But if the homoclinic orbit is continued in 'opposite direction' along the curve, there is the possibility that the real eigenvalues merge at 0 and become imaginary, such that the equilibrium becomes a centre. Studies in [67, 24] show that in the singular limit the homoclinic orbit shrinks to a point. Investigations in [61] for reversible Hamiltonian systems concern the behaviour of two-homoclinic orbits in such a transition.

We now return to the bifurcations that have been considered in this thesis.

Homoclinic orbits to degenerate equilibria

The studies in Chapters 2 and 3 of this thesis have concerned homoclinic orbits to degenerate equilibria. We have introduced appropriate 'centre manifolds' $W^c_{loc,\lambda}$ and have studied the existence of homoclinic orbits to these manifolds. We could completely describe bifurcating one-homoclinic orbits and, moreover, analyse their asymptotic behaviour by a projection along stable fibres.

In the last part of Chapter 2 we have taken a next step and have analysed the existence of two-homoclinic orbits. There we have chosen to rely on a geometric approach, motivated by studies for singularly perturbed ODEs. The difficulties have become evident. One of the main obstacles is the 'complex' dynamics in $W^c_{loc,\lambda}$ which makes it difficult to analyse the behaviour in a neighbourhood of this manifold geometrically.

Therefore, one of the major directions of future research is to either improve the geometric approach or to develop an analytical technique for the study of further recurrent dynamics near the primary orbit. It would, for instance, be desirable to further generalize Lin's method, such that the case of homoclinic orbits to nonhyperbolic equilibria can be analysed completely. It seems likely that, just as in the geometric considerations in Section 2.5, this method decomposes into two parts, one dealing with the local behaviour near $W^c_{loc,\lambda}$ and the other with the 'global flight'. For the local part, exponential expansions as in [27] will be crucial. Rigorous results are still missing.

Let us discuss interesting aspects of the bifurcation scenarios that have been established in Chapters 2 and 3. The bifurcation scenario for the reversible homoclinic pitchfork bifurcation implies that for $\lambda < 0$ the homoclinic orbits to the equilibria η, $R_2\eta$ and the (small) heteroclinic cycle in $W^c_{loc,\lambda}$ form a bellows configuration. The results of Section 2.5 and the numerical computations for the system f^- suggest that at the same time N-homoclinic (and N-heteroclinic) orbits to the equilibria exist. Similarly, in the case of a local transcritical bifurcation, treated in Chapter 3 we find a homoclinic orbit which is composed of the primary orbit and the small homoclinic orbit Υ, see panel b) in Figure 3.7. This orbit can also be viewed as a two-homoclinic orbit near the bellows configuration.

These observations remarkably differ from the results in [46], where it is proved that

generically *no* N-homoclinic orbits exist near a bellows configuration. Of course, since in our case the bellows configuration emerges in another bifurcation itself, it is not surprising that the results do not fall into the general frame. But still, this is an interesting difference. Moreover, it is shown in [46] that N-periodic orbits exist near the bellows configuration, and that in general, one finds complex dynamics, caused by heteroclinic orbits between periodic orbits near the bellows. It is interesting to see, how far this result applies to our scenarios.

In each of the bifurcation scenarios in Chapter 3 we have encountered a reversible orbit flip bifurcation of the primary orbit. General results by Sanstede et. al. in [74] show that this bifurcation typically leads to the emergence of N-homoclinic orbits. See also [15] for a numerical investigation of this bifurcation for the 5-th order KdV-equation (3.5), where the presence of a Hamiltonian structure implies that the bifurcation is degenerate compared with the analysis of [74]. These results concern orbits which are composed of copies of the fast decaying homoclinic orbit alone. In our case, however, there is the possibility of an even richer dynamics in that it includes orbits being composed of copies of the primary orbit and of parts that are governed by the dynamics in $W^c_{loc,\lambda}$.

Of similar interest is the existence of N-homoclinic solutions for parameter values where the origin is a saddle centre. Here, general results are available which explain the accumulation of such solutions on parameter values where the primary orbit exists, see [16] for the reversible case and [68, 61] for the case of systems that are additionally Hamiltonian. An interesting point is that these studies show differences in the behaviour of systems that are purely reversible and of those are also Hamiltonian. In Section 3.5 of the present paper we have established a possible reason for these differences, namely the fact that the Hamiltonian property does not allow a transverse intersection of the centre-stable and unstable manifolds. This will certainly be reflected in results concerning bifurcating N-homoclinic orbits. Thus, an analysis may also give further insight into qualitative differences between reversible and Hamiltonian systems, see [16] for some related remarks.

Hence, the fundamental problem in a future analysis of homoclinic orbits to degenerate equilibria lies in the study of bifurcating N-homoclinic orbits.

Let us finally turn to the application in Section 3.6 where we have considered the transition gap soliton / embedded soliton (ES). From a PDE point of view a further important project is the study of the stability of solutions. More precisely an open question is what happens to the stability of the ESs when they cross the critical parameter value to become structurally stable objects. For a variety of model equations, including two of the examples studied in this thesis, the property of semi-stability of embedded solitons has been established by a mixture of numerical, asymptotic and rigorous arguments [71, 95, 93, 94]. Does this semi-stability necessarily transform into true exponential stability when the embedded soliton becomes a gap soliton? A general rigorous answer to this question is of course beyond the realm of the finite-dimensional dynamical systems theory used in Chapter 3.

The broom bifurcation

Our analysis of the broom bifurcation from the bellows structure in Chapter 4 have focussed on a specific part of the dynamics, namely bifurcating N-homoclinic orbits. The bifurcation results resemble those for single homoclinic orbits: If the equilibrium is a complex saddle focus, then infinitely many N-homoclinic orbits exist. But in the transition of the equilibrium each one of these orbits approaches the primary configuration, and no N-homoclinic orbits exist in the saddle region.

It is interesting to study further dynamics near the bellows. As we have described above, homoclinic orbits to saddle foci are typically accompanied by an incredibly rich dynamics. In particular, infinitely many N-homoclinic and N-periodic orbits exist near such homoclinic orbits [41]. Note, however, that it is not fully clear for purely reversible systems whether shift-dynamics necessarily occurs near homoclinic orbits to saddle foci. If the system is additionally Hamiltonian, then before-mentioned results by Devaney [28] ensure this.

Now, consider what happens when the associated equilibrium changes its type. If a single homoclinic orbit is concerned, then the results are similar to those for the N-homoclinic orbits, namely each N-periodic solution will be destroyed in the process. However, the investigations in [46] about the dynamics near a bellows configuration show that the configuration is accompanied by infinitely many N-periodic orbits, even in the saddle case. Thus, there is a possibility for N-homoclinic orbits to survive the equilibrium's change. So, what happens with N-periodic orbits near the bellows if the equilibrium becomes a saddle?

The umbilic systems

Let us conclude the thesis with some remarks about the umbilic systems (1.1). As we have remarked, these systems are of importance, since they describe the behaviour near equilibria with fourfold eigenvalue zero in a class of reversible Hamiltonian systems.

Our studies demonstrate that in an unfolding of such an equilibrium a great variety of homoclinic and heteroclinic phenomena can be observed. This is of interest in applications. In Appendix A we describe our motivation for the study of (1.1), which stems from a model in nonlinear optics. In this context it is interesting to study the relation of our results to the physical problem. Because of a certain degeneracy in the corresponding model this is by no means trivial.

APPENDIX A

The umbilic systems

A.1. Introduction

In this appendix we collect various results in connection with the umbilic systems (1.1). We start with some details on how the system have been derived as unfoldings of an equilibrium with fourfold eigenvalue zero. In Section A.2 we then review results about the bifurcation of equilibria and existence results for connecting orbits, derived in the author's Diploma thesis [88], see also [91]. Of particular importance are existence results for a homoclinic orbit γ_{hom}, stated in Theorems A.1 and A.3, and for a heteroclinic cycle $\{\gamma_{het}, R_1\gamma_{het}\}$ in Theorems A.2 and A.4. We also discuss two techniques that facilitate the analysis of the umbilic systems.

The heteroclinic cycle is again the subject of Section A.3, where we extend the existence results from [88]. The results of that section have already found their way into [91]. In Section A.3 we explain the corresponding analysis in detail.

Let us for the sake of completeness look back on fundamental properties of the umbilic systems (1.1) that have already been explained in the first introductory chapter. First, recall that the systems read

$$\dot{x} = f^{\pm}(x, \alpha, \beta) = \begin{pmatrix} x_2 \\ 2x_1x_3 + 2\alpha x_1 \\ x_4 \\ -x_1^2 \pm x_3^2 \mp 2\alpha x_3 - \beta \end{pmatrix}$$

for $x = (x_1, x_2, x_3, x_4) \in \mathbb{R}^4$, depending on parameters α, $\beta \in \mathbb{R}$. We view the systems (1.1) as (parameter dependent) dynamical systems induced by the vector fields $f^{\pm}$. We refer to the vector field f^- as the reversible hyperbolic umbilic; the other case f^+ is referred to as the reversible elliptic umbilic.

The vector fields $f^{\pm}$ are reversible and $\mathbb{Z}_2$-symmetric. Indeed, we have seen that $f^{\pm}$ are

reversible with respect to

$$R_1 : (x_1, x_2, x_3, x_4) \mapsto (x_1, -x_2, x_3, -x_4)$$

and

$$R_2 : (x_1, x_2, x_3, x_4) \mapsto (-x_1, x_2, x_3, -x_4).$$

As a result, the map $S := R_1 \circ R_2$ describes a $\mathbb{Z}_2$-symmetry for (1.1), that is

$$Sf^{\pm}(x, \alpha, \beta) - f^{\pm}(Sx, \alpha, \beta) = 0.$$

An immediate consequence of this equality is that the fixed space $\mathrm{Fix}\,(S)$ is invariant with respect to the the flow of $f^{\pm}$.

Finally, the umbilic systems are *Hamiltonian* with a Hamilton function given by

$$H^{\pm}(x, \alpha, \beta) = -\frac{1}{2}x_2^2 + \frac{1}{2}x_4^2 + x_1^2 x_3 \mp \frac{1}{3}x_3^3 + \alpha(x_1^2 \pm x_3^2) + \beta x_3.$$

Because of the indefinite quadratic form in $H^{\pm}$ the systems belong to the class of *indefinite Hamiltonian systems*.

We have already mentioned a number of times that (1.1) are unfoldings of an equilibrium with fourfold eigenvalue zero. Indeed, setting $\alpha = \beta = 0$ a quick calculation shows that

$$D_1 f^{\pm}(0,0,0) = \begin{pmatrix} 0 & 1 & 0 & 0 \\ 0 & 0 & 0 & 0 \\ 0 & 0 & 0 & 1 \\ 0 & 0 & 0 & 0 \end{pmatrix}. \tag{A.1}$$

Why are we interested in equilibria of this type?

The physical background

Our motivation comes from a problem in nonlinear optics that concerns the existence of solitary light waves in an optical fibre. We are interested in the special case of so-called $\chi^{(2)}$-solitons. These are solitary light waves that exist in a medium with $\chi^{(2)}$-nonlinearity, see [13, 11] for comprehensive reviews. In this case light propagation is adequately described by the following system of PDEs

$$\begin{aligned} i\frac{\partial w}{\partial \xi} + r\frac{\partial^2 w}{\partial t^2} - w + w^* v &= 0 \\ i\sigma\frac{\partial v}{\partial \xi} + s\frac{\partial^2 v}{\partial t^2} - \alpha v + \frac{1}{2}w^2 &= 0 \end{aligned} \tag{A.2}$$

for the complex functions v and w, representing the envelope amplitudes of the fundamental and second-harmonic waves, respectively. The evolution variable ξ measures

the distance along the optical fibre. The second variable t describes distance or retarded time, depending on whether we deal with a spatial or temporal problem. The parameters r, s can only take values ± 1. Their sign is determined by the signs of the dispersion/diffraction coefficients. The parameter σ measures the ratio of the dispersion/diffraction, and α is a dimensionless real parameter. System (A.2) is obtained from the model for $\chi^{(2)}$ second-harmonic generation of type I by a normalization procedure and the insertion of an appropriate ansatz, see [13, 97, 96].

Solitary waves and kinks are stationary solutions of (A.2), i.e. solutions depending on t only. The search for real stationary solutions then leads to the study of homoclinic and heteroclinic solutions of a system of second-order ODEs

$$\begin{aligned} rw'' - w + wv &= 0 \\ sv'' - \alpha v + w^2/2 &= 0, \end{aligned} \tag{A.3}$$

where the prime denotes differentiation with respect to t. It is not hard to see that (A.3) is an indefinite Hamiltonian which is reversible with respect to the involutions R_1 and R_2, introduced above.

If $r = -1$, $s = 1$ one is interested in the existence of heteroclinic orbits of (A.3), corresponding to kink solutions of (A.2). For $\alpha > 0$ there is a chance for such orbits as we find two equilibria

$$(w_{1/2},\ w'_{1/2},\ v_{1/2},\ v'_{1/2}\ ) = (\pm\sqrt{2\alpha}, 0, 1, 0)$$

on the same level set of the corresponding Hamiltonian. (The symmetries of the system imply that heteroclinic orbits will not come alone but in pairs forming a cycle, and thus describe fronts in the physical system.)

If $\alpha \geq 8$ the equilibria are real saddles, that is, their linearization possesses four real eigenvalues. In this region heteroclinic orbits can be found by a shooting technique for indefinite Hamiltonian systems, developed in [44]. (We touch upon this method in Appendix A.) For $0 < \alpha < 8$, however, the equilibria are complex saddle foci, and therefore the situation is more involved. Our idea was to attack the existence problem for this region at the special value $\alpha = 0$. Here the two equilibria emerge in some (degenerate) pitchfork bifurcation of an equilibrium ξ_0 and a local bifurcation analysis combined with path-following arguments should provide information about the existence of heteroclinic orbits.

A calculation shows that the linearization at the degenerate equilibrium ξ_0 is precisely as in (A.1). Such matrices are of codimension two in the class of reversible and Hamiltonian matrices, according to results by Hoveijn [48]. One would thus expect an unfolding of the local bifurcation of ξ_0 to require two parameters. But unfortunately this is not the case. The particular singularity ξ_0 of (A.3) is of infinite codimension, since there exists a manifold of equilibria at $\alpha = 0$. This circumstance makes a rigorous analytical treatment almost impossible. We have thus decided to drop the concrete physical problem. Instead,

our goal is to analyse the generic local behaviour near equilibria with fourfold eigenvalue zero in a corresponding class of reversible indefinite Hamiltonian systems.

In a first step we have aimed at deriving a standard form for the degenerate equilibrium and a corresponding unfolding. In general this is a very hard problem and only few results can be found in the literature. One problem similar to ours is studied by Iooss via normal form theory in [51]. We have chosen to exploit the Hamiltonian structure and have performed an unfolding of the singular Hamilton function using techniques from Catastrophe Theory. (Note that a degenerate equilibrium corresponds to a singularity of the Hamilton function.) This method has successfully been applied to planar Hamiltonian systems in [8, 40]. We refer to [88, 91] for details of the procedure in the present case.

We have found the singularity of the Hamilton function to be of codimension two in the class of reversible systems. Obviously, this agrees with the results by Hoveijn about the linear codimension. The procedure shows that two cases have to be distinguished which differ in the sign of a third order term in the singular Hamilton function, namely the reversible hyperbolic hyperbolic umbilic with Hamilton function H^- and the reversible elliptic umbilic with Hamilton function H^+. The chosen procedure also yields unfoldings of the singular Hamilton functions and we consequently obtain the vector fields $f^\pm$ that bear the names of the corresponding Hamilton function.

Although we could obtain the vector fields $f^\pm$ in a straightforward way, the chosen procedure does not allow us to prove that they are indeed versal unfoldings of the singular systems (with $\alpha = \beta = 0$). It therefore remains to investigate whether bifurcation results that have been obtained for the umbilic systems occur robustly near singularities with fourfold eigenvalue zero. In many cases it is possible to prove this robustness. In particular, we can show that the bifurcation results in Appendix A are generic, see [91] for details. We therefore hope to convince the reader that the umbilic systems are more than just suitable examples for the numerical studies in the first chapter. On the contrary, they are of mathematical importance since the results obtained for the systems also increase the understanding of the generic behaviour near such equilibria.

Also, we are not aware of any physical application of $f^\pm$ or any direct relation to the physical system (A.3). But again, bifurcations that will be observed for $f^\pm$ are of interest in physical applications, as we have demonstrated for example in Chapter 3.

A.2. Summary of analytical results

In the following we collect various analytical results about $f^\pm$. We present bifurcation diagrams for equilibria and existence results for connecting orbits.

A.2.1. The hyperbolic umbilic f^-

Many bifurcation results are completely analogous for both of the umbilic systems and can be derived in a similar way. In our discussion of the analytical results we will therefore focus on the reversible hyperbolic umbilic f^-, as usual. The results for the elliptic umbilic are summarized afterwards.

Bifurcations of equilibria

Equilibria of f^- can be computed directly as solutions of the system of equations $f^-(x, \alpha, \beta) = 0$. It is also straightforward to compute the eigenvalues of the equilibria using computer algebra programs. We find two equilibria

$$\xi_{1,2} = (0, 0, \alpha \pm \sqrt{\alpha^2 - \beta}, 0)$$

if $\beta \leq \alpha^2$ and two additional equilibria

$$\xi_{3,4} = (\pm\sqrt{-3\alpha^2 - \beta}, 0, -\alpha, 0)$$

if $\beta < -3\alpha^2$. The bifurcation diagram is presented in Figure A.1. This diagram shows the number of equilibria of the systems in certain regions or curves in the parameter plane. For each equilibrium the position of its eigenvalues in the complex plane is indicated in the corresponding small box. Single eigenvalues are denoted by a '•' whereas for double eigenvalues (meaning eigenvalues of algebraic multiplicity two) we use '×'. (Note that the notation in the diagram slightly differs from the one in [91].)

Local bifurcation of equilibria occur on two parabolas

$$\mathcal{B}_1 \cup \mathcal{B}_2 := \{\beta = \alpha^2\} \quad \text{and} \quad \mathcal{B}_3 \cup \mathcal{B}_4 := \{\beta = -3\alpha^2\}.$$

From Figure A.1 we conclude that a reversible saddle-centre bifurcation occurs for $\beta = \alpha^2$ while for $\beta = -3\alpha^2$ a reversible pitchfork bifurcation takes place.

We note that all equilibria are R_1-symmetric, that is, $R_1\xi_i = \xi_i$, $i = 1, \ldots, 4$. But only ξ_1 and ξ_2 are R_2-symmetric, whereas $R_2\xi_3 = \xi_4$. We furthermore note that ξ_3 and ξ_4 are the only equilibria on the same level set of the Hamiltonian H^-.

For certain parameter values one finds qualitative changes in the linearizations of equilibria that may lead to a bifurcation of orbits in their neighbourhood. Of interest to us is the behaviour on the parabola

$$\mathcal{B}_5 \cup \mathcal{B}_6 := \{\beta = -4\alpha^2\}.$$

If this parabola is crossed with decreasing β then either $\xi_{3,4}$ turn from centres into complex saddle foci and lose their stability in a reversible 1:1-resonance or Hamiltonian-Hopf bifurcation [50, 85] if $\alpha < 0$, or the equilibria turn from real saddles into complex saddle foci if $\alpha > 0$. The latter case is considered in Chapter 4.

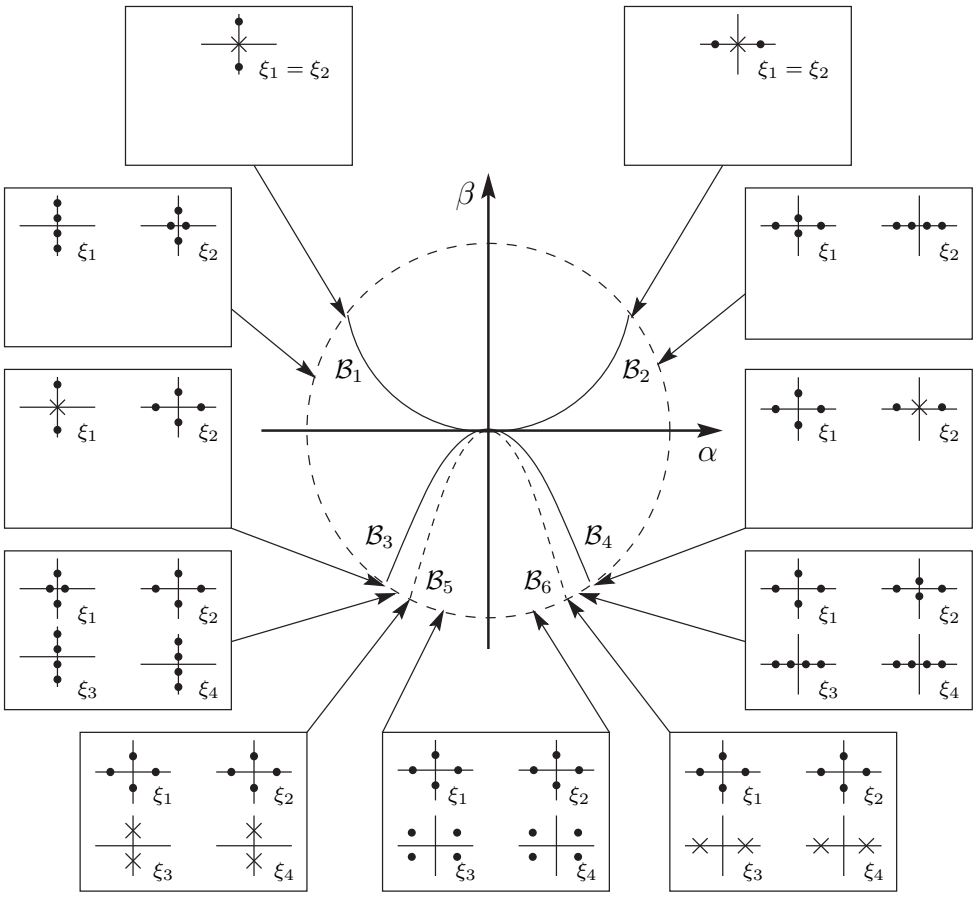

Figure A.1.: Bifurcation diagram for equilibria of f^-. It shows the equilibria ξ_i of the system in the α, β-plane and the position of their eigenvalues in the complex plane. Each of the small boxes refers to a region or bifurcation curve in the parameter plane. Within the boxes single eigenvalues are denoted by '$\bullet$', for double eigenvalues we use '$\times$'. On the solid curves $\mathcal{B}_1 \cup \mathcal{B}_2 := \{\beta = \alpha^2\}$ and $\mathcal{B}_3 \cup \mathcal{B}_4 := \{\beta = -3\alpha^2\}$ local bifurcations of equilibria occur, whereas the dashed curve $\mathcal{B}_5 \cup \mathcal{B}_6 := \{\beta = -4\alpha^2\}$ is related to a qualitative change of the eigenvalues of the equilibria $\xi_{3,4}$.

Homoclinic orbits

We will now show the existence of a homoclinic orbit to the equilibrium ξ_2. The key to this is the invariance of the plane

$$\mathrm{Fix}\,(S) := \{x : Sx = x\} = \{x = (x_1, x_2, x_3, x_4) : x_1 = x_2 = 0\},$$

which has already been observed above. Within $\mathrm{Fix}\,(S)$ the reduced system is also Hamiltonian and it can be shown that a homoclinic orbit is created in the reversible

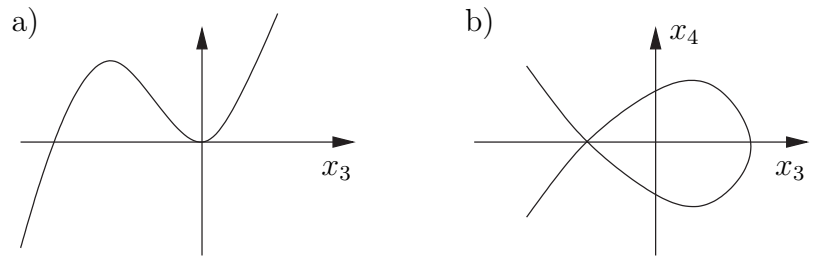

Figure A.2.: Existence of a homoclinic orbit of $f^-(x, \alpha, \beta)$ for $\beta < \alpha^2$: panel (a) shows the potential $V(x_3, \alpha, \beta) = x^3/3 - \alpha x_3^2 + \beta x_3$ for the system in Fix (S), panel (b) shows γ_{hom} itself.

saddle-centre bifurcation on $\mathcal{B}_1 \cup \mathcal{B}_2$, see Figure A.2. It is also possible to derive an analytical expression for the corresponding solution. We obtain

Theorem A.1. *For $\beta < \alpha^2$ the vector field f^- possesses a homoclinic orbit γ_{hom} to the equilibrium ξ_2. The orbit is symmetric with respect to both R_1 and R_2, that is $R_i\gamma_{hom} = \gamma_{hom}$, $i = 1, 2$. The corresponding solution x_{hom} with $x_{hom}(0) \in Fix(R_1) \cap Fix(R_2)$ is given by $x_{hom}(t) = (0, 0, r(t), \dot{r}(t))$, where*

$$r(t) = 3\sqrt{\alpha^2 - \beta} \cdot sech^2 \left(\frac{\sqrt[4]{\alpha^2 - \beta}}{\sqrt{2}}\, t \right) + \alpha - \sqrt{\alpha^2 - \beta}.$$

Theorem A.1 shows the existence of γ_{hom} for all parameter values where ξ_2 exists. Let us discuss this result. We distinguish two cases.

For parameter values between $\mathcal{B}_2$ and $\mathcal{B}_4$ the equilibrium ξ_2 is hyperbolic and the robust existence of γ_{hom} is compatible with the fact that homoclinic orbits to hyperbolic equilibria are of codimension-zero in the class of reversible or Hamiltonian systems. It is possible to prove that γ_{hom} is non-degenerate for parameter values between $\mathcal{B}_2$ and $\mathcal{B}_4$ (Lemma 2 in [91]). This explains the robust existence of the orbit for parameter values in this region.

If, however, we choose parameters *not* between $\mathcal{B}_2$ and $\mathcal{B}_4$ the equilibrium ξ_2 is nonhyperbolic and the above transversality arguments do not apply to the orbit in the full four-dimensional phase space. Indeed, a homoclinic orbit to a nonhyperbolic equilibrium should break up under perturbations even in the case of a reversible or Hamiltonian system. But for γ_{hom} the $\mathbb{Z}_2$-symmetry of f^- does not allow this, since we can repeat the transversality arguments for the situation within the space Fix (S).

The transition of ξ_2 from a hyperbolic equilibrium (real saddle) to a nonhyperbolic equilibrium (saddle centre) occurs for parameter values on $\mathcal{B}_4$. By Theorem A.1 the transition does not affect the orbit γ_{hom} itself. But still, one can expect a bifurcation of orbits from γ_{hom}. In Chapter 2 it is demonstrated that the situation on $\mathcal{B}_4$ leads to a *reversible homoclinic pitchfork bifurcation.*

Heteroclinic orbits

Heteroclinic orbits between equilibria of Hamiltonian systems can only exist if these equilibria belong to the same level set of the Hamiltonian. Since ξ_3 and ξ_4 are the only equilibria of f^- on the same level set of H^-, heteroclinic orbits can only exist between these equilibria. Because of the R_1-reversibility of f^-, and since $\xi_{3,4} \in \mathrm{Fix}\,(R_1)$, such orbits will not come alone but in pairs forming a heteroclinic cycle. We will show that such a cycle exists for parameter values between $\mathcal{B}_4$ and $\mathcal{B}_6$.

It is instructive to consider the local bifurcation of ξ_2 on $\mathcal{B}_4$ first. Here the equilibrium undergoes a (reversible) pitchfork bifurcation giving rise to the two real saddles $\xi_{3,4}$ and turning from a real saddle to a saddle centre itself. A normal form calculation for this bifurcation shows that a small heteroclinic cycle between ξ_3 and ξ_4 emerges in this bifurcation. Hence, the pitchfork bifurcation is of *eye type*, compare also with Figure 1.1.

For the actual proof of existence of such a heteroclinic cycle we employ a shooting method for indefinite Hamiltonian systems developed by Hofer and Toland [44]. The investigations in [44] concern systems with a Hamilton function of the form

$$\widetilde{H}(q,\dot{q}) = \frac{1}{2}\langle S\dot{q},\dot{q}\rangle + V(q),$$

where S is an indefinite matrix, possessing exactly one negative eigenvalue, and V is the potential. It is proved that certain periodic, homoclinic or heteroclinic orbits exist, if the potential V satisfies certain assumptions. In particular, the method is not restricted to any local regime as the discussion of the local bifurcation of ξ_2 above. An application of the method to f^- yields the following theorem.

Theorem A.2. *Consider f^- with parameter values $\alpha > 0$ and $-4\alpha^2 \leq \beta < -3\alpha^2$. Then the equilibria ξ_3 and ξ_4 are connected by a heteroclinic cycle $\{\gamma_{het}, R_1\gamma_{het}\}$.*

Theorem A.2 ensures the existence of the heteroclinic cycle for all parameter values between $\mathcal{B}_4$ and $\mathcal{B}_6$, that is, for all parameter values where the equilibria are real saddles. It has been an open question in [88] what happens to the cycle when we vary parameters such that $\mathcal{B}_6$ is crossed. On this curve the equilibria $\xi_{3,4}$ change their type from real saddles to saddle foci. It is important to note that the shooting method can only be applied to the region where the equilibria are real saddles since it yields a certain monotonicity for the detected orbits, see [44, 91] for details. (We also return to this point in Section A.3 below.) This monotonicity is not shared by orbits that are asymptotic to equilibria of saddle focus type because of the behaviour in a neighbourhood of the equilibrium. In Section A.3 we exploit a topological property of γ_{het} to derive further existence (continuation) results.

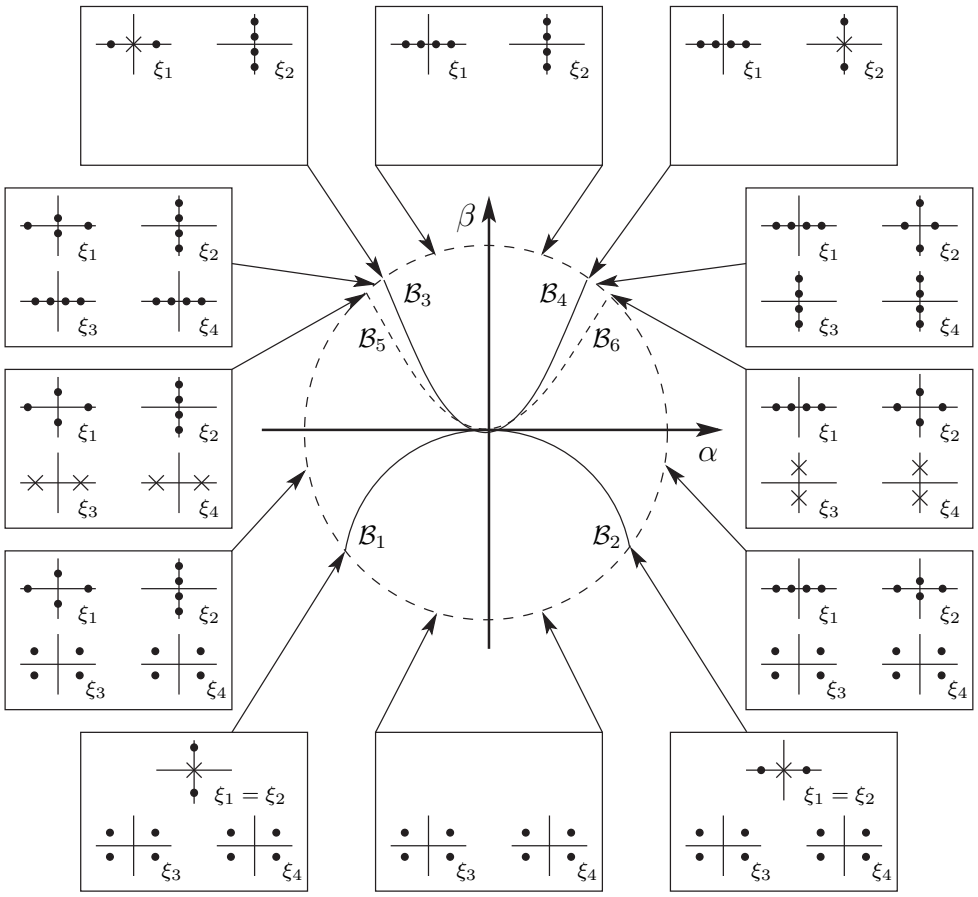

Figure A.3.: Bifurcation diagram of f^+. It shows the equilibria ξ_i of the system in the α, β-plane and the position of their eigenvalues in the complex plane. Each of the small boxes refers to a region or bifurcation curve in the parameter plane. Within the boxes single eigenvalues are denoted by '•', for double eigenvalues we use '×'. On the solid curves $\mathcal{B}_1 \cup \mathcal{B}_2 := \{\beta = 3\alpha^2\}$ and $\mathcal{B}_3 \cup \mathcal{B}_4 := \{\beta = -\alpha^2\}$ local bifurcations of equilibria occur, whereas the dashed curve $\mathcal{B}_5 \cup \mathcal{B}_6 := \{\beta = 2\alpha^2\}$ is related to a qualitative change of the eigenvalues of the equilibria $\xi_{3,4}$.

A.2.2. The elliptic umbilic f^+

The elliptic umbilic f^+ can be analysed in the same way as f^- above. The equilibria of the system and their eigenvalues can again be computed directly. We summarize the results in the bifurcation diagram in Figure A.3. We note that in contrast to f^- the vector field f^+ possesses equilibria for each parameter values.

The results about connecting orbits for f^+ are completely analogous to the ones obtained in the last section. They read as follows.

Theorem A.3. *For $\beta > -\alpha^2$ the vector field f^+ possesses a homoclinic orbit γ_{hom} to the equilibrium ξ_1. The orbit is symmetric with respect to both R_1 and R_2, that is $R_i\gamma_{hom} = \gamma_{hom}$, $i = 1, 2$. The corresponding solution x_{hom} with $x_{hom}(0) \in Fix(R_1) \cap Fix(R_2)$ is given by $x_{hom}(t) = (0, 0, r(t), \dot{r}(t))$, where*

$$r(t) = -3\sqrt{\alpha^2+\beta} \cdot sech^2\left(\frac{\sqrt[4]{\alpha^2+\beta}}{\sqrt{2}}\, t\right) + \alpha + \sqrt{\alpha^2+\beta}.$$

Theorem A.4. *Consider f^+ with parameter values $\alpha < 0$ and $2\alpha^2 \leq \beta < 3\alpha^2$. Then the equilibria ξ_3 and ξ_4 are connected by a heteroclinic cycle $\{\gamma_{het}, R_1\gamma_{het}\}$.*

A.2.3. Two methods to simplify the systems

We present two techniques that will simplify the analysis of (1.1). By a suitable scaling we establish that vector fields $f^{\pm}(\cdot, \alpha_1, \beta_1)$ and $f^{\pm}(\cdot, \alpha_2, \beta_2)$ are equivalent if the parameters lie on the same arc of a parabola $\beta = c\alpha^2$, $c \in \mathbb{R}$. Thus, in a lot of cases it suffices to consider the system under variation of one of the parameters. Afterwards we discuss a technique that allows us to unify the treatment of homoclinic and heteroclinic orbits. Using suitable coordinates we can factor out the $\mathbb{Z}_2$-symmetry of (1.1) and classify homoclinic and heteroclinic orbits as certain homoclinic orbits in the new phase space. In deriving these two results we again concentrate on the hyperbolic case f^-. The computations for f^+ run completely along the same lines and are omitted.

A suitable scaling

For convenience we rewrite f^- as a system of second order ODEs

$$\begin{aligned} \ddot{x}_1 &= 2x_1x_3 + 2\alpha x_1 \\ \ddot{x}_3 &= -x_1^2 - x_3^2 + 2\alpha x_3 - \beta \end{aligned} \tag{A.4}$$

and introduce a new parameter by setting $\lambda = \alpha^2\mathrm{sgn}(\alpha)$. This straightens parabolas in the (α, β)-plane to lines in the (λ, β)-plane. Here we introduce polar coordinates

$$\begin{aligned} \lambda &= \begin{cases} \mathbf{r}\cos\boldsymbol{\phi} & : \quad \lambda \geq 0 \\ -\mathbf{r}\cos(\pi - \boldsymbol{\phi}) & : \quad \lambda < 0 \end{cases} \\ \beta &= \mathbf{r}\sin\varphi \end{aligned}$$

with $\boldsymbol{\phi} \in [-\frac{\pi}{2}, \frac{\pi}{2})$ and $\mathbf{r} \in \mathbb{R}^+$. With no loss of generality we restrict to $\lambda > 0$ in the following. Then (A.4) can be written as

$$\begin{aligned} \ddot{x}_1 &= 2x_1x_3 + 2\sqrt{\mathbf{r}\cos\boldsymbol{\phi}}\, x_1 \\ \ddot{x}_3 &= -x_1^2 - x_3^2 + 2\sqrt{\mathbf{r}\cos\boldsymbol{\phi}}\, x_3 - \mathbf{r}\sin\boldsymbol{\phi}. \end{aligned}$$

Finally, setting $\tilde{x}_1 := x_1/\sqrt{\mathbf{r}}$, $\tilde{x}_3 := x_3/\sqrt{\mathbf{r}}$ and scaling time by $\tau(t) := \sqrt[4]{\mathbf{r}} \cdot t$, we obtain differential equations for $X_{\boldsymbol{\phi},\mathbf{r}}(t) := \tilde{x}_1(\tau(t))$, $Y_{\boldsymbol{\phi},\mathbf{r}}(t) := \tilde{x}_3(\tau(t))$ which read

$$\begin{aligned} \ddot{X}_{\boldsymbol{\phi},\mathbf{r}} &= 2X_{\boldsymbol{\phi},\mathbf{r}}Y_{\boldsymbol{\phi},\mathbf{r}} + 2\sqrt{\cos\boldsymbol{\phi}}\, X_{\boldsymbol{\phi},\mathbf{r}} \\ \ddot{Y}_{\boldsymbol{\phi},\mathbf{r}} &= -X^2_{\boldsymbol{\phi},\mathbf{r}} - Y^2_{\boldsymbol{\phi},\mathbf{r}} + 2\sqrt{\cos\boldsymbol{\phi}}\, Y_{\boldsymbol{\phi},\mathbf{r}} - \sin\boldsymbol{\phi}. \end{aligned} \tag{A.5}$$

Obviously, equation (A.5) depends on $\boldsymbol{\phi}$ alone. Translated backwards into our original parameters we obtain in consequence

Lemma A.5. *Consider $f^{\pm}$ with parameter values (α_1, β_1) and (α_2, β_2) such that α_1, α_2 have the same sign and such that either $\alpha_1 = \alpha_2 = 0$ or $\beta_1/\alpha_1^2 = \beta_2/\alpha_2^2$. Then the vector fields $f^{\pm}(\cdot, \alpha_1, \beta_1)$ and $f^{\pm}(\cdot, \alpha_2, \beta_2)$ are equivalent.*

Let us discuss this result in detail. Lemma A.5 implies that bifurcations (of equilibria, periodic orbits, or connecting orbits) can only occur on parabolas $\{\beta = c\alpha^2\}$ in the parameter plane. Hence, we can also perform the numerical analysis of such bifurcations by keeping one parameter fixed and vary only the other. Moreover, we can use parameters of arbitrary size and we are not chained to some local regime. Finally, the lemma also allows to check the validity of numerical computations, since detected bifurcations should appear only on arcs of parabolas in the (α, β) parameter plane.

Reducing the symmetry

In the final part of this short summary of results for (1.1) we show how the treatment of homoclinic and heteroclinic orbits between the equilibria $\xi_{3,4}$ can be unified. For this we factor out the $\mathbb{Z}_2$-symmetry and consider the systems in *orbit space*, i.e. in the space of orbits of the action of the symmetry group $\{id, S\}$ of (1.1). The equilibria $\xi_{3,4}$ correspond to an equilibrium $\hat{\xi}$ in this space and both homoclinic and heteroclinic orbits to $\xi_{3,4}$ correspond to homoclinic orbits. This makes the general analysis of Chapter 4 applicable to the systems.

We can perform the reduction to orbit space for (1.1) explicitly. Again we focus on the hyperbolic umbilic f^-. Here the calculations proceed as follows. First recall that

$$S : (x_1, x_2, x_3, x_4) \mapsto (-x_1, -x_2, x_3, x_4).$$

Thus, $\mathrm{Fix}\,(S) := \{x_1 = x_2 = 0\}$ and we will transform the (x_1, x_2)-coordinates only. Here, the map S acts as a rotation by π. Returning to the original form in (1.1) we consider f^- as a first order system and rewrite the equations for (x_1, x_2)

$$\begin{aligned} \dot{x_1} &= x_2 \\ \dot{x_2} &= 2x_1x_3 + 2\alpha x_1 \end{aligned} \tag{A.6}$$

For the moment we think of x_3 as a parameter in these equations. It is not hard to calculate that in polar-coordinates

$$x_1 = \mathbf{r}\cos(\boldsymbol{\phi}), \quad x_2 = \mathbf{r}\sin(\boldsymbol{\phi}),$$

system (A.6) becomes

$$\begin{aligned} \dot{\mathbf{r}} &= \frac{\mathbf{r}}{2}\cdot\sin(2\boldsymbol{\phi}) + (x_3+\alpha)\cdot\mathbf{r}\sin(2\boldsymbol{\phi}) \\ \dot{\boldsymbol{\phi}} &= \cos(2\boldsymbol{\phi}) + \left(x_3+\alpha-\frac{1}{2}\right)\cdot(1+\cos(2\boldsymbol{\phi})). \end{aligned}$$

In this version the action of S is immediate, as the system is invariant under $\boldsymbol{\phi}\mapsto\boldsymbol{\phi}+\pi$. We divide out this symmetry by setting $\boldsymbol{\psi}=2\boldsymbol{\phi}$. Geometrically, this map achieves the following: The sides of a quadrant in the (x_1,x_2)-plane are identified ("glued together") in a way such that both the vertical and horizontal sides have different directions, respectively. The resulting surface is known as the real projective plane. One can thus consider the resulting vector field on this surface. But we will not pursue this geometric point of view, as it is of no importance for us.

We go back to 'cartesian' coordinates by setting

$$y_1 = \mathbf{r}\cos(\boldsymbol{\psi}), \quad y_2 = \mathbf{r}\sin(\boldsymbol{\psi}).$$

It is then straightforward to calculate the ODEs for (y_1,y_2) and to adapt those for $(y_3,y_4)=(x_3,x_4)$. They read

$$\begin{aligned} \dot{y_1} &= (1-2y_3-2\alpha)\cdot y_2 - \left(\frac{1}{2}+y_3+\alpha\right)\cdot\frac{y_1\cdot y_2}{\sqrt{(y_1^2+y_2^2)}} \\ \dot{y_2} &= \left(\frac{1}{2}+y_3+\alpha\right)\cdot\frac{2y_1^2+y_2^2}{\sqrt{(y_1^2+y_2^2)}} + (2y_3+2\alpha-1)\cdot y_1 \\ \dot{y_3} &= y_4 \\ \dot{y_4} &= -\frac{(y_1^2+y_2^2)}{2} - \frac{\sqrt{(y_1^2+y_2^2)}}{2}y_1 - y_3^2 + 2\alpha y_3 - \beta. \end{aligned} \tag{A.7}$$

The vector field in (A.7) is well-defined everywhere and smooth in all points, except for the plane $y_1=y_2=0$. This plane corresponds to the fixed space $\mathrm{Fix}\,(S)$ of the $\mathbb{Z}_2$-symmetry in original x-coordinates. Here the vector field is merely continuous, but not differentiable. But since $\mathrm{Fix}\,(S)$ is invariant for the original system, and since $\xi_{3,4}\notin\ \mathrm{Fix}\,(S)$ homoclinic and heteroclinic orbits to these equilibria stay away from this space. Hence, the lack of smoothness in (A.7) is not of concern to us in this setting.

Homoclinic and heteroclinic orbits to $\xi_{3,4}$ of the original system are homoclinic orbits of (A.7) to the equilibrium

$$\hat{\xi} = (\sqrt{-3\alpha^2-\beta}, 0, -\alpha, 0).$$

Note that such orbits correspond to different types of orbits in the original system. If we want to lift back results from orbit space to the original phase space we can distinguish these types by their 'path' in (y_1, y_2)-space. Orbits, whose paths do not encircle the origin in this space necessarily describe homoclinic orbits to ξ_3 and ξ_4. Note that the symmetry implies that such orbits appear in pairs. On the other hand, if the path encircles the point $y_1 = y_2 = 0$, the corresponding pair of orbit in the original space can either be homoclinic or heteroclinic. (Think of the cycle $\{\gamma_{het}, R_1\gamma_{het}\}$ or a pair of homoclinic orbits to $\xi_{3,4}$ close to this cycle.) We can distinguish these two possibilities by the number of their windings. If the number is odd, then the orbit represents a heteroclinic orbit between ξ_3 and ξ_4. In the other case it represents a homoclinic orbit.

A.3. Continuation of a heteroclinic cycle

In this section we consider the heteroclinic cycle $\{\gamma_{het}, R_1\gamma_{het}\}$ of the umbilic systems in detail. Existence results for this cycle have been stated in Theorems A.2 and A.4. The results there only concern values of the parameters α, β for which $\xi_{3,4}$ are real saddles. We show now that the cycle exists at least in some small region in parameter space where the equilibria are complex saddle foci. We do not attack the existence problem directly, but perform a continuation of the known heteroclinic cycle. For this we exploit a topological property of the orbit.

We have seen before that homoclinic and heteroclinic orbits generically exist robustly in reversible or Hamiltonian systems. (The arguments have concerned homoclinic orbits, but they easily generalize to the case of heteroclinic cycles.) Recall that *non-degeneracy* of a symmetric orbit is sufficient for its robust existence. This means that the corresponding stable and unstable manifolds intersect as cleanly as possible along the orbit. Unfortunately, it is very difficult to prove that a specific orbit is non-degenerate, since this requires a detailed knowledge of the behaviour of those manifolds. Since the cycle $\{\gamma_{het}, R_1\gamma_{het}\}$ has been found by a shooting method we do not know enough about the orbits to prove their non-degeneracy.

Remark A.1. We note that there are examples of fourth-order equations for which it could be shown that homoclinic orbits, found by shooting, are non-degenerate, see [9, 84]. But the proofs in these papers are rather specific and do not apply to our case.

Instead of analysing the non-degeneracy of γ_{het} (and consequently $R_1\gamma_{het}$) we focus on a weaker property and show that this cycle exists due to a *topologically transverse* intersection of the stable and unstable manifolds of $\xi_{3,4}$. This idea has been developed by Buffoni in [10] where it has been applied to a heteroclinic cycle in the Extended Fisher-Kolmogorov equation. The precise definition of topological transversality needs additional concepts from differential topology and will be given below. But a good example to have in mind is the intersection of the graph of $F : x \mapsto x^3$ with the x-axis at

0. This intersection is not transverse but, as we will see, it is topologically transverse. An important observation is that this intersection cannot be destroyed. Hence, topological transversality is also sufficient for the continuation of connecting orbits. Note, however, that there may exist additional points of intersection in perturbations.

We will prove that for all values of α, β where $\xi_{3,4}$ are real saddles the cycle exists due to a topologically transverse intersection of the stable and unstable manifolds of $\xi_{3,4}$. Therefore, we can continue the cycle at least to some small region in parameter space where the equilibria are complex saddle foci. This continuation method is closely related to the shooting method in [44] and extensively uses the fact that (1.1) are indefinite Hamiltonian systems. It is therefore useful to return to the presentation of (1.1) as systems of second-order ODEs

$$S\ddot{q} + \nabla V(q, \alpha, \beta) = 0 \tag{A.8}$$

with $q = (x_1, x_3)$. In these coordinates the Hamiltonian reads

$$\widetilde{H}^{\pm}(q, \dot{q}, \alpha, \beta) = \frac{1}{2}\langle S\dot{q}, \dot{q}\rangle + V(q, \alpha, \beta),$$

as above, with an indefinite quadratic form $\langle S\cdot, \cdot\rangle$ and potential V.

As usual, we do not deal with both systems (1.1) in detail, but we focus on the hyperbolic umbilic f^- in the following. All calculations can repeated for the elliptic case without any difficulties. The results of this section have already appeared in [91], the proofs and technical details are taken from the preprint [89]. We first provide the necessary background from differential geometry.

A.3.1. Topological transversality

The notion of topological transversality is closely related to the concept of intersection numbers. Our approach to this subject is similar to [10]. We start with the concept of intersection numbers of manifolds (see also [43, 38]) which is afterwards generalized to compact pieces of manifolds.

Let M be a finite-dimensional orientable C^1-manifold without boundary and let K, N be finite-dimensional orientable C^1-manifolds without boundary such that K is a closed submanifold of N and

$$\dim M + \dim K = \dim N.$$

Let $F \in C^1(M, N)$ be transverse to K in the classic sense. This means that for each $k \in K$ for which there exists $m \in M$ such that $F(m) = k$ it holds

$$\operatorname{im}(d_m F) \oplus T_k K = T_k N.$$

If the natural orientation of $\operatorname{im}(d_m F)$ completed with the orientation of $T_k K$ gives the orientation of $T_k N$ then the *orientation number* $O(F, m, K)$ of F at x is set to

$O(F, m, K) = +1$, and $O(F, m, K) = -1$ otherwise. Now, the *intersection number* of F and K can be defined as an integer $I(F, K)$ satisfying the following:

I-1) If F is transverse to K, then $F^{-1}(K)$ is a finite set of points [38] and

$$I(F, K) := \sum_{m \in F^{-1}(K)} O(F, m, K).$$

I-2) If F_0 and F_1 are homotopic then $I(F_0, K) = I(F_1, K)$.

I-3) If $I(F, K) \neq 0$ then $F^{-1}(K) \neq \emptyset$.

I-4) If $\Delta \in C^1(N, N')$ is a diffeomorphism, then $I(\Delta \circ F, \Delta(K)) = \pm I(F, K)$.

I-5) Suppose that intersection theory is applicable for M_i, K_i, N_i, F_i. Then

$$I(F_1 \times \cdots \times F_k, K_1 \times \cdots \times K_k) = \prod_{i=1}^{k} I(F_i, K_i).$$

It is important to note that the intersection number is continuous, i.e. it is constant under small perturbations of F or K. Also note that every map F is homotopic to a map $\tilde{F}$ transverse to K, where $\tilde{F}$ can be chosen as close to F as necessary.

Assume now that M is also included in N and denote the inclusion by $i : M \hookrightarrow N$. Then the intersection number of M and K is denoted by $I(M, K)$ and is defined by

$$I(M, K) := I(i, K).$$

The intersection of the manifolds M and K is said to be *topologically transverse* provided that $I(M, K) \neq 0$.

For the application of this concept to the heteroclinic cycle of f^- we have to generalize the concept of topological transversality to *compact pieces of manifolds* as in [10]. Let $\tilde{M}$ be a finite-dimensional orientable C^1-manifold without boundary. A compact subset $M \neq \emptyset$ of $\tilde{M}$ with $\mathrm{cl}\,(\mathrm{int}\, M) = M$ is called a *compact piece of manifold*. We refer to [10] for a precise definition of intersection numbers of compact pieces of manifolds which slightly differs from the one above. We only mention that the characteristic properties *I-1)* to *I-5)*, which are essential in later computations, also hold in the generalized frame provided that one restricts to *admissible maps*. A map $F : M \to N$ which can be extended to a map $\tilde{F} \in C^1(\tilde{M}, N)$ is called admissible if $F^{-1}(K) \subset \mathrm{int}\, M$. For the intersection number of two compact pieces of manifolds $M_1 \subset N$, $M_2 \subset N$ the assumption of admissibility means $\dim M_1 + \dim M_2 = \dim N$ and $M_1 \cap M_2 \subset \mathrm{int}\, M_1 \cap \mathrm{int}\, M_2$. As above, the intersection of M_1 and M_2 is called topologically transverse if $I(M_1, M_2) \neq 0$.

A.3.2. Shooting for heteroclinic orbits

We consider the reversible hyperbolic umbilic f^- for parameter values $\alpha > 0$ and $-4\alpha^2 \leq \beta < -3\alpha^2$. In this case the equilibria ξ_3 and $\xi_4 = R_2\xi_3$ are real saddles. We show that

their two-dimensional stable and unstable manifolds intersect topologically transversally in some suitably chosen cross section Σ. We work in $(q, \dot{q})$-coordinates and use a (beforementioned) monotonicity property of orbits of the system that allows a reduction to q-space.

For this it is convenient to modify the potential V such that the equilibria $\xi_{3,4}$ are contained in the zero level set of $\widetilde{H}^-$. This can easily be achieved by considering

$$V(q, \alpha, \beta) = q_1^2 q_2 + \frac{1}{3} q_2^3 + \alpha(q_1^2 - q_2^2) + \beta q_2 + \frac{4}{3}\alpha^3 + \alpha\beta,$$

which, of course, leads to the same systems of ODEs.

We now introduce the following cones in $\mathbb{R}^2$

$$\begin{aligned} K_0 &:= \{p = (p_1, p_2) \in \mathbb{R}^2 : |p_2| < |p_1|, p_1 > 0\} \\ K_1 &:= \{p = (p_1, p_2) \in \mathbb{R}^2 : |p_2| > |p_1|, p_2 > 0\} \\ K_2 &:= \{p = (p_1, p_2) \in \mathbb{R}^2 : |p_2| < |p_1|, p_1 < 0\} \\ K_3 &:= \{p = (p_1, p_2) \in \mathbb{R}^2 : |p_2| > |p_1|, p_2 < 0\}. \end{aligned}$$

We also introduce a component C of the set $\{q : V(q, \alpha, \beta) > 0\}$ which we take as the region bounded by the line $q_2 = -\alpha$ and by the curve $3q_1^2 + q_2^2 - 4\alpha q_2 + 3\beta + 4\alpha^2 = 0$ (see Figure A.4 for an impression of this set). For $q \in \partial C$ we have $V(q, \alpha, \beta) = 0$.

From now on we only consider solutions in the zero level set $\mathcal{H}_0$ of the Hamiltonian. For such orbits the sign of $\langle S\dot{q}, \dot{q} \rangle$ only changes if the sign of $V(q, \alpha, \beta)$ changes. Therefore $\dot{q}$ is forced to stay in one of the cones K_i as long as $V(q, \alpha, \beta) \neq 0$. In particular, if $(q, \dot{q})$ is a solution of (A.8) such that $q(0) \in C$, $\dot{q}(0) \in K_0$ then either $\lim_{t\to\infty} q(t) = \xi_4$ or the *path* $q(t)$ has to leave C at some finite *exit time* τ^+ (see also [44]). Furthermore, if $q_2(\tau^+) = -\alpha$ (i.e. the path leaves through the upper boundary of C) then $\dot{q}(\tau^+) \neq 0$ and $\dot{q}(\tau^+) \in \partial K_0 \cap \partial K_1$. In the other case we have $\dot{q}(\tau^+) \neq 0$ and $\dot{q}(\tau^+) \in \partial K_0 \cap \partial K_3$.

Now for $x \in [-\sqrt{-3\alpha^2 - \beta}, 0]$ let $Q_x := \{q \in \operatorname{cl} C, q_1 \leq x\}$ and suppose that $(q, \dot{q})$ is a solution with $q(0) \in \operatorname{cl} C$ and $\dot{q}(0) \in \operatorname{cl} K_0$. Then the path $q(t)$ leaves Q_x in some finite exit-time $\tau_x^+(q(0), \dot{q}(0))$ and the related point of leaving in $(q, \dot{q})$-space will be denoted by

$$\Gamma_x(q(0), \dot{q}(0)) := \left(q\left(\tau_x^+(q(0), \dot{q}(0))\right), \dot{q}\left(\tau_x^+(q(0), \dot{q}(0))\right)\right).$$

If $q(0) \notin Q_x$ then we set $\tau_x^+(q(0), \dot{q}(0)) = 0$ and $\Gamma_x(q(0), \dot{q}(0)) = (q(0), \dot{q}(0))$. This construction is applied to some set $\mathcal{A}$ which for $\varepsilon > 0$ sufficiently small is defined by

$$\mathcal{A} := \{(q, \dot{q}) \in W^u_{loc}(\xi_3) : q_1 = -\sqrt{-3\alpha^2 - \beta} + \varepsilon, q \in \operatorname{cl} C\}.$$

Here $W^u_{loc}(\xi_3)$ denotes the local unstable manifold of ξ_3. (We refer to Figure A.4 for an impression of some of the sets previously defined.) The next lemma describes properties of $\mathcal{A}$.

Lemma A.6. *Consider (A.8) with $-4\alpha^2 \leq \beta < -3\alpha^2$ and let $\mathcal{A}$ be defined as above with $\varepsilon > 0$ sufficiently small. Then for every $q \in \operatorname{cl} C$ with $q_1 = -\sqrt{-3\alpha^2 - \beta} + \varepsilon$ there exists a unique $\dot{q} \in \operatorname{cl} K_0$ such that $(q, \dot{q}) \in \mathcal{A}$. If $q(0) \in \partial C$ with $q_2(0) = -\alpha$ then $\dot{q}(0) \in \partial K_0 \cap \partial K_1$, else if $q(0) \in \partial C$ with $q_2(0) < -\alpha$ then $\dot{q}(0) \in \partial K_0 \cap \partial K_3$. Finally, let $(q, \dot{q})$ be a solution with $(q(0), \dot{q}(0)) \in \mathcal{A}$. Then for every $t < 0$ it holds $q(t) \in C$.*

Proof. The proof of the first part of Lemma A.6 uses explicit calculations for the linearized vector field near the equilibrium ξ_3 and the fact that $W^u_{loc}(\xi_3)$ is tangent to the unstable eigenspace of this problem. More precisely, we can flatten out $W^u_{loc}(\xi_3)$ by an appropriate transformation, so that the results below carry over from the linear to the nonlinear problem. The actual computations have been performed using computer algebra programmes. As they involve some lengthy expressions we will reduce their presentation to a minimum.

Dropping the parameters for convenience and denoting the linearization at ξ_3 by A we find that

$$\sigma(A) = \left\{ \pm\sqrt{2\alpha \pm \sqrt{4\alpha^2 + \beta}} \right\}.$$

Let $\mathfrak{e} = (\mathfrak{e}_1, \ldots, \mathfrak{e}_4)$ and $\mathfrak{f} = (\mathfrak{f}_1, \ldots, \mathfrak{f}_4)$ denote the eigenvectors of A corresponding to the positive eigenvalues $\sqrt{2\alpha \pm \sqrt{4\alpha^2 + \beta}}$. Note that for $\beta = -4\alpha^2$ there is only one positive eigenvalue of geometric multiplicity 1. In this case let $\mathfrak{e}$ denote the eigenvector and let $\mathfrak{f}$ be a suitably chosen vector in the generalized eigenspace, complementary to $\mathfrak{e}$.

Let us now choose $q \in \operatorname{cl} C$ with $q_1 := x_0 + \varepsilon$. In order to show that there exists a unique $\dot{q}$ such that $(q, \dot{q}) \in \mathcal{A}$ we consider the linear problem. Here this assertion follows from

$$\det \begin{pmatrix} \mathfrak{e}_1 & \mathfrak{f}_1 \\ \mathfrak{e}_2 & \mathfrak{f}_2 \end{pmatrix} \neq 0.$$

(Note that we work in $(q, \dot{q})$-phase space such that the first two components of $\mathfrak{e}$, $\mathfrak{f}$ correspond to the q-variables.)

For the proof of the next assertions observe that for each $(q, \dot{q})$ in $\mathcal{A}$ with $q \in C$ the velocity $\dot{q}$ is bound to lie in the same cone K_i since $V(q, \alpha, \beta) > 0$ in C and since $\mathcal{A} \subset \mathcal{H}_0$. We can therefore restrict to consider the situation on ∂C. Suppose for instance that $(q, \dot{q}) \in \mathcal{A}$ with $q \in \partial C$ and $q_2 = -\alpha$, and let us show that $\dot{q} \in \partial K_0 \cap \partial K_1$. In the linear problem a simple computation shows that for $\mathfrak{g} = (\mathfrak{g}_1, \ldots, \mathfrak{g}_4) \in \mathit{span}\{\mathfrak{e}, \mathfrak{f}\}$ with $\mathfrak{g}_1 = \varepsilon$, $\mathfrak{g}_2 = 0$ it holds $\mathfrak{g}_3 > 0$, $\mathfrak{g}_4 > 0$. Since in the nonlinear problem $V(q, \alpha, \beta) = 0$ for $q \in \partial C$ the result follows.

For the last part of the lemma we have to show that for $(q, \dot{q}) \in \mathcal{A}$ we have $\tau^-(q, \dot{q}) = -\infty$. Seeking a contradiction we assume that there exists $(q, \dot{q}) \in \mathcal{A}$ with $\tau^-(q, \dot{q}) = \tau_0 < \infty$. Without loss of generality we further assume that $q(\tau_0) = (q_0, q_1(q_0))$, i.e. that the corresponding path leaves C through the lower boundary. Then $\dot{q}(\tau_0) \in \partial K_0 \cap \partial K_1$ and we have $\dot{q}(t) \in K_1$ for $t < \tau_0$ close to τ_0. From Figure A.4 it can be seen that in this case

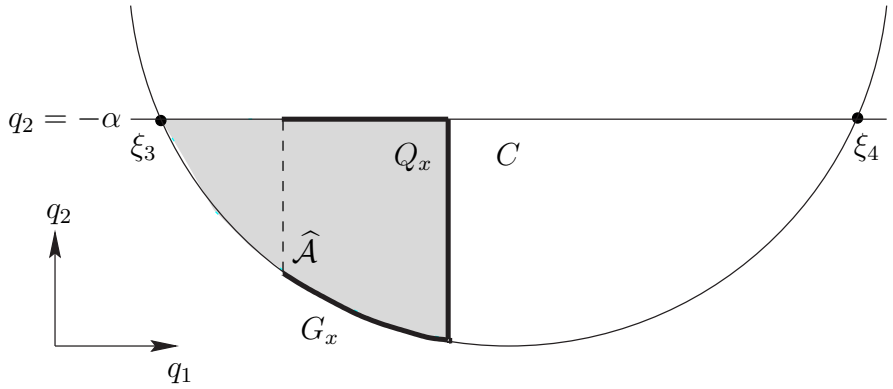

Figure A.4.: Sketch of the set C. By $\widehat{\mathcal{A}}$ we denote the projection of $\mathcal{A}$ onto q-space.

$V(q(t), \alpha, \beta) \leq 0$ and therefore $\dot{q} \in K_1$ for all $t < \tau^-$. This contradicts $(q, \dot{q}) \in W^u(\xi_3)$ (see again Figure A.4). □

Lemma A.6 allows to consider $\mathcal{M} := \Gamma_0(\mathcal{A})$. Clearly, $\mathcal{M} \subset W^u(\xi_3)$ and, by reversibility, $R_2\mathcal{M} \subset W^s(\xi_4)$. We will show that $\mathcal{M}$ and $R_2\mathcal{M}$ intersect topologically transversally in

$$\Sigma := \{(q, \dot{q}) \in \mathcal{H}_0 : q \in C, q_1 = 0, \dot{q} \in K_0\}.$$

Note that $\dim \mathcal{M} = \dim R_2\mathcal{M} = 1$ and $\dim \Sigma = 2$. Moreover, since for $(q, \dot{q}) \in \mathcal{M} \cap \Sigma$ we have $\dot{q} \in K_0$ and therefore $\dot{q}_1 > 0$. We can thus view Σ as a cross section to $W^u(\xi_3)$ in $\mathcal{H}_0$.

Before the calculation of the intersection number we need another technical result.

Lemma A.7. *For $x \in [-\sqrt{-3\alpha^2 - \beta}, 0]$ define $\tau_x^+(q, \dot{q})$ and $\Gamma_x(q, \dot{q})$ as above. Then $\tau_x^+(\cdot, \cdot)$ and $\Gamma_x(\cdot, \cdot)$ are continuous in $\mathcal{A}$.*

Proof. The continuity of Γ_x is an immediate consequence of the continuity of τ_x, so we show the latter using similar arguments as in the proof of Lemma 7 in [44].

First choose $(q_0, \dot{q}_0) \in \mathcal{A}$ and consider the case $\tau_x^+(q_0, \dot{q}_0) = 0$. Then for each $\epsilon > 0$ sufficiently small it holds $q_0(\epsilon) \notin Q_x$. By continuous dependence on the initial value there exists a neighbourhood U of $(q_0, \dot{q}_0)$ in $\mathcal{A}$ such that for each $(q, \dot{q}) \in U$ we have $q(\epsilon) \notin Q_x$. This implies continuity in the first case.

For $\tau_x^+(q_0, \dot{q}_0) > 0$ arguments as above show the existence of a neighbourhood U of $(q_0, \dot{q}_0)$ in $\mathcal{A}$ such that for each $(q, \dot{q}) \in U$ we have $q(\tau_x^+(q_0, \dot{q}_0) + \epsilon) \notin Q_x$ for $\epsilon > 0$ sufficiently small. Stated differently, this means $\tau_x^+(q, \dot{q}) \leq \tau_x^+(q_0, \dot{q}_0) + \epsilon$. It remains to show that $\tau_x^+(q, \dot{q}) \geq \tau_x^+(q_0, \dot{q}_0) - \epsilon$. For this assume U to be compact. From the fact that $\dot{q} \in K_0$, i.e. that $\dot{q}_1 > 0$, for each $(q, \dot{q}) \in U$ and since $\dot{q}$ is bounded in U we can infer the existence of $\delta > 0$ such that for all $(q, \dot{q}) \in U$ it holds $\tau_x^+(q, \dot{q}) \geq \delta > 0$. Furthermore, since $\operatorname{int} Q_x$ is an open neighbourhood of the set $\{q_0(t) : t \in [\delta/2, \tau_x^+(q_0, \dot{q}_0) - \epsilon]\}$ there

exists a neighbourhood V of $(q_0, \dot{q}_0)$ in $\mathcal{A}$ such that $q(t) \in \operatorname{int} Q_x$ for $(q, \dot{q}) \in V$ and $t \in [\delta/2, \tau_x^+(q_0, \dot{q}_0) - \epsilon]$. Now each $(q, \dot{q}) \in V \cap U$ meets our requirements which proves continuity of τ_x^+. □

Calculation of the intersection number

Let us now come to the calculation of the intersection number of $\mathcal{M}$ and $R_2\mathcal{M}$ in Σ as defined above. We note that in Σ the involution R_2 coincides with $\widetilde{R}_2 : (q_1, q_2, \dot{q}_1, \dot{q}_2) \mapsto (q_1, q_2, \dot{q}_1, -\dot{q}_2)$. In the following it will be more convenient to use $\widetilde{R}_2$.
We use a homotopy which is constructed with

$$G_x := \{q = (q_1, q_2) \in \partial C : -\sqrt{-3\alpha^2 - \beta} + \varepsilon \leq q_1 \leq x\} \cup \{q \in C : q_1 = x\}.$$

The set G_x is homeomorphic to $[-1, 1]$ (see again Figure A.4). The corresponding homeomorphism is denoted by $\delta_x : G_x \to [-1, 1]$. For $q \in C$ we can assume δ_x to be a diffeomorphism. We also define the map

$$\begin{aligned} \Delta_x : (G_x \times \operatorname{cl} K_0) \cap \mathcal{H}_0 &\to [-1, 1] \times \mathbb{R} \\ (q, v) &\mapsto (\delta_x(q), v_2). \end{aligned}$$

which also is a homeomorphism, and a diffeomorphism for $q \in C$. Note that the domain of Δ_0 contains the cross section Σ.
In order to work within the general frame of Section A.3.1 above we can restrict $\mathcal{M}$, $R_2\mathcal{M}$ to an appropriate closed subset of Σ such that the restrictions are compact manifolds with boundary. Recall from above that $\dim \mathcal{M} = \dim R_2\mathcal{M} = 1$ and $\dim \Sigma = 2$ and therefore intersection theory is applicable. Setting $x_0 := -\sqrt{-3\alpha^2 - \beta}$ we obtain the following sequence of equations

$$\begin{aligned} I(\mathcal{M}, R_2\mathcal{M}) &= I\left(\mathcal{M}, \widetilde{R}_2\mathcal{M}\right) \\ &= I\left(\Gamma_0(\mathcal{A}), \widetilde{R}_2\Gamma_0(\mathcal{A})\right) \\ &= \pm I\left((\Delta_0 \circ \Gamma_0)(\mathcal{A}), (\Delta_0 \circ \widetilde{R}_2\Gamma_0)(\mathcal{A})\right) \\ &= \pm I\left((\Delta_x \circ \Gamma_x)(\mathcal{A}), (\Delta_x \circ \widetilde{R}_2\Gamma_x)(\mathcal{A})\right) \quad \forall x \in [x_0 + \varepsilon, 0] \\ &= \pm I\left((\Delta_{x_0+\varepsilon} \circ \Gamma_{x_0+\varepsilon})(\mathcal{A}), (\Delta_{x_0+\varepsilon} \circ \widetilde{R}_2\Gamma_{x_0+\varepsilon})(\mathcal{A})\right). \end{aligned}$$

Here we have used the fact that Δ_0 is a diffeomorphism in Σ and the homotopy property of the intersection number. The latter requires to check the admissibility of the homotopy which amounts to prove the next Lemma.

Lemma A.8. *Let $\partial\mathcal{A} := \{(q, \dot{q}) \in \mathcal{A} : q \in \partial C\}$. Then for each $x \in [x_0 + \varepsilon, 0]$ it holds*

$$(\Delta_x \circ \Gamma_x)(\partial\mathcal{A}) \cap (\Delta_x \circ \widetilde{R}_2\Gamma_x)(\mathcal{A}) = \emptyset.$$

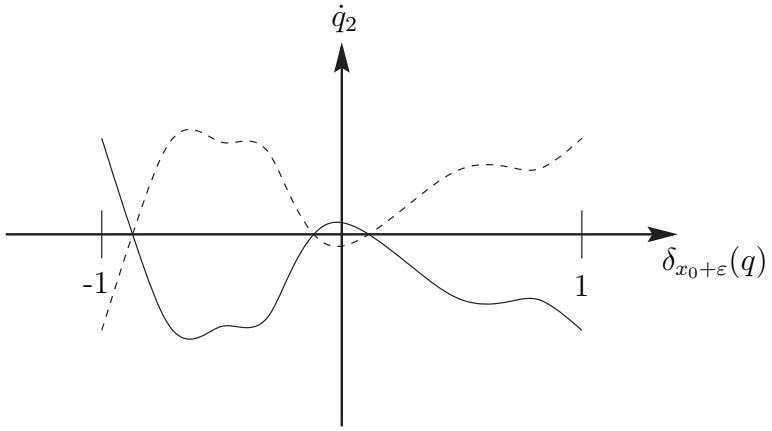

Figure A.5.: Possible graphs of $\Delta_{x_0+\varepsilon}$ and $(\Delta_{x_0+\varepsilon} \circ \widetilde{R}_2)$

Proof. Assume that there exists $x \in [x_0 + \varepsilon, 0]$ for which the condition is not fulfilled, i.e. that there exists $a \in \Gamma_x(\partial\mathcal{A})$ with $a \in \widetilde{R}_2\Gamma_x(\mathcal{A})$. Since, however, $\Gamma_x(\partial\mathcal{A}) = \partial\mathcal{A}$, $(\widetilde{R}_2\Gamma_x)(\partial\mathcal{A}) = \widetilde{R}_2(\partial\mathcal{A})$ we would have $a \in \partial\mathcal{A} \cap \widetilde{R}_2(\partial\mathcal{A})$. For $a := (q, \dot{q})$ this implies $\dot{q}_2 = 0$ and therefore $\dot{q}_1 = 0$ by Lemma A.6 which gives a contradiction. □

It remains to calculate

$$I\left((\Delta_{x_0+\varepsilon} \circ \Gamma_{x_0+\varepsilon})(\mathcal{A}), (\Delta_{x_0+\varepsilon} \circ \widetilde{R}_2\Gamma_{x_0+\varepsilon})(\mathcal{A})\right) = I\left(\Delta_{x_0+\varepsilon}(\mathcal{A}), (\Delta_{x_0+\varepsilon} \circ \widetilde{R}_2)(\mathcal{A})\right).$$

For this observe that $\partial\mathcal{A} = \{(q^t, \dot{q}^t), (q^b, \dot{q}^b)\}$, where $\dot{q}_2^t > 0$ and $\dot{q}_2^b < 0$ by Lemma A.6. Whence, for $(p^t, \dot{p}^t) := \widetilde{R}_2(q^t, \dot{q}^t)$ and $(p^b, \dot{p}^b) := \widetilde{R}_2(q^b, \dot{q}^b)$ we have $\dot{p}_2^t < 0$ and $\dot{p}_2^b > 0$, respectively (see also Figure A.5.)

As pointed out in Section A.3.1 we can with no loss of generality assume that the intersection of $\Delta_{x_0+\varepsilon}(\mathcal{A})$ and $(\Delta_{x_0+\varepsilon} \circ \widetilde{R}_2)(\mathcal{A})$ is transverse. (If necessary, the intersection can be modified by a homotopy.) Then there necessarily exists an odd number of intersection points and we conclude that

$$I\left(\Delta_{x_0+\varepsilon}(\mathcal{A}), (\Delta_{x_0+\varepsilon} \circ \widetilde{R}_2)(\mathcal{A})\right) \neq 0.$$

We have thus proved that there exists a topologically transverse intersection of subsets of $W^u(\xi_3)$ and $W^s(\xi_4)$ for all parameter values $\alpha > 0$ and $-4\alpha^2 \leq \beta < -3\alpha^2$. An immediate consequence is the final theorem.

Theorem A.9. *There exists $\delta > 0$ such that for $\alpha > 0$ and $-4\alpha^2 - \delta < \beta < -4\alpha^2$ the vector field f^- possesses a heteroclinic cycle connecting the equilibria ξ_3 and ξ_4.*

We finally like to point out that this theorem indeed concerns the heteroclinic cycle $\{\gamma_{het}, R_1\gamma_{het}\}$. For parameter values near $\mathcal{B}_5$ centre manifold theory demonstrates that

there exists only one 'small' cycle between ξ_3 and ξ_4. But this cycle necessarily lies in the intersection $\mathcal{M} \cap R_2\mathcal{M}$ and is also the one which is detected by the shooting method, i.e. it is the cycle $\{\gamma_{het}, R_1\gamma_{het}\}$. Hence, Theorem A.9 allows us to continue this cycle to parameter values where $\xi_{3,4}$ are saddle foci. It has been one of the open questions in [88] if this is possible.

We can say even more. Using the scaling property of f^-, established above, we can conclude that there exists a further arc - say $\mathcal{B}_H$ - of a parabola $\{\beta = c\alpha^2\}$ in parameter space such that the cycle exists for parameter values between $\mathcal{B}_H$ and $\mathcal{B}_6$. Since the heteroclinic cycle does not 'survive' the Hamiltonian-Hopf bifurcation of $\xi_{3,4}$ on $\mathcal{B}_5$ the bifurcation curve $\mathcal{B}_H$ lies between $\mathcal{B}_5$ and $\mathcal{B}_6$. The numerical studies in Section 1.4 reveal $\mathcal{B}_H$ to be given by $\beta \approx -5.5\alpha^2$, $\alpha < 0$. For these parameter values the cycle undergoes a saddle-node bifurcation with a second heteroclinic cycle between $\xi_{3,4}$ and disappears.

Bibliography

[1] N. Akhmediev and A. Ankiewicz. *Solitons: Nonlinear pulses and beams*. Chapman and Hall, London, 1997.

[2] C.J. Amick and J.F. Toland. Homoclinic orbits in the dynamic phase-space analogy of an elastic strut. *European J. Appl. Mech.*, 3:97–114, 1992.

[3] D. G. Aronson, M. Golubitsky, and Krupa M. Coupled arrays of josephson junctions and bifurcation of maps with S_n symmetry. *Nonlinearity*, 4:861–902, 1991.

[4] L. A. Belyakov and L. P. Shilnikov. Homoclinic Curves and Complex Solitary Waves. *Selecta Mathematic Sovietica*, 9:219–228, 1990.

[5] G. D. Birkhoff. Nouvelles recherche sur les systèmes dynamiques. *Mem. Pontif. Acad. Sci. Novi Lyncaei*, 53:85–216, 1935.

[6] P. Bolle and B. Buffoni. Multibump homoclinic solutions to a centre equilibrium in a class of autonomous Hamiltonian systems. *Nonlinearity*, 12:1699–1716, 1999.

[7] J. P. Boyd. *Weakly Nonlocal Solitary Waves and Beyond-All-Orders Asymptotics*. Kluwer, Dodrecht, Boston, London, 1998.

[8] H. W. Broer, S. N. Chow, Y. Kim, and G. Vegter. A normally elliptic Hamiltonian bifurcation. *Z. Angew. Math. Phys.*, 44:389–432, 1993.

[9] B. Buffoni, A. R. Champneys, and J. F. Toland. Bifurcation and coalescence of a plethora of homoclinic orbits for a Hamiltonian system. *J. Dyn. Diff. Eqns.*, 8:221–281, 1996.

[10] B. Buffoni. Shooting methods and topological transversality. *Proc. Roy. Soc. Edin. A*, 129:1137–1155, 1999.

[11] A. V. Buryak, P. Di Trapani, D. V. Skryabin, and S. Trillo. Optical solitons due to quadratic nonlinearities: from basic physics to futuristic applications. *Physics Reports*, 370:63–235, 2002.

[12] A. V. Buryak. Stationary soliton bound states existing in resonance with linear waves. *Physical Review E*, 52:1156–1163, 1995.

[13] A. V. Buryak. *Solitons due to quadratic nonlinearities*. PhD thesis, Australian National University, 1996.

[14] D. C. Calvo and T. R Akylas. On the formation of bound states by interacting

nonlocal solitary waves. *Physica D*, 101:270–288, 1997.

[15] A. R. Champneys and M. D. Groves. A global investigation of solitary wave solutions to a two-parameter model for water waves. *J. Fluid Mech.*, 342:199–229, 1997.

[16] A. R. Champneys and J. Härterich. Cascades of homoclinic orbits to a saddle-centre for reversible and perturbed Hamiltonian systems. *Dynamical Systems*, 15:231–252, 2000.

[17] A. R. Champneys, B. A. Malomed, and M. J. Friedman. Thirring solitons in the presence of dispersion. *Phys. Rev. Lett.*, 80:4168–4171, 1998.

[18] A. R. Champneys, B. A. Malomed, J. Yang, and D. J. Kaup. Embedded solitons: solitary waves in resonance with the linear spectrum. *Physica D*, 152:340–354, 2001.

[19] A. R. Champneys and B. A. Malomed. Embedded solitons in a three-wave system. *Phys. Rev. E*, 61:463–466, 1999.

[20] A. R. Champneys and B. A. Malomed. Moving embedded solitons. *Phys. Rev. A*, 32:547–553, 1999.

[21] A. R. Champneys and J. F. Toland. Bifurcation of a plethora of multi-modal homoclinic orbits for autonomous Hamiltonian systems. *Nonlinearity*, 6:665–772, 1993.

[22] A. R. Champneys. Homoclinic orbits in reversible systems and their applications in mechanics, fluids and optics. *Physica D*, 112(1-2):158–186, 1998.

[23] A. R. Champneys. Homoclinic orbits in reversible systems II: Multi-bumps and saddle-centres. *CWI Quarterly*, 12(3-4):185–212, 1999.

[24] A. R. Champneys. Codimension-one persistence beyond all orders of homoclinic orbits to singular saddle centres in reversible systems. *Nonlinearity*, 14(87-112), 2001.

[25] P. Chossat and R. Lauterbach. *Methods in Equivariant Bifurcation Theory and Dynamical Systems*. World Scientific, 2000. Adv. Series in Nonlinear Dynamics.

[26] L. Debnath. *Nonlinear water waves*. Academic Press, Boston, 1994.

[27] B. Deng. Homoclinic bifurcations with nonhyperbolic equilibria. *SIAM J. Math. Anal.*, 21(3):693–720, 1990.

[28] R. L. Devaney. Homoclinic orbits in Hamiltonian systems. *J. Diff. Eqns.*, 21:431–438, 1976.

[29] R. L. Devaney. Reversible diffeomorphisms and flows. *Trans. Amer. Math. Soc.*, 218:89–113, 1976.

[30] R. L. Devaney. Blue sky catastrophes in reversible and Hamiltonian systems. *Indiana Univ. Math. J.*, 26:247–263, 1977.

[31] C. M. de Sterke and J. E. Sipe. Gap solitons. *Progress in Optics*, 33:203–260, 1993.

[32] E. J. Doedel, A. R. Champneys, T. R. Fairgrieve, Yu. A. Kuznetsov, B. Sandstede, and X. J. Wang. AUTO97 continuation and bifurcation software for ordinary differ-

ential equations, 1997. Available by anonymous ftp from FTP.CS.CONCORDIA.CA, directory PUB/DOEDEL/AUTO.

[33] F. Dumortier. Local study of planar vector fields: singularities and their unfoldings. *Structures in Dynamics,* Studies in Mathematical Physics, 2:161–242, 1991.

[34] B. Fiedler and D. Turaev. Coalescence of reversible homoclinic orbits causes elliptic resonance. *Int. J. Bifurcation Chaos*, 6:1007–1027, 1996.

[35] J. Fujioka and A. Espinosz. Soliton-like solution of an extenced NLS equation existing in resonance with linear dispersive waves. *Journal of the Physical Society of Japan*, 66:2601–2607, 1997.

[36] R. Grimshaw and P. Cook. Solitary waves with oscillatory tails. In A. T. Chwang, J. H. W. Lee, D. Y. C. Leung, and A. A. Balkema, editors, *Proceedings of Second International Conference on Hydrodynamics, Hong Kong 1996*, pages 327–336. Hydrodynamics: Theory and Applications, volume 1, 1996.

[37] J. Guckenheimer and P. Holmes. *Nonlinear Oscillations, Dynamical Systems and Bifurcations of Vector Fields.* Springer-Verlag, New York, U.S.A., 1983.

[38] V. Guillemin and A. Pollack. *Differential Topology.* Prentice-Hall, 1974.

[39] J. Hale and X.-B. Lin. Heteroclinic orbits for retarded functional differential equations. *Journal of Differential Equations*, 65:175–202, 1986.

[40] H. Hanßmann. The reversible umbilic bifurcation. *Physica D*, 112(1-2):81–94, 1998.

[41] J. Härterich. Cascades of homoclinic orbits in reversible dynamical systems. *Physica D*, 112:187–200, 1997.

[42] G. M. Hek. *Bifurcations of homoclinic orbits in singularly perturbed flows.* PhD thesis, Utrecht University, 2000.

[43] M. W. Hirsch. *Differential Topology.* Springer, 1976.

[44] H. Hofer and J.F. Toland. Homoclinic, heteroclinic and periodic orbits for a class of indefinite Hamiltonian systems. *Math. Annalen*, 268:387–403, 1984.

[45] P. Holmes, A. Doelman, G. M. Hek, and G. Domokos. Homoclinic orbits and chaos in three- and four-dimensional flows. *Phil. Trans. Roy. Soc. Lond. A*, 359:1429–1438, 2001.

[46] A. J. Homburg and J. Knobloch. Multiple homoclinic orbits in conservative and reversible systems. *Transactions of the AMS*, 2003. submitted.

[47] A. J. Homburg. *Some global aspects of homoclinic bifurcations of vector fields.* PhD thesis, Rijkuniversiteit Groningen, 1993.

[48] I. Hoveijn. Versal deformations and normal forms for reversible and Hamiltonian linear systems. *Journal of Differential Equations*, 126(2):408–442, 1996.

[49] G. Iooss and Adelmeyer M. *Topics in Bifurcation Theory and Applications.* World Scientific, 1992. Adv. Series in Nonlinear Dynamics 3.

[50] G. Iooss and M.C. Peroueme. Perturbed homoclinic solutions in reversible 1:1

resonance vector fields. *J. Diff. Eq.*, 102:62–88, 1993.

[51] G. Iooss. A codimension-two bifurcation for reversible vector fields. *Fields Institute Communications*, 4:201–217, 1995.

[52] C. K. R. T. Jones, T. J. Kaper, and N. Kopell. Tracking invariant manifolds up to exponentially small errors. *SIAM J. Math. Anal.*, 27(2):558–577, 1996.

[53] C. K. R. T. Jones and N. Kopell. Tracking invariant manifolds with differential forms in singularly perturbed systems. *J. Diff. Eq.*, 108(1):64–88, 1994.

[54] C. K. R. T. Jones. Geometric singular perturbation theory. In R. Johnson, editor, *Dynamical Systems, Montecatibi Terme*, volume 1609 of *Lecture Notes in Math.*, pages 44–118. Springer, 1994.

[55] T. J. Kaper. An introduction to geometric methods and dynamical systems theory for singular perturbation problems. In J. Cronin and R. E. O'Malley, editors, *Analyzing multiscale phenomena using singular perturbation methods*, volume 56 of *Proc. Symposia Appl. Math.*, pages 85–132. American Mathematical Society, 1999.

[56] S. Kichenassamy and P. J. Olver. Existence and non-existence of solitary wave solutions to higher-order model evolution equations. *SIAM J. Math. Anal.*, 23:1141–1166, 1996.

[57] J. Klaus and J. Knobloch. Bifurcation of homoclinic orbits to a saddle-center in reversible systems. *Int. Journal of Bifurcation of Chaos*, 13(9):2603–2622, 2003.

[58] J. Knobloch, T. Rieß, and T. Wagenknecht. Numerical study of connecting orbits in systems of second order ODEs. *in preparation*, 2003.

[59] J. Knobloch. Bifurcation of degenerate homoclinics in reversible and conservative systems. *J. Dynamics. Diff. Eqns.*, 9:472–494, 1997.

[60] J. Knobloch. Chaotic behaviour near non-transversal homoclinic points with quadratic tangencies. *Preprint, TU Ilmenau*, 07/00, 2000.

[61] K. Kolossovski, A. R. Champneys, A. V. Buryak, and R. A. Sammut. Multipulse embedded solitons as bound states of quasi-solitons. *Physica D*, 171(3):153–177, 2002.

[62] O.Yu Koltsova and L. M. Lerman. Periodic orbits and homoclinic orbits in a two-parameter unfolding of a Hamiltonian system with a homoclinic orbit to a saddle-center. *Int. J. Bifurcation Chaos*, 5:397–408, 1995.

[63] J. S. W. Lamb and J. A. G Roberts. Time-reversal symmetry in dynamical systems: A survey. *Physica D*, 112:1–39, 1998.

[64] J. S. W. Lamb and Capel H. W. Local bifurcations on the plane with reversing point group symmetry. *Chaos, Solitons and Fractals*, 5:271–293, 1995.

[65] J. S. W. Lamb. *Reversing symmetries in dynamical systems.* PhD thesis, University of Amsterdam, 1994.

[66] X.-B. Lin. Using Melnikov's method to solve Shil'nikov's problems. *Proc. Roy. Soc. Edinburgh, A*, 116:295–325, 1990.

[67] E. Lombardi. *Oscillatory Integrals and Phenomena Beyond all Orders; With Applications to Homoclinic Orbits in Reversible Systems*. Number 1741 in LNM. Springer, 2000.

[68] A. Mielke, P. Holmes, and O. O'Reilly. Cascades of homoclinic orbits to, and chaos near, a Hamiltonian saddle-center. *J. Dynamics Diff. Eqns.*, 4:95–126, 1992.

[69] J. D. Murray. *Mathematical Biology*. Springer-Verlag, 1993.

[70] B. E. Oldeman, A. R. Champneys, and B. Krauskopf. Homoclinic branch switching: a numerical implementation of Lin's method. *Int. Journal of Bifurcation and Chaos*, 13(10):2977–3000, 2003.

[71] D. E. Pelinovsky and J. Yang. A normal form for nonlinear resonance of embedded solitons. *Proc. Roy. Soc. Lond. A*, 458:1469–1497, 2002.

[72] H. Poincaré. Sur le problème des trois corps et les équations de la dynamique (mémoire couronné du prise de s.m. le roi oscar de suède. *Acta Math.*, 13:1–270, 1890.

[73] M. Remoissenet. *Waves called solitons: concepts and experiments*. Springer, 1996.

[74] B. Sandstede, C. K. R. T. Jones, and J. C. Alexander. Existence and stability of N-pulses on optical fibres with phase-sensitive amplifiers. *Physica D*, 106:167–206, 1997.

[75] B. Sandstede. *Verzweigungstheorie homokliner Verdopplungen*. PhD thesis, University of Stuttgart, 1993.

[76] B. Sandstede. Instability of localised buckling modes in a one-dimensional strut model. *Phil. Trans. Roy. Soc. Lond. A*, 355:2083–2097, 1997.

[77] B. Sandstede. Stability of multiple-pulse solutions. *Trans. Amer. Math. Soc.*, 350:429–472, 1998.

[78] L.P. Shilnikov. A case of the existence of a countable number of periodic motions. *Sov. Math. Dokl.*, 6:163–166, 1965.

[79] L. P. Shilnikov, A. L. Shilnikov, D. V. Turaev, and L. O. Chua. *Methods of Qualitative Theory in Nonlinear Dynamics. Part I*. World Scientific, 1998.

[80] S. Smale. Differentiable dynamical systems. *Bull. Amer. Math. Soc.*, 73:747–817, 1967.

[81] A. Vanderbauwhede and B. Fiedler. Homoclinic period blow-up in reversible and conservative systems. *Z. Angew. Math. Phys.*, 43:292–318, 1992.

[82] A. Vanderbauwhede. Centre manifolds, normal forms and elementary bifurcations. In U. Kirchgraber and O. Walther, editors, *Dynamics Reported*, pages 89–169. Wiley/Teubner, New York, 1989.

[83] A. Vanderbauwhede. Bifurcation of degenerate homoclinics. *Results in Mathematics*, 21(1/2):211–223, 1992.

[84] J. B. van den Berg. The phase-plane picture for a class of fourth-order conservative differential equations. *J. Differential Equations*, 161:110–153, 2000.

[85] J. C. van der Meer. *The Hamiltonian Hopf bifurcation.* Number 1160 in LNM. Springer, 1985.

[86] T. Wagenknecht and A. R. Champneys. When gap solitons become embedded solitons; an unfolding via lin's method. *ANM Preprint*, 2002.4, 2002.

[87] T. Wagenknecht and A. R. Champneys. When gap solitons become embedded solitons: a generic unfolding. *Physica D*, 177:50–70, 2003.

[88] T. Wagenknecht. An analytical study of a two degrees of freedom Hamiltonian system associated to the reversible hyperbolic umbilic. Diploma Thesis, TU Ilmenau, 1999.

[89] T. Wagenknecht. Continuation of heteroclinic cycles using topological transversality. *Preprint*, M02/01, 2001.

[90] T. Wagenknecht. About a homoclinic pitchfork bifurcation in reversible systems with additional $\mathbb{Z}_2$-symmetry. *Nonlinearity*, 15(6):2097–2119, 2002.

[91] T. Wagenknecht. Bifurcation of a reversible Hamiltonian system from a fixed point with fourfold eigenvalue zero. *Dynamical Systems*, 17(1):29–45, 2002.

[92] S. Wiggins. *Global Bifurcations and Chaos : Analytical Methods.* Springer-Verlag, New York, U.S.A., 1988.

[93] J. Yang, B. A. Malomed, and Kaup D. J. Embedded-solitons in second-harmonic-generating systems. *Phys. Rev. Lett.*, 83:1958–1961, 1999.

[94] J. Yang, B. A. Malomed, D. J. Kaup, and A. R. Champneys. Embedded solitons: a new type of solitary waves. *Mathematic and Computers in Simulation*, 56:585–600, 2001.

[95] J. Yang. Dynamics of embedded solitons in the extended KdV equations. *Stud. Appl. Math.*, 106:337–365, 2001.

[96] A. C. Yew, A. R. Champneys, and P. J. McKenna. Multiple solitary-waves due to second harmonic generation in quadratic media. *J. Nonlin. Sci.*, 9:33–52, 1999.

[97] A. C. Yew. *An analytical study of solitary-waves in quadratic media.* PhD thesis, Brown University, 1998.

Zusammenfassung

Dieser Abschnitt enthält eine Zusammenfassung der Arbeit in deutscher Sprache. Sämtliche Referenzen beziehen sich auf den vorderen englischsprachigen Teil. Die Bezeichnungen sind ebenfalls beibehalten worden.

Einführung

Seit längerer Zeit besteht ein großes Interesse an homoklinen und heteroklinen Phänomenen in gewöhnlichen Differentialgleichungen. Homokline und heterokline Orbits sind zum einen von mathematischer Bedeutung, da sie häufig organisierende Zentren für die Dynamik in ihrer Umgebung darstellen. Zum anderen finden Homoklinen Anwendungen als solitäre Wellenlösungen (Pulslösungen) partieller Differentialgleichungen. Heteroklinen beschreiben in diesem Zusammenhang sogenannte Fronten. Die partielle Differentialgleichung wird dabei durch einen entsprechenden Ansatz für laufende Wellenlösungen zu einer gewöhnlichen Differentialgleichung reduziert. In einer Vielzahl von Beispielen implizieren Symmetrien der partiellen Differentialgleichung, dass die zugeordnete gewöhnliche Differentialgleichung *reversibel* ist. Die Arbeit betrachtet zwei neue Typen homokline Bifurkationen in Systemen reversibler gewöhnlicher Differentialgleichungen. Diese können durch eine Änderung im Typ der assoziierten Gleichgewichtslage (GGL) charakterisiert werden. Beide Bifurkationen verlangen einen mindestens vierdimensionalen Phasenraum.

Im Hauptteil der Arbeit werden Homoklinen an GGLn betrachtet, welche selbst in einer lokalen Bifurkation verzweigen. Dabei geht die GGL über vom Typ des reellen Sattels (mit führenden reellen Eigenwerten) in den Typ des Sattel-Zentrums (mit einem Paar rein imaginärer Eigenwerte). Hier kommt es zu einem Zusammenspiel lokaler und globaler Bifurkationseffekte. Dies erfordert eine neuartige Behandlung. Wir gewinnen Bifurkationsszenarien für verzweigende homokline Orbits in verschiedenen Klassen reversibler Systeme.

Der zweite Teil behandelt Homoklinen an GGLn, welche ihren Typ vom reellen Sattel zum komplexen Sattel-Fokus ändern. Es ist wohlbekannt [22], dass dieser Übergang zu einer dramatischen Veränderung in der Dynamik nahe des Orbits führt. Wir betrach-

ten diese Bifurkation für zwei Orbits in Blasebalg-Konfiguration und beschreiben die Verzweigung N-homokliner Orbits. Dabei ist ein N-homokliner Orbit eine Homokline, die N Umläufe entlang der Orbits des Blasebalgs macht.

Die allgemeinen Resultate der Bifurkationsanalyse werden in numerischen Untersuchungen an mathematischen Modellgleichungen und physikalischen Problemen illustriert.

Die gewonnenen Resultate liefern neue Beiträge zur Bifurkationstheorie homokliner Orbits.

Homokline Orbits an degenerierte Gleichgewichtslagen

Im Hauptteil der Arbeit betrachten wir Bifurkationen von Homoklinen an degenerierte GGLn. Dabei wird zunächst in Kapitel 2 der Fall reversibler und $\mathbb{Z}_2$-symmetrischer Systeme betrachtet. Wir betrachten einparametrige Familien solcher Systeme $\dot{x} = f(x, \lambda)$, $\lambda \in \mathbb{R}$, die zum Parameterwert $\lambda = 0$ eine Homokline Γ an eine GGL mit singulärer Linearisierung besitzen. Die Homokline wird als symmetrisch vorausgesetzt, d.h. sie soll im Fixraum der $\mathbb{Z}_2$-Symmetrie enthalten sein und invariant unter der zeitreversiblen Symmetrie sein. Der Parameter λ entfaltet die lokale Bifurkation der GGL, siehe Abschnitt 2.2.

Wir analysieren zunächst die lokale Bifurkation mittels Zentrumsmannigfaltigkeit-Reduktion auf Mannigfaltigkeiten $W^c_{loc,\lambda}$. Es ist wohl bekannt, dass unter den gemachten Voraussetzungen die GGL typischerweise in einer Heugabel-Bifurkation verzweigt [64]. Wir unterscheiden Typ I *(eye case)* und II *(figure-eight case)* mit unterschiedlichen Vorzeichen im Term dritter Ordnung in einer Normalform.

Der Zentrumsmannigfaltigkeiten-Satz erlaubt es uns geeignete zentrumsstabile und zentrumsinstabile Mannigfaltigkeiten $W^{cs(cu)}_\lambda$ zu erklären, die alle Lösungen enthalten, welche asymptotisch zu den $W^c_{loc,\lambda}$ für $t \to \pm\infty$ sind. Wir bestimmen den Schnitt $W^{cs}_\lambda \cap W^{cu}_\lambda$ und damit Homoklinen an $W^c_{loc,\lambda}$. Diese umfassen insbesondere alle von Γ verzweigenden Homoklinen an GGLn und periodische Orbits.

Zur Bestimmung von $W^{cs}_\lambda \cap W^{cu}_\lambda$ werden die Symmetrien des Systemes und von Γ entscheidend genutzt. Es kann bewiesen werden, dass Γ unter Störungen erhalten bleibt und dass zwei Familien von symmetrischen 1-Homoklinen an die $W^c_{loc,\lambda}$ existieren. Der geometrische Zugang wird unterstützt durch eine analytische Methode, die ähnlich Lins Methode Gleichungen für das Aufsplitten von W^{cs}_λ und W^{cu}_λ liefert. Analytische Details sind in Abschnitt 2.3 zu finden.

Um das asymptotische Verhalten der homoklinen Orbits an $W^c_{loc,\lambda}$ zu analysieren führen wir eine Projektion entlang stabiler Fasern durch. Nun zeigt sich der entscheidende Einfluss der lokalen Bifurkation der GGL. Während im Typ II lediglich Homoklinen an periodische Orbits von Γ verzweigen (Satz 2.12), kommt es beim Typ I zu einer homoklinen reversiblen Heugabel-Bifurkation. Parallel zur lokalen Bifurkation, bei der aus der GGL zwei neue GGLn η, $R_2\eta$ verzweigen, verzweigen homokline Orbits an η, $R_2\eta$

von Γ. Außerdem entsteht ein heterokliner Zykel nahe Γ an diese GGLn (Satz 2.11).

Im Abschnitt 2.5 wird die Existenz von 2-heteroklinen Zykeln zwischen η, $R_2\eta$ nachgewiesen. Dazu wird eine entsprechende Poincaré-Abbildung untersucht und ein nichtleerer Schnitt von W^{cu}_λ mit dem Fixraum einer reversiblen Symmetrie nachgewiesen.

In Kapitel 3 werden die entwickelten Methoden benutzt um Bifurkationsszenarien in weiteren Klassen reversibler Differentialgleichungen zu beschreiben. Den Schwerpunkt bildet dabei die Analyse rein reversibler Systeme. Hier sind homokline Orbits an eine Sattel-GGL strukturell stabil, während Homoklinen an ein Sattel-Zentrum von Kodimension-1 sind. Deshalb wird ein zweiter Parameter in der Entfaltung benötigt. Die lokale Bifurkation der GGL ist nun im generischen Fall transkritisch.

Unter Verwendung des oben beschriebenen Zugangs und einer geeigneten Transversalitätsbedingung können wir sehr einfach Bifurkationsdiagramme für 1-Homoklinen an $W^c_{loc,\lambda}$ gewinnen und die Existenz homokliner Orbits an GGLn und periodische Orbits diskutieren (Satz 3.3 und Bemerkungen danach). Es wird bewiesen, dass beim Übergang in die Sattel-Zentrum-Region Homoklinen auf zwei verschiedene Arten vernichtet werden; entweder durch Sattel-Knoten Bifurkation mit einer zweiten Homokline oder über ein algebraisches Abklingen zur GGL. Von besonderem Interesse sind reversible Hamilton-Systeme. Hier wird gezeigt, dass die allgemeinen Resultate auf die Bifurkation symmetrischer Orbits zutreffen. Allerdings können im Gegensatz zum rein reversiblen Fall auch nichtsymmetrische Orbits verzweigen. Der Grund dafür liegt in einer Degeneriertheit der Klasse der Hamilton-Systeme. In dieser Klasse kann die grundlegende Transversalitätsbedingung 3.5 nicht erfüllt werden.

Die allgemeine Theorie wird in numerischen Untersuchungen von physikalischen Problemen aus der Wasserwellen-Theorie und nichtlinearen Optik und von mathematischen Modellgleichungen bestätigt.

Der Hauptteil der Arbeit fußt im wesentlichen auf den Veröffentlichungen [90, 87].

Bifurkation einer homoklinen Blasebalg-Konfiguration

In Kapitel 4 wird die Bifurkation von Homoklinen in reversiblen Systemen betrachtet, deren assoziierte GGL ihren Typ von reellem Sattel zu komplexem Sattel-Fokus ändert. Dabei wird die Existenz zweier symmetrischer Homoklinen, Γ_1 und Γ_2, vorausgesetzt, die eine Blasebalg-Konfiguration bilden. Dies bedeutet, dass sie sich der GGL aus der jeweils gleichen Richtung für $t \to \pm\infty$ nähern, siehe Hypothese 4.3.

Eine oben beschriebene Änderung der GGL erfolgt an einem kritischen Parameterwert, an dem die führenden Eigenwerte der Linearisierung reell, doppelt und nicht-halbeinfach sind. Die Entfaltung dieser Situation benötigt einen Parameter. Es werden Nicht-Degeneriertheitsforderungen an die Γ_i gestellt, so dass deren globale Bifurkation von Kodimension-1 ist.

Wir untersuchen die Existenz von N-Homoklinen in einer Umgebung des Blasebalgs. Dazu werden Bifurkationsgleichungen nach der Methode von Lin [66, 75] hergeleitet. Hauptquelle hierfür ist [75], die Darstellung beschräkt sich auf wesentliche Details. Nach Ausnutzen der Symmetrien können wir N-Homoklinen durch Lösung von $[N/2]$-Gleichungen finden. (Hier bezeichnet $[\cdot]$ die *größte ganze* Funktion.)

Die Lösung der Gleichungen zeigt ein analoges Verhalten zum bereits untersuchten Fall [21] eines einzelnen homoklinen Orbits. Für Parameterwerte, bei denen die GGL ein Sattel ist, existieren keine weiteren Homoklinen nahe $\Gamma_1 \cup \Gamma_2$. Ist die GGL allerdings ein Sattel-Fokus, so existieren unendlich viele Homoklinen.

Genauer gesagt, können wir bei beliebigem N eine beliebige symmetrische Abfolge $\kappa \in \{1,2\}^N$ vorgeben, die angibt, in welcher Reihenfolge die gesuchte Homokline Γ_1 und Γ_2 folgen soll. Dann existieren zu dieser Abfolge unendlich viele N-Homoklinen nahe $\Gamma_1 \cup \Gamma_2$. Werden die führenden Eigenwerte der GGL reell, so lösen sich alle N-Homoklinen an $\Gamma_1 \cup \Gamma_2$ auf.

Zwei Modellgleichungen

Die Untersuchungen der Arbeit werden insbesondere für zwei Modellsysteme von Differentialgleichungen zweiter Ordnung angewendet. Diese Systeme wurden in der Diplomarbeit [88] des Autors als Entfaltungen einer GGL mit vierfachem 0-Eigenwert in einer Klasse reversibler Hamilton-Systeme gewonnen. Sie beschreiben das typische Verhalten in der Umgebung einer solchen GGL. Numerische Untersuchungen der Gleichungen motivieren und illustrieren die allgemeine Bifurkations-Analyse. Die zugrunde liegenden analytischen Resultate sind in einem Anhang zusammengefasst.

Die gewonnenen Resultate, sowie ergänzende numerische Studien zeigen, dass in Störungen der GGL eine reichhaltige Dynamik vorliegt. Insbesondere können zahlreiche homokline und heterokline Bifurkationsphänomene beobachtet werden. Dies ist von Interesse für ein zugeordnetes physikalisches Problem aus der nichtlinearen Optik.

Danksagung (Acknowledgements)

Die vorliegende Arbeit ist das Ergebnis eines vierjährigen Promotionsstudiums im Fachbereich Analysis und Dynamische Systeme des Instituts für Mathematik der TU Ilmenau. Zahlreiche Kollegen und Freunde, Verwandte und Bekannte haben zu ihrem Gelingen beigetragen. Ihnen allen möchte ich auf diesem Weg recht herzlich danken.

Mein erster Dank gilt meinen Betreuern Dr. Jürgen Knobloch und Prof. Dr. Bernd Marx für ihre Unterstützung während meiner Promotion.

Die zahlreichen Diskussionen mit Jürgen Knobloch sind der Grundstein für viele Ergebnisse dieser Arbeit. Seine Ideen sind fast immer inspirierend; seine kritischen Kommentare halfen manche Darstellung zu verbessern. Unsere gemeinsamen Bemühungen die weite Welt der dynamischen Systeme in Forschungsseminaren zu erkunden sind ein wertvoller Bestandteil meines Promotionsstudiums gewesen. Danke, Knobi!

Meinem zweiten Betreuer, Bernd Marx, danke ich für sein stetes Interesse an meiner Arbeit und seinen Einsatz, wenn es darum ging mal wieder ein Gutachten für ein Stipendium zu verfassen. In fachlichen Gesprächen, gemeinsamen Seminaren und Lehrveranstaltungen konnte ich von seinem Wissen profitieren.

Genauso herzlich danke ich meinen anderen Mitkämpfern an der Homoklinen-Front, Jenny Klaus und Thorsten Rieß für die zahlreichen Gespräche rund um Homoklinen und andere Dinge. Insbesondere danke ich Thorsten für seine Hilfe bei den numerischen Berechnungen.

Die Diskussionen und wertvollen Hinweise in den Seminaren des Fachbereiches Analysis trugen wesentlich zu dieser Dissertation bei, und das kollegiale Miteinander machte meine Promotion zu einer sehr angenehmen Erfahrung. Dafür danke ich allen Angehörigen des Fachbereiches.

My six month stay at the Department of Engineering Mathematics at the University of Bristol has been a marvellous experience. I thank the Applied Nonlinear Mathematics Group for the hospitality. I deeply enjoyed working with Alan Champneys on homoclinic bifurcations and thank him for explaining the corresponding physical background to me. I also appreciate Bart Oldeman's patience in explaining how the AUTO-program is supposed to work.

Zu weiten Teilen wurde meine Promotion finanziert durch ein Stipendium des Freistaates

Thüringen sowie ein Forschungsstipendium des Deutschen Akademischen Austauschdienstes. Beides wurde dankend angenommen.

Zum Abschluss möchte ich mich bei meinen Eltern und meiner ganzen Familie für die jahrelange menschliche, fachliche und finanzielle Unterstützung bedanken. Ohne Euch wäre diese Arbeit so nie entstanden.